

CASE FILE
COPY

NASA TECHNICAL
MEMORANDUM



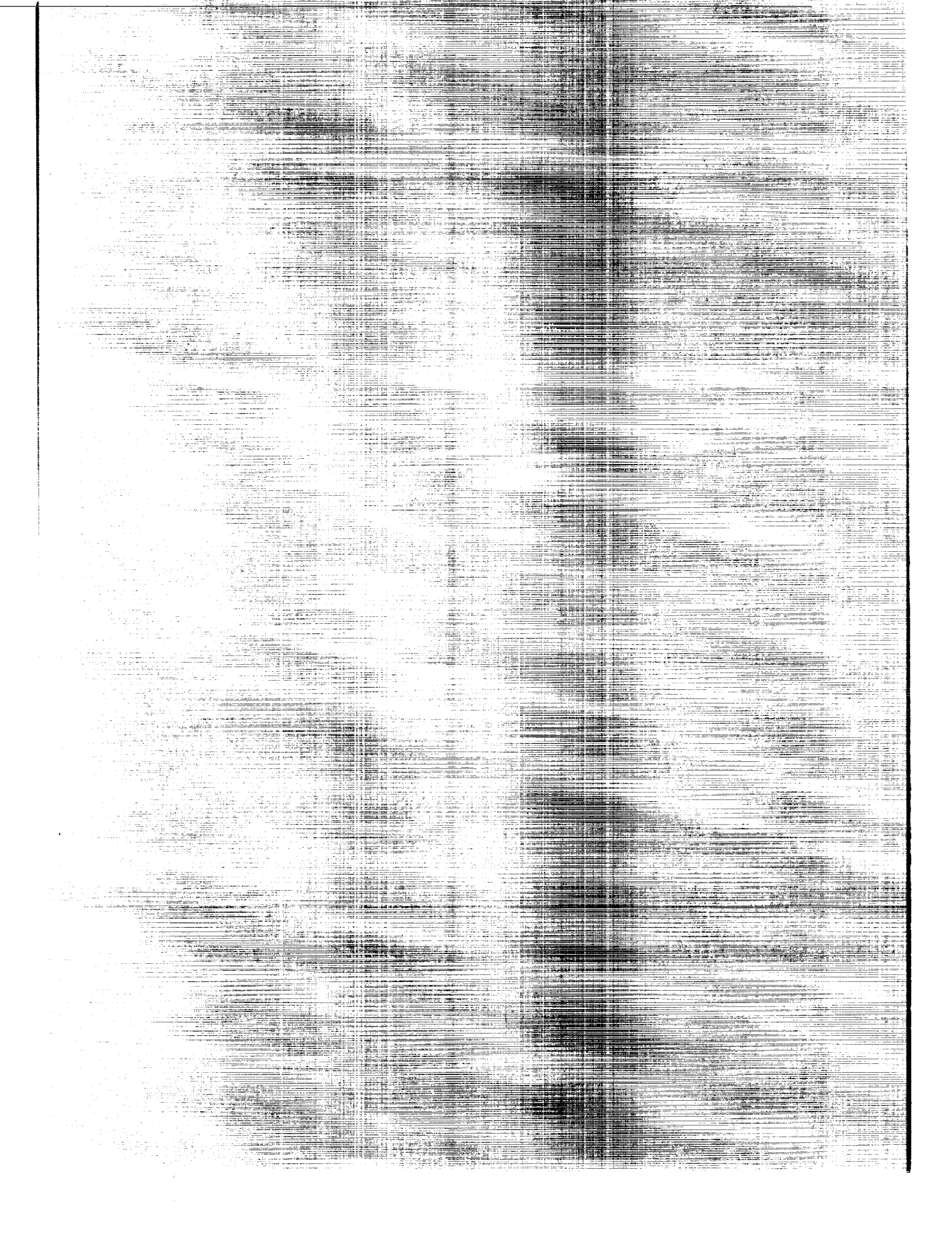
NASA TM X-3293

SEP 1 1975

EFFECTS OF FORWARD CONTOUR MODIFICATION
ON THE AERODYNAMIC CHARACTERISTICS
OF THE NACA 64-212 AIRFOIL SECTION

*Raymond M. Hicks, Joel P. Mendoza,
and Angelo Bandettini*
Ames Research Center
Moffett Field, Calif. 94035





1. Report No. NASA TM X-3293	2. Government Accession No.	3. Recipient's Catalog No.	
4. Title and Subtitle EFFECTS OF FORWARD CONTOUR MODIFICATION ON THE AERO-DYNAMIC CHARACTERISTICS OF THE NACA 64 ₁ -212 AIRFOIL SECTION		5. Report Date September 1975	6. Performing Organization Code
		8. Performing Organization Report No. A-6018	10. Work Unit No. 505-10-12
7. Author(s) Raymond M. Hicks, Joel P. Mendoza, and Angelo Bandettini		11. Contract or Grant No.	
9. Performing Organization Name and Address Ames Research Center Moffett Field, California 94035		13. Type of Report and Period Covered Technical Memorandum	
		14. Sponsoring Agency Code	
12. Sponsoring Agency Name and Address National Aeronautics and Space Administration Washington, D.C. 20546		15. Supplementary Notes	
16. Abstract Two different forward contour modifications designed to increase the maximum lift coefficient of the NACA 64 ₁ -212 airfoil section were evaluated experimentally at low speeds. One modification consisted of a slight droop of the leading edge with an increased leading-edge radius; the other modification incorporated increased thickness over the forward 35 percent of the upper surface of the profile. Both modified airfoil sections were found to provide substantially higher maximum lift coefficients than the 64 ₁ -212 section. The drooped leading-edge modification incurred a drag penalty of approximately 10 percent at low and moderate lift coefficients and exhibited a greater nosedown pitching moment than the 64 ₁ -212 profile. The upper-surface modification produced about the same drag level as the 64 ₁ -212 section at low and moderate lift coefficients and less nosedown pitching moment than the 64 ₁ -212 profile. Both modified airfoil sections had lower drag coefficients than the 64 ₁ -212 section at high lift coefficients.			
17. Key Words (Suggested by Author(s)) Airfoil Optimization Wing		18. Distribution Statement Unclassified - Unlimited STAR Category - 02	
19. Security Classif. (of this report) Unclassified	20. Security Classif. (of this page) Unclassified	21. No. of Pages 78	22. Price* \$4.75

NOMENCLATURE

c	airfoil chord, cm (in.)
c_d	section drag coefficient
c_l	section lift coefficient
c_m	section pitching-moment coefficient referenced to quarter chord
C_p	pressure coefficient, $\frac{p_L - p_\infty}{q_\infty}$
h	tunnel height, m (ft)
k	roughness diameter, cm (in.)
p	static pressure, N/m ² (lb/ft ²)
q	dynamic pressure, N/m ² (lb/ft ²)
Re	Reynolds number based on free-stream conditions and airfoil chord
x	airfoil abscissa, cm (in.)
y	airfoil ordinate, cm (in.)
α	angle of attack, deg

Subscripts

max	maximum
L	local
∞	free-stream conditions

EFFECTS OF FORWARD CONTOUR MODIFICATION ON THE AERODYNAMIC CHARACTERISTICS OF THE NACA 64₁-212 AIRFOIL SECTION

Raymond M. Hicks, Joel P. Mendoza, and Angelo Bandettini

Ames Research Center

SUMMARY

Two different forward contour modifications designed to increase the maximum lift coefficient of the NACA 64₁-212 airfoil section were tested at Mach numbers of 0.2, 0.3, and 0.4 and Reynolds numbers of 1 million, 1.5 million, and 1.9 million. The unmodified 64₁-212 profile was also tested for comparison with the modified sections. One modification consisted of a slight leading-edge droop along with an increased leading-edge radius; the other modification incorporated increased thickness over the forward 35 percent of the upper surface of the airfoil profile.

Lift and pitching moment were determined by integrating surface pressure measurements and the profile drag was obtained from wake pressures. The models were tested at all the Mach numbers and Reynolds numbers with a narrow strip of roughness located at 12 percent of the chord and without roughness at $M = 0.2$ and $Re = 1.9$ million.

Both modified profiles were found to provide substantially higher maximum lift coefficients than the NACA 64₁-212 section. The drooped leading edge incurred a drag penalty of approximately 10 percent at low and moderate lift coefficients and exhibited a greater nosedown pitching moment than the 64₁-212 profile. Relative to the 64₁-212 section, the upper-surface modification produced nearly the same drag level at low and moderate lift coefficients and less nosedown pitching moment. Both modified profiles had lower drag coefficients than the 64₁-212 section at lift coefficients above 0.8.

INTRODUCTION

Airfoils that produce high maximum lift coefficients are desirable for airplanes designed for short takeoff and landing (STOL) capability and for maximum turning performance during maneuvers. On the other hand, airfoils that produce low drag coefficients are needed for airplanes designed for high-speed applications. After World War II, many general aviation airplanes were designed with emphasis on the high-speed requirements rather than the slow-flight or maneuvering capabilities. This led many designers to use the NACA laminar-flow sections in the hope of achieving the low drag coefficients exhibited by these airfoil sections during wind-tunnel testing when operated near the design lift coefficient. Such sections rarely achieve the low drag in flight because of manufacturing roughness or poor care of the wing surfaces during service. Furthermore, the laminar-flow sections exhibit a greater decrease in maximum lift coefficient with decreasing Reynolds number below 3 million than do most of the NACA 4- and 5-digit sections. Because of the relatively poor maximum lift characteristics of the 6-series airfoils and the realization on the part of many designers that large amounts of laminar flow are not generally achieved in practice, several efforts have been made to modify the contour of the NACA 6-series sections to achieve greater maximum lift coefficients.

The most widely used contour modification for increasing the maximum lift coefficient has been a droop of the leading edge with or without an increased leading-edge radius (e.g., refs. 1-4). A relatively little used contour modification for increasing maximum lift is to increase the thickness of the forward section of the upper surface of the airfoil. Such a modification is suggested in reference 5. The main advantage of the forward upper-surface modification is that the maximum lift is increased without incurring the drag penalty generally found with the drooped leading edge. Furthermore, the upper-surface modification produces less nosedown pitching moment than a drooped leading edge. Because of these advantages and because of the need to further investigate upper-surface modifications, a study was undertaken to compare the two types of forward contour modifications.

As noted earlier, the 6-series profiles have relatively poor maximum lift characteristics at low Reynolds numbers; hence a 6-series section was deemed most appropriate for this study. Since NACA 63-, 64-, and 65-series profiles are being used on many general aviation airplanes, a 64-series section was chosen as representative of this class of airfoils. Thickness ratios ranging from 6 percent to 18 percent are in use on general aviation airplanes, hence, a 12 percent thick section was selected for this investigation. The concept demonstrated here should be applicable to NACA 6-series profiles with thickness ratios between 6 and 18 percent.

DESIGN OF AIRFOIL SECTION

The design of profiles for high maximum lift coefficient is usually carried out by consideration of the surface pressure distribution since no reliable methods are available for direct calculation of $c_{l_{max}}$. The procedure used here was to reshape the forward region of the airfoil so that the peak pressure coefficient and adverse pressure gradient near the leading edge on the upper surface are reduced without significantly changing the basic camber of the 64₁-212 profile, thereby retaining the original design lift coefficient. The modified airfoil sections are shown in figure 1 along with the NACA 64₁-212 profile. The theoretical pressure distributions for $M = 0.1$ and $Re = 1.0 \times 10^6$ are presented in figures 2(a) and 2(b). Note the decrease in pressure peak and improved pressure gradient exhibited by both Modification (Mod.) A and Mod. B profiles for $\alpha = 6^\circ$ when compared with the pressure distribution of the 64₁-212 section (fig. 2(a)). These modified pressure distributions were achieved by repeated iterations utilizing drafting tools and a high-speed computer. Each iteration consisted of drawing a different forward contour for the 64₁-212 profile and then calculating the pressure distribution and aerodynamic force coefficients for the modified airfoil section by the theory of reference 6 (a CDC 7600 computer was used). Seven iterations were required to develop Mod. A profile and 6 iterations to develop Mod. B. Note that the final pressure distribution for Mod. B at $\alpha = 6^\circ$ exhibits a greater peak pressure coefficient than Mod. A. The test results presented later show a slightly lower maximum lift coefficient for Mod. B than for Mod. A, which is consistent with the relative values of peak pressure coefficients shown here. It might have been possible to further reduce the pressure peak for Mod. B if more iterations had been attempted. However, because of the time involved in producing the large-scale drawings and generating the "inputs" for the computer for each iteration, the process was terminated after six iterations. In the future, such contour modifications will be carried out very rapidly by the numerical optimization technique described in reference 7.

The main disadvantage in drooping the leading edge to increase the maximum lift coefficient is illustrated in figure 2(b), which shows theoretical pressure distributions for $\alpha = 0^\circ$. Note the pressure "spike" near the leading edge of the lower surface of Mod. A. The steep adverse pressure gradient following the "spike" will cause the boundary layer to thicken with an attendant increase in drag. If the leading edge is drooped enough to produce reflexed curvature behind the leading edge on the lower surface, the pressure "spike" will be accentuated and the drag increase will be greater. The experimental results presented later show a higher drag level for Mod. A than for either Mod. B or the 64₁-212 profile at low lift coefficients, which tends to support the predicted effect of the lower surface adverse gradient. Note that the lower surface pressure distribution of Mod. B is very similar to that of the 64₁-212 airfoil section whereas the upper-surface pressure distribution shows a modest "hump" near the 10-percent chord station followed by a relatively "flat" adverse pressure gradient. A gradient of this magnitude should have only a minor effect on the boundary-layer development and hence little effect on pressure drag.

The coordinates for the unmodified NACA 64₁-212 section and the two modified profiles are given in tables 1 to 3.

APPARATUS AND TEST PROCEDURE

Models

Three airfoil models with the NACA 64₁-212, Mod. A, and Mod. B profiles were machined from aluminum billets. Each model had a nominal chord of 15.24 cm (6 in.) and a span of 60.96 cm (24 in.). The models were equipped with 21 upper-surface orifices and 22 lower-surface orifices drilled normal to the surface, which, together with the necessary pressure leads, made it possible to determine the pressure distributions on the model surfaces. The pressure leads from each orifice were set in milled slots in the models, resulting in minute wavyness of the upper and lower surfaces. It was felt that such an imperfection was fairly realistic since most manufacturing processes produce some wavyness of aircraft skins.

Wind Tunnel

The tests were conducted in the Ames 2- by 2-Foot Transonic Wind Tunnel, a variable-speed, continuous flow, ventilated wall, variable pressure facility. The tunnel can be used for two-dimensional testing by replacing the ventilated side walls with solid walls where model-supporting thick glass windows are mounted. The windows can be rotated by a motorized drive system to change the angle of attack. An 82-tube drag rake located 1.75 chords behind the model trailing edge is used to survey the model wake. Figures 3(a) and 3(b) show the Mod. B airfoil installed in the tunnel along with the drag rake. Airfoil models are mounted spanning the horizontal dimension of the tunnel test section so that the center of rotation of the side windows is near the 25-percent chord station on the model. The gaps between the ends of the model and the side windows were sealed with silicone rubber adhesive sealant.

Instrumentation

Measurements of the model surface pressures and the wake rake pressures were made by automatic pressure-scanning system that utilizes precision pressure transducers. Basic tunnel pressures were measured with precision mercury manometers. Angle of attack was measured with a potentiometer operated by the drive gear for the rotating side windows. Data were obtained by a high-speed, data-acquisition system and recorded on paper tape.

Tests

The section aerodynamic characteristics of the three airfoils were obtained at $M = 0.2$ and 0.3 at $Re = 1.0 \times 10^6$, 1.5×10^6 , and 1.9×10^6 and at $M = 0.4$ at $Re = 1.0 \times 10^6$, 1.9×10^6 , and 3.0×10^6 . (The Reynolds numbers are based on the model chord.) The angles of attack ranged from approximately -3° to 18° , depending on the stalling angle of each model. The models were not tested without the wake rake installed since previous investigations in the 2- by 2-Foot Wind Tunnel have shown that the effect of the wake rake on the model surface pressures is negligible for the rake position used in the present tests. Data were obtained at all test conditions with a 0.159 cm (0.0625 in.) wide strip of 0.0064 cm (0.0025 in.) (nominal) diameter glass balls located at the 12-percent chord station in an effort to simulate manufacturing roughness. Data were also taken at $M = 0.2$ and $Re = 1.9 \times 10^6$ without roughness.

Pressure coefficients were determined from surface pressure measurements. Section normal force coefficients, chord force coefficients, and pitching-moment coefficients were obtained from an integration of the pressure coefficients. The pitching-moment coefficients were referenced to the quarter-chord point. Section profile drag was calculated from the wake-rake total and static-pressure measurements.

The model angle of attack was corrected for the presence of the tunnel walls by the following equation:

$$\Delta\alpha = \delta(c/h)c_l$$

where $\Delta\alpha$, δ , c/h , and c_l are the angle-of-attack correction, correction factor, model chord/tunnel height ratio, and section lift coefficient respectively. The angle-of-attack correction factor (δ) is a function of Mach number. The following values were used and the corresponding $\Delta\alpha$, converted to units of degrees, was added algebraically to the model geometric angle of attack:

<u>M</u>	<u>δ</u>
0.2	-0.095
.3	-.150
.4	-.186

(These correction factors (δ) were determined during a tunnel calibration conducted by Mr. L. S. Stivers, Jr.) The Mach number corrections due to the presence of the tunnel walls were negligible for the Mach numbers of the present investigation.

RESULTS AND DISCUSSION

Aerodynamic Characteristics

Lift. – The basic force coefficients for the three airfoils tested with roughness are presented in figure 4(a) through 4(i). Both Mod. A and B airfoils gave substantially greater maximum lift than the NACA 64₁-212 section. At $Re = 1.0 \times 10^6$ and $M = 0.2$, both modifications had the same maximum lift coefficient but the stall of Mod. B was somewhat more abrupt than the stall of Mod. A or the 64₁-212 airfoil (fig. 4(a)). At $Re = 1.5 \times 10^6$ and 1.9×10^6 , Mod. A has the highest maximum lift coefficient (figs. 4(b) and (c)). Both modified sections stalled more abruptly than the 64₁-212. At all test Reynolds numbers at $M = 0.3$ and 0.4 , the two modified airfoils produced nearly equal maximum lift coefficients and showed similar stall characteristics (figs. 4(d)–(i)), except at $M = 0.3$ and $Re = 1.0 \times 10^6$ where Mod. A showed a more gradual stall (fig. 4(d)) than both Mod. B and the 64₁-212 airfoil. The two types of forward contour modification considered during this study had little effect on the basic camber distribution of the 64₁-212 airfoil as evidenced by the nearly constant values of c_l at $\alpha = 0^\circ$ for the three airfoils at all test conditions. As discussed previously, a constant value of design lift coefficient was one of the criteria used to develop these contour modifications. This is important if such modifications are considered for retrofit of existing aircraft.

Summary plots of $c_{l_{max}}$ versus Reynolds number for the three test Mach numbers are presented in figures 5(a) through 5(c). These figures clearly show the small difference in $c_{l_{max}}$ for the two contour modifications studied. Further work will be done to optimize the upper-surface modification (Mod. B) in an effort to further improve $c_{l_{max}}$ since this type of modification does not incur the drag penalty found with Mod. A (see the following discussion). The values of $c_{l_{max}}$ shown here may be lower than that achieved in actual use on general aviation airplanes since the landing Mach number of most light planes is 0.1 or less and previous NACA data have shown that $c_{l_{max}}$ can decrease substantially as the Mach number is increased from 0.1 to 0.2 (ref. 8).

Drag. – The profile drag data in figure 4 generally show that the drag level of the Mod. B airfoil is about the same as that of the NACA 64₁-212 section at low lift coefficients with Mod. A exhibiting higher drag for these conditions. An exception to this result is found at $M = 0.2$ and $Re = 1.0 \times 10^6$ where Mod. B shows slightly more drag than the 64₁-212 airfoil (fig. 4(a)). However, such a combination of Mach number and Reynolds number is not representative of the cruise condition for most general aviation airplanes and hence is of interest only academically. At all test conditions, both modified airfoils showed lower drag at moderate and high lift coefficients than the 64₁-212 airfoil (figs. 4(a)–(i)). Note that Mod. B had lower drag than Mod. A at high lift coefficients at all test conditions.

The fact that both modified airfoils extend the low drag range of the 64₁-212 airfoil to higher lift coefficients should be of particular interest to general aviation manufacturers since this means lower drag during climb and hence better climb performance, which is important from a safety standpoint. For example, the data in figure 4(c) show that the section lift/drag ratio of Mod. B varies from 80 at $c_l = 0.9$ to 86 at $c_l = 1.10$, which compares with lift/drag ratios of 67 to 70 for the 64₁-212 airfoil over the same lift coefficient range.

Pitching moment.— The pitching moment data in figure 4 show that Mod. A had a greater nosedown pitching moment than the NACA 64₁-212 airfoil, whereas Mod. B produced less nosedown pitching moment than either of the other two airfoils at all test conditions. These results show another advantage of using an upper-surface contour modification to increase $c_{l_{max}}$ instead of a drooped leading edge since less nosedown pitching moment means less trim drag. This is an important consideration in choosing a retrofit modification for an existing airplane.

Effect of Surface Roughness

The data in figure 6 show the effect of roughness on the section characteristics of the three airfoils at $M = 0.2$ and $Re = 1.9 \times 10^6$. A strip of glass balls, 0.159 cm (0.0625 in.) wide, with a nominal diameter of 0.0064 cm (0.0025 in.) located at the 12-percent chord station was used to achieve a mostly turbulent boundary layer and thereby simulate the surface condition found on most general aviation airplanes in normal service. The major effect of surface roughness was to increase the section profile drag coefficient of all models. The drag increase for the 64₁-212 airfoil was greater than for the other two sections since the 6-series airfoils were designed to achieve large amounts of laminar flow for a range of lift coefficients above and below the design point. Since extensive laminar flow is rarely attained in practice, the data obtained with roughness are more realistic.

Comparison of Experiment with Theory

A comparison of experimental and theoretical aerodynamic force data is presented in figure 7 (the viscous theoretical program used here is described in ref. 6). Data are shown for the NACA 64₁-212 section at $M = 0.2, 0.3,$ and 0.4 at $Re = 1.5 \times 10^6$ and for Mods. A and B at $M = 0.2$ and $Re = 1.5 \times 10^6$. In general, the agreement between experiment and theory is acceptable for the lift and pitching-moment data for angles of attack where the boundary layer is attached, whereas the theory consistently overestimates the profile drag for all three models. The inaccurate drag predictions are due in part to the technique used to determine the pressure drag, the integration of the theoretical surface pressures. This procedure is always difficult to use because the pressures are poorly defined near the leading edge of the profile. A new method is currently under development which will use the momentum defect in the wake to calculate profile drag, thereby eliminating the most serious inaccuracy in the theory. Note that the theory predicts the lift and pitching-moment characteristics of the 64₁-212 section slightly better than for the two modified airfoils. It is interesting that the agreement between experiment and theory is as good at $M = 0.4$ as at $M = 0.2$ or 0.3 since the theory was not intended to be applicable above $M = 0.3$.

Figure 8 compares experimental and theoretical pressure distributions. Data are presented for the 64₁-212 airfoil at $M = 0.2, 0.3,$ and 0.4 at $Re = 1.5 \times 10^6$ and for Mods. A and B at $M = 0.2$ and $Re = 1.5 \times 10^6$. Again the agreement between experiment and theory is acceptable at angles of attack where the boundary layer is not separated. As noted with the force data, the agreement between experiment and theory is somewhat better for the 64₁-212 section than for either modified airfoil.

CONCLUSIONS

Wind-tunnel tests were conducted to determine the section aerodynamic characteristics of two types of forward contour modifications designed to increase the maximum lift coefficient of the NACA 64₁-212 airfoil section. The unmodified 64₁-212 section was tested for comparison. The experimental data were compared with theoretical predictions. The tests were conducted at $M = 0.2$ and 0.3 at $Re = 1.0 \times 10^6$, 1.5×10^6 , and 1.9×10^6 and at $M = 0.4$ at $Re = 1.0 \times 10^6$, 1.9×10^6 , and 3.0×10^6 . The following results were established:

1. Increasing the upper-surface thickness over the forward 35 percent of the chord was nearly as effective as a drooped leading edge with an increased leading radius for increasing the maximum lift coefficient of the 64₁-212 section. Both modifications produced about 30 percent more maximum lift than the 64₁-212 profile.

2. The forward upper-surface modification did not incur the drag penalty of the drooped leading-edge modification at lift coefficients in the cruise range of most general aviation airplanes. The drag of the airfoil with upper-surface modification was equal to that of the 64₁-212 section at cruise conditions when both airfoils were tested with a mostly turbulent boundary layer.

3. The forward upper-surface modification produced nearly a 25-percent reduction in nose-down pitching moment compared with the unmodified 64₁-212 airfoil, whereas the drooped leading-edge modification showed approximately 30 percent more nosedown pitching moment than the 64₁-212.

4. Both types of forward contour modification produced less drag at moderate and high lift coefficients than the 64₁-212 airfoil, the drag of the profile having the upper-surface modification being less than that of the airfoil with a drooped leading edge at high lift coefficients. The lift/drag ratio of the airfoil with upper-surface modification was about 23 percent greater than that of the 64₁-212 airfoil at $M = 0.2$ and $Re = 1.9 \times 10^6$ at $c_l = 1.10$.

5. A comparison of experimental values of lift coefficient, pitching-moment coefficient, and pressure distributions with those calculated by a viscous-flow theory was acceptable at all test Mach numbers for angles of attack where the boundary layer remained attached. However, the drag prediction was poor for all test conditions. A new viscous theory under development should improve drag estimates considerably.

Further research will be done, aided by a numerical optimization program, to develop optimum forward upper-surface modifications since such contour modifications appear most promising for attaining high maximum lift coefficients, low cruise drag, and low pitching-moment coefficients.

Ames Research Center

National Aeronautics and Space Administration
Moffett Field, Calif., 94035, April 21, 1975

REFERENCES

1. Kelly, John A.: Effects of Modifications to the Leading-Edge Region on the Stalling Characteristics of the NACA 63₁-012 Airfoil Section. NACA TN 2228, 1950.
2. Anderson, Seth B.; Matteson, Fredrick H.; and Van Dyke, Rudolph D., Jr.: A Flight Investigation of the Effect of Leading-Edge Camber on the Aerodynamic Characteristics of a Swept-Wing Airplane. NACA RM A52L16a, 1953.
3. Demele, Fred A.; and Sutton, Fred B.: The Effects of Increasing the Leading-Edge Radius and Adding Forward Camber on the Aerodynamic Characteristics of a Wing with 35° of Sweepback. NACA RM A50K28a, 1951.
4. Goradia, Suresh H.; and Lyman, Victor: Laminar Stall Prediction and Estimation of $C_{L(max)}$. Journal of Aircraft, vol. 11, no. 9, Sept. 1974, pp. 528-536.
5. Wortman, F. X.: Design of Airfoils with High Lift at Low and Medium Subsonic Mach Numbers. Advisory Group for Aerospace Research and Development. Fluid Dynamics of Aircraft Stalling. AGARD CP 102, 1972.
6. Stevens, W. A.; Goradia, S. H.; and Braden, J. A.: Mathematical Model for Two-Dimensional Multi-Component Airfoils in Viscous Flow. NASA CR-1843, 1971.
7. Hicks, Raymond M.; and Vanderplaats, Garret N.: Design of Low-Speed Airfoils by Numerical Optimization. Paper 750524 presented at SAE Business Aircraft Meeting, Wichita, Kansas, April 1975.
8. Racisz, Stanley F.: Effects of Independent Variation of Mach Number and Reynolds Number on the Maximum Lift Coefficients of Four NACA 6-Series Airfoil Sections. NACA TN 2824, 1952.

TABLE 1.— NACA 64₁-212 AIRFOIL COORDINATES

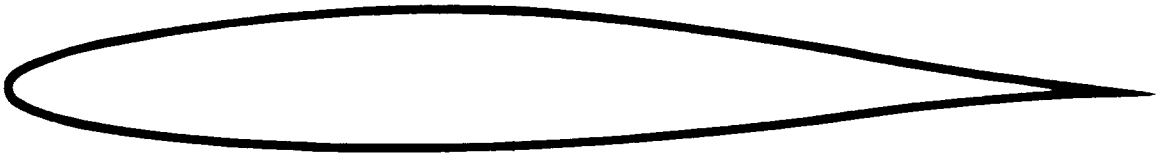
Upper surface		Lower surface	
x/c	y/c	x/c	y/c
0.00000	0.00000	0.00000	0.00000
.00418	.01025	.00582	-.00925
.00659	.01245	.00841	-.01105
.01147	.01593	.01353	-.01379
.02382	.02218	.02618	-.01846
.04868	.03123	.05132	-.02491
.07364	.03815	.07636	-.02967
.09865	.04386	.10135	-.03352
.14872	.05291	.15128	-.03945
.19886	.05968	.20114	-.04376
.24903	.06470	.25097	-.04680
.29921	.06815	.30079	-.04871
.34941	.07008	.35059	-.04948
.39961	.07052	.40039	-.04910
.44982	.06893	.45018	-.04703
.50000	.06583	.50000	-.04377
.55016	.06151	.54984	-.03961
.60029	.05619	.59971	-.03477
.65039	.05004	.64961	-.02944
.70045	.04322	.69955	-.02378
.75047	.03590	.74953	-.01800
.80045	.02825	.79955	-.01233
.85038	.02054	.84962	-.00708
.90027	.01303	.89973	-.00269
.95013	.00604	.94987	.00028
1.00000	.00000	1.00000	.00000

TABLE 2.— MOD. A AIRFOIL COORDINATES

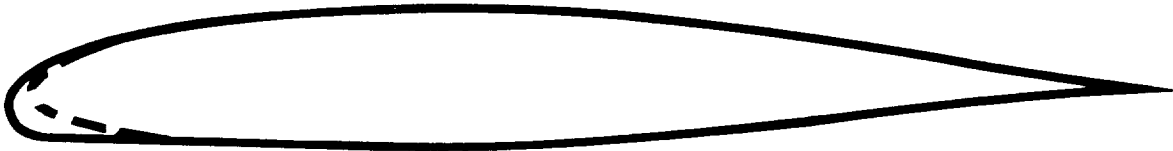
Upper surface		Lower surface	
x/c	y/c	x/c	y/c
-0.01850	-0.02000	-0.01850	-0.02000
-.01700	-.00600	-.01700	-.02680
-.01400	.00100	-.01400	-.03110
-.01000	.00650	-.01000	-.03450
-.00500	.01180	-.00500	-.03700
.00000	.01560	.00500	-.03900
.01000	.02200	.01500	-.03980
.02000	.02810	.04000	-.04060
.03000	.03250	.08000	-.04180
.04320	.03940	.12000	-.04300
.07364	.04650	.16000	-.04410
.09865	.05200	.20000	-.04540
.14872	.05880	.24000	-.04680
.19886	.06310	.30079	-.04871
.24903	.06640	.35059	-.04948
.29921	.06900	.40039	-.04910
.34941	.07008	.45018	-.04703
.39961	.07052	.50000	-.04377
.44982	.06893	.54984	-.03961
.50000	.06583	.59971	-.03477
.55016	.06151	.64961	-.02944
.60029	.05619	.69955	-.02378
.65039	.05004	.74953	-.01800
.70045	.04322	.79955	-.01233
.75047	.03590	.84962	-.00708
.80045	.02825	.89973	-.00269
.85038	.02054	.94987	.00028
.90027	.01303	1.00000	.00000
.95013	.00604		
1.00000	.00000		

TABLE 3.— MOD. B AIRFOIL COORDINATES

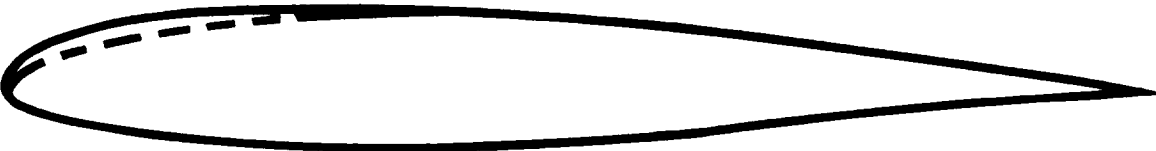
Upper surface		Lower surface	
x/c	y/c	x/c	y/c
0.00000	0.00000	0.00000	0.00000
.00418	.01640	.00582	-.00925
.00659	.01970	.00841	-.01105
.01147	.02500	.01353	-.01379
.02382	.03480	.02618	-.01846
.04868	.04820	.05132	-.02491
.07364	.05730	.07636	-.02967
.09865	.06310	.10135	-.03352
.14872	.06820	.15128	-.03945
.19886	.07000	.20114	-.04376
.24903	.07080	.25097	-.04680
.29921	.07100	.30079	-.04871
.34941	.07100	.35059	-.04948
.39961	.07052	.40039	-.04910
.44982	.06893	.45018	-.04703
.50000	.06583	.50000	-.04377
.55016	.06151	.54984	-.03961
.60029	.05619	.59971	-.03477
.65039	.05004	.64961	-.02944
.70045	.04322	.69955	-.02378
.75047	.03590	.74953	-.01800
.80045	.02825	.79955	-.01233
.85038	.02054	.84962	-.00708
.90027	.01303	.89973	-.00269
.95013	.00604	.94987	.00028
1.00000	.00000	1.00000	.00000



NACA 64₁ 212



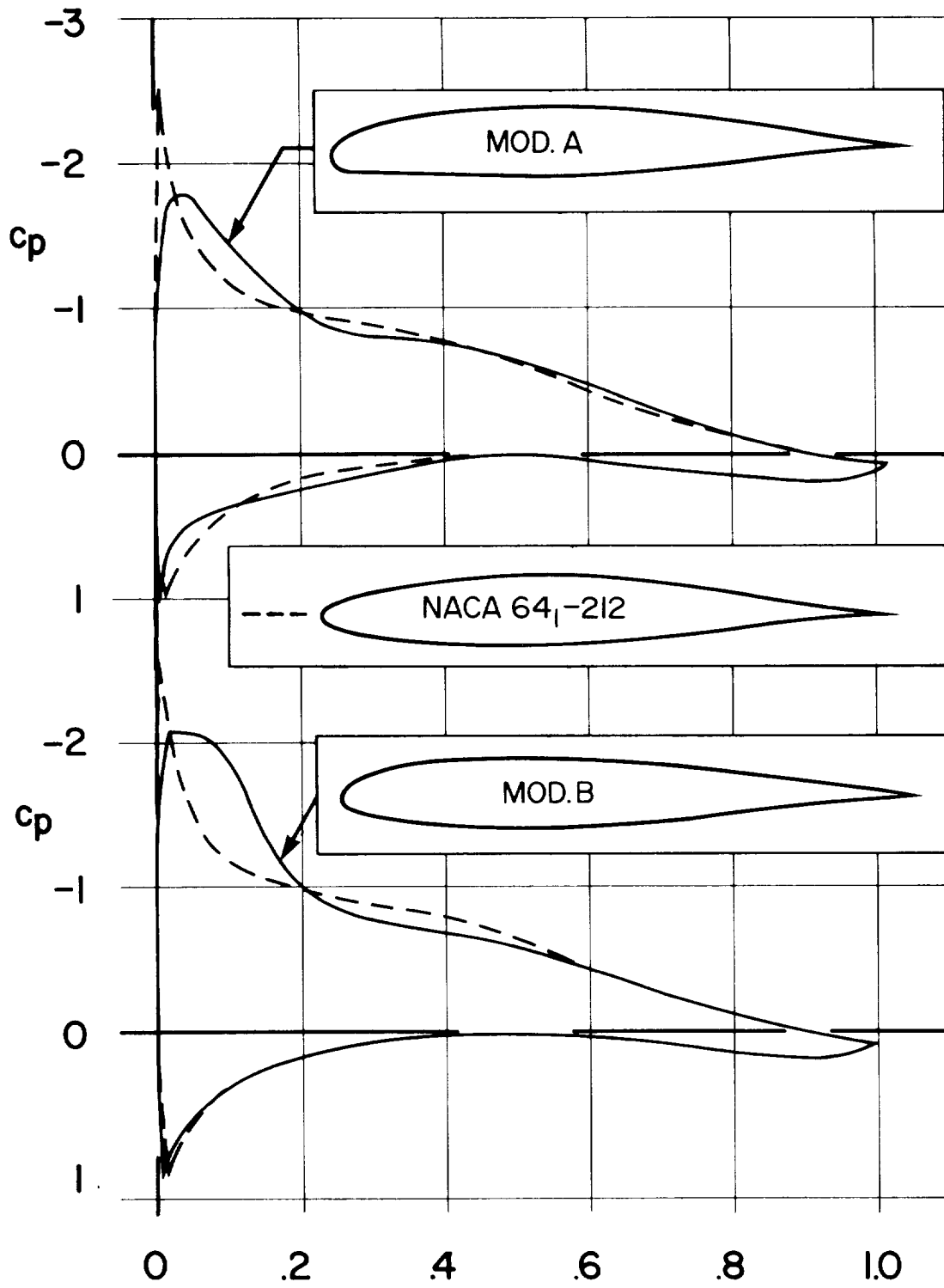
Mod. A



Mod. B

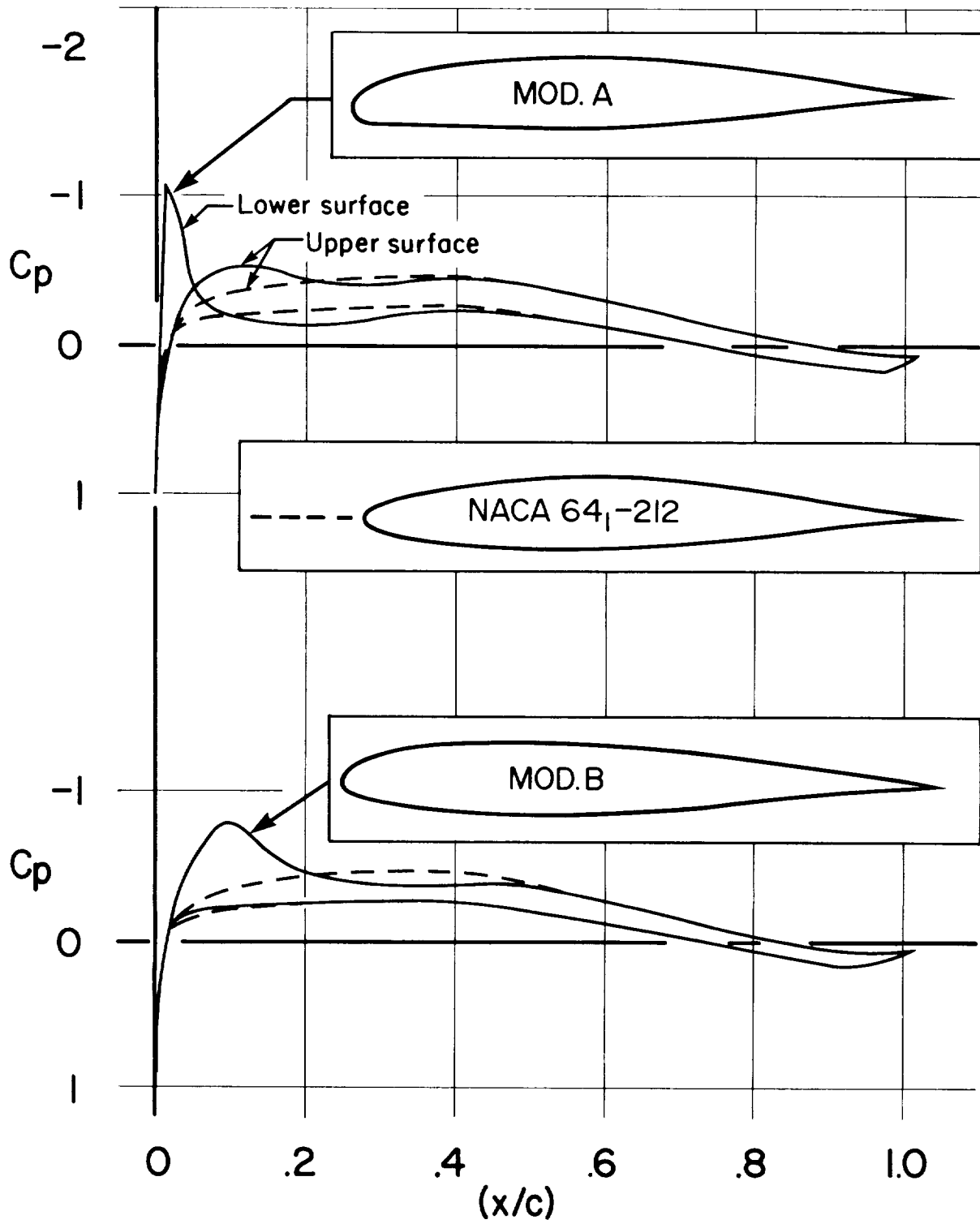
----- NACA 64₁-212

Figure 1.— Airfoil sections tested.



(a) $\alpha = 6^\circ$, $c_l \sim 0.75$.

Figure 2.— Theoretical pressure distributions for $M = 0.1$, $Re = 1.0 \times 10^6$.



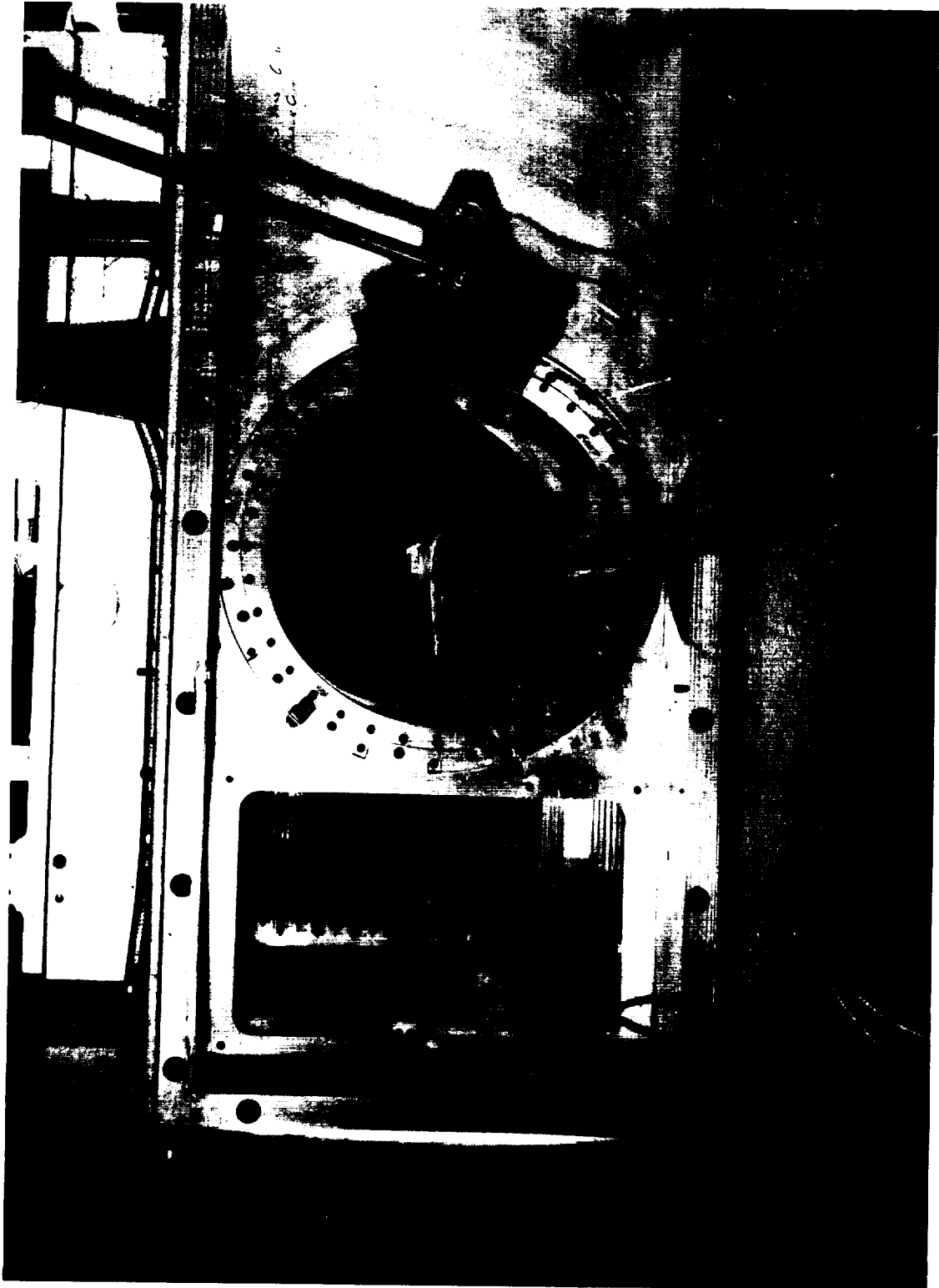
(b) $\alpha = 0^\circ$, $c_l \sim 0.15$.

Figure 2.— Concluded.



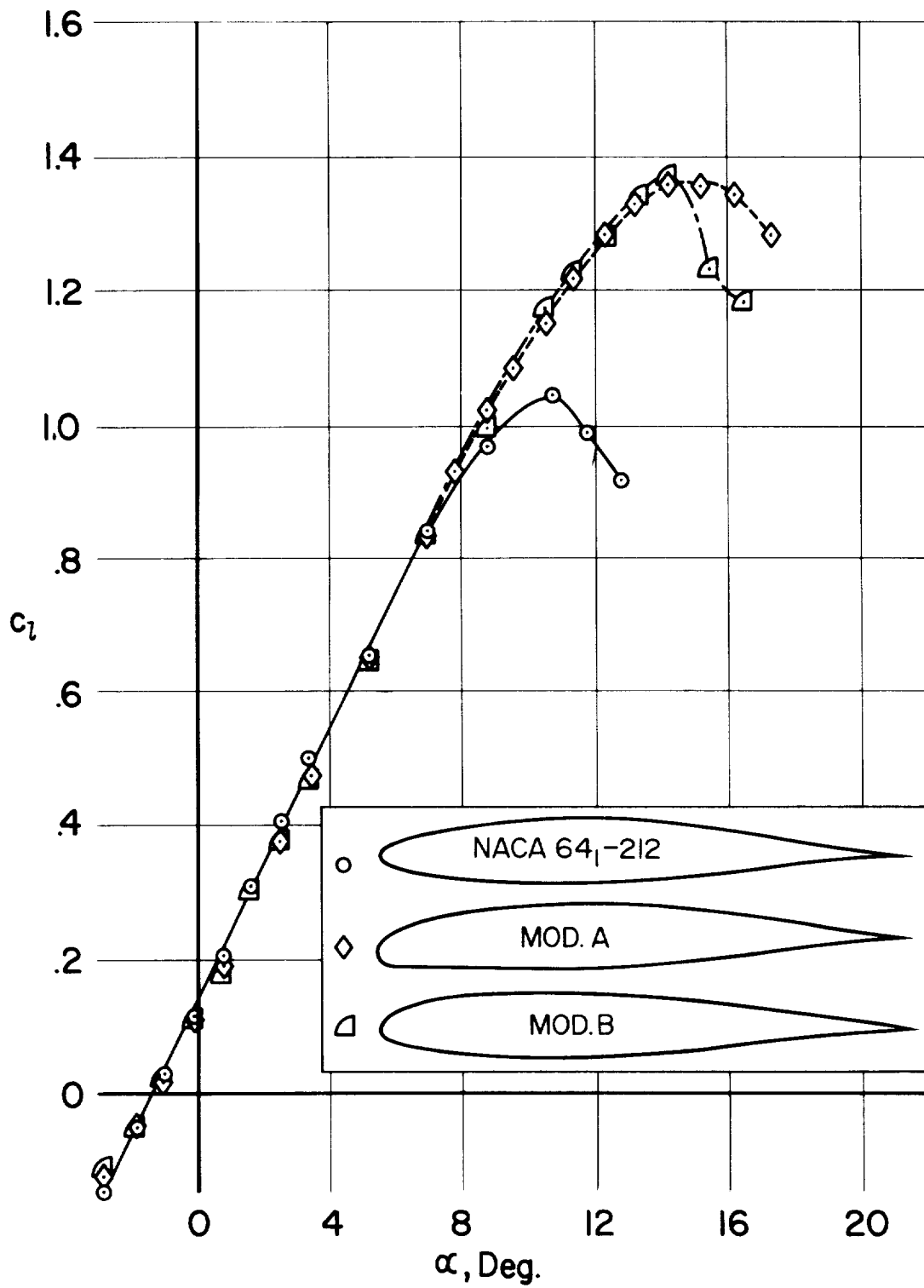
(a) Forward quarter view.

Figure 3. — Mod B airfoil installed in the Ames 2X2 Foot Wind Tunnel with wake rake.



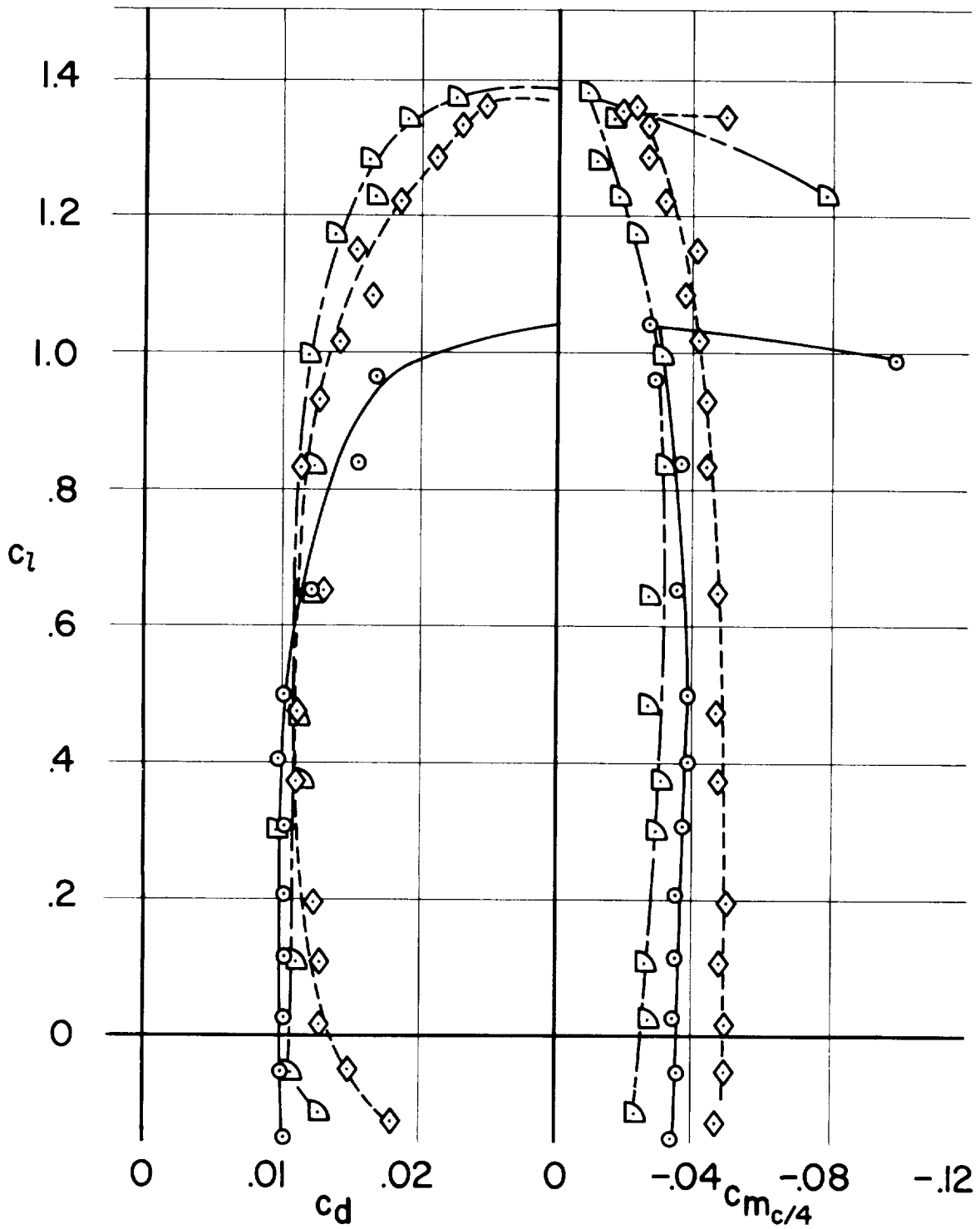
(b) Side view.

Figure 3.— Concluded.



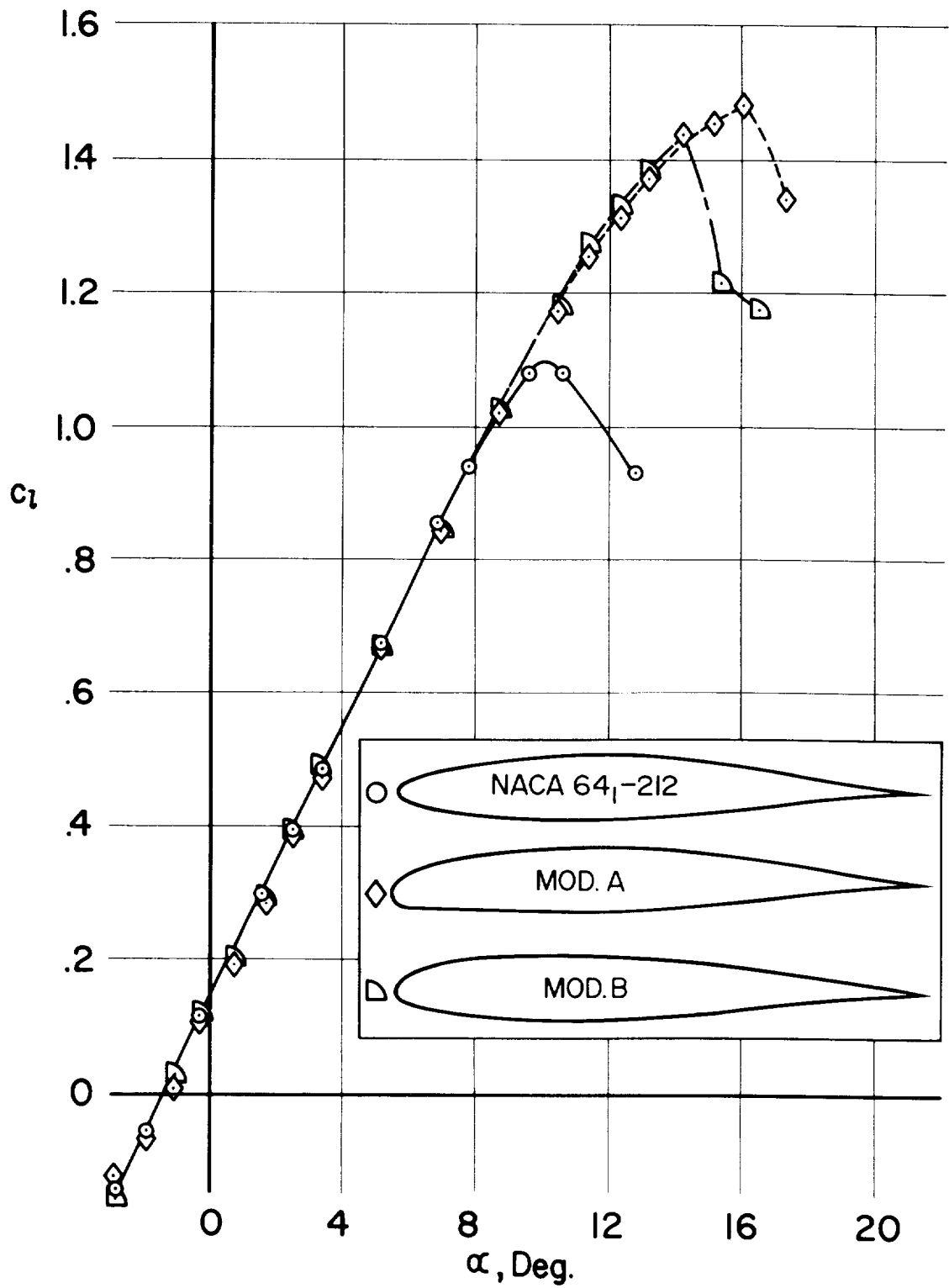
(a) $M = 0.2, Re = 1.0 \times 10^6$.

Figure 4.— Effect of airfoil contour modification on section characteristics, roughness at $0.12c$.



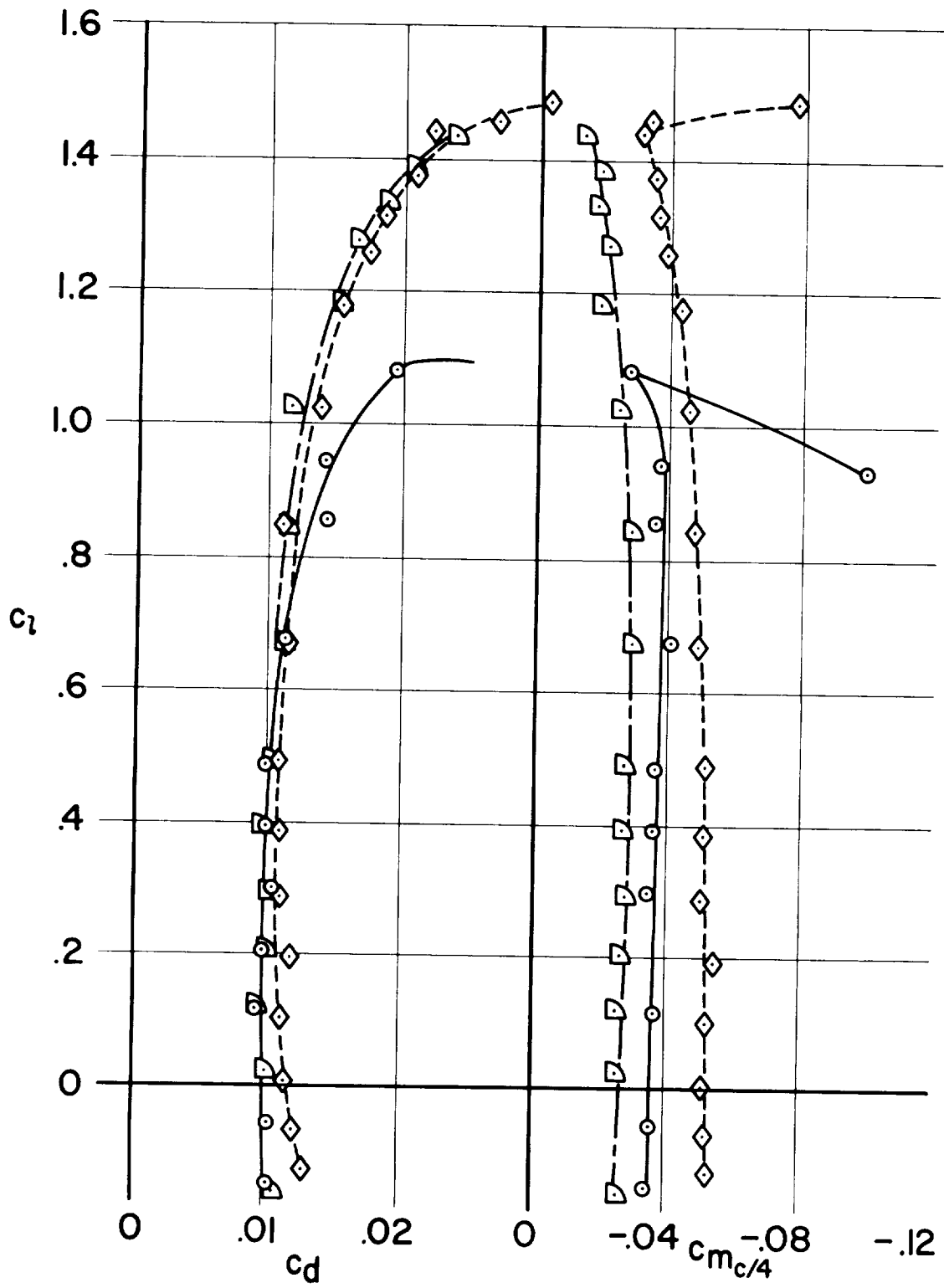
(a) $M = 0.2, Re = 1.0 \times 10^6$ - Concluded.

Figure 4.- Continued.



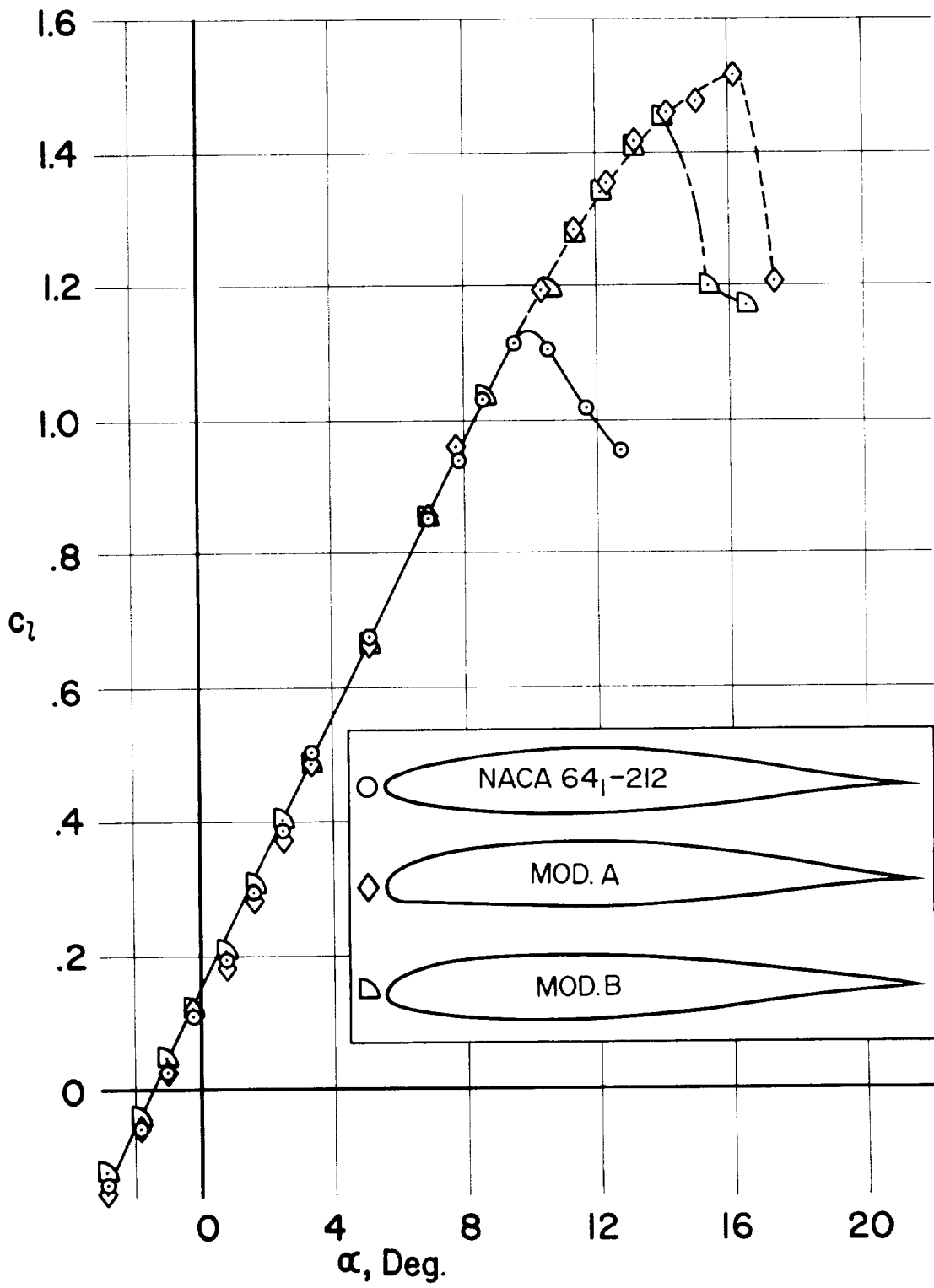
(b) $M = 0.2, Re = 1.5 \times 10^6$.

Figure 4.— Continued.



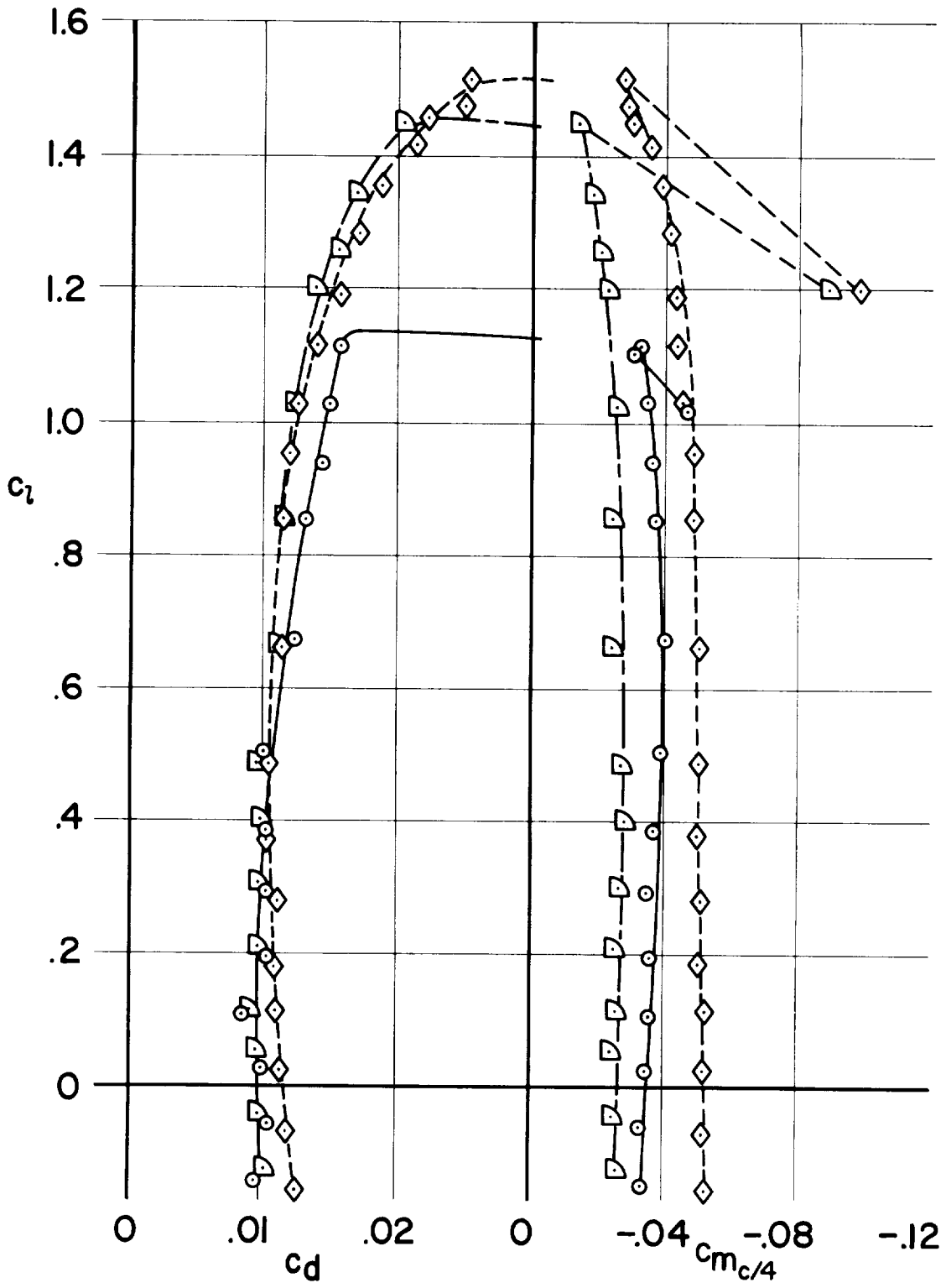
(b) $M = 0.2, Re = 1.5 \times 10^6$ - Concluded.

Figure 4.- Continued.



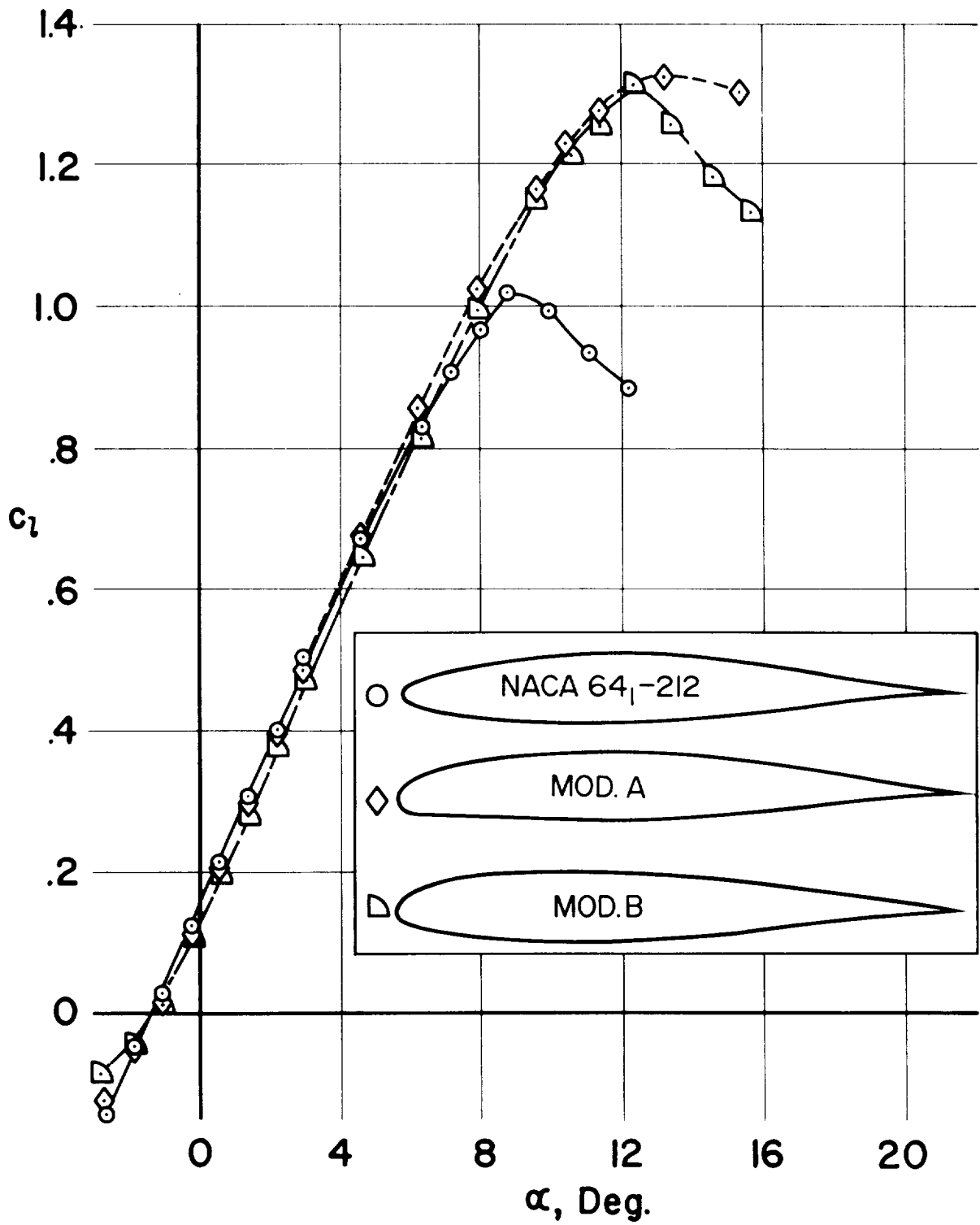
(c) $M = 0.2, Re = 1.9 \times 10^6$.

Figure 4.— Continued.



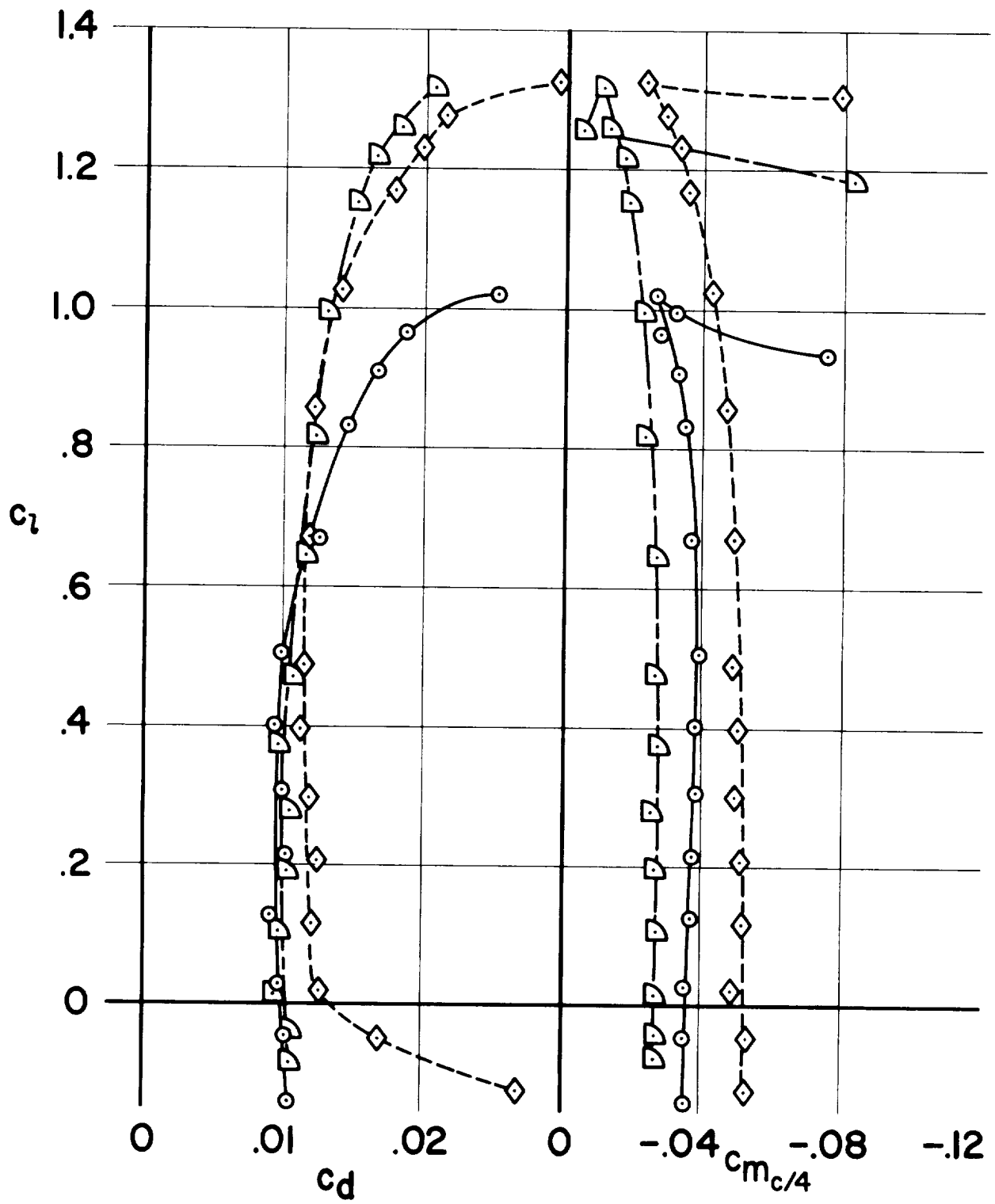
(c) $M = 0.2, Re = 1.9 \times 10^6$ - Concluded.

Figure 4.- Continued.



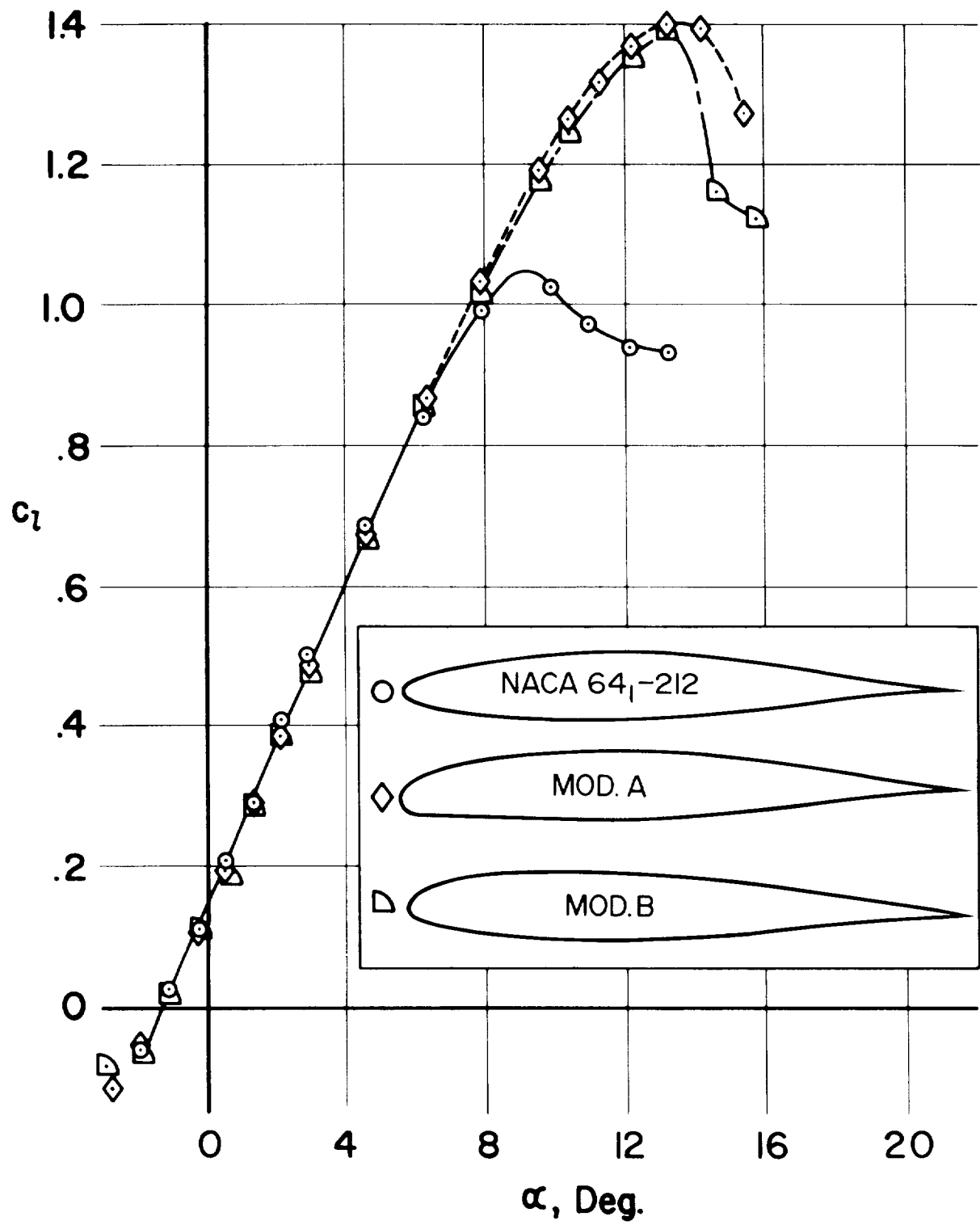
(d) $M = 0.3, Re = 1.0 \times 10^6$.

Figure 4.— Continued.



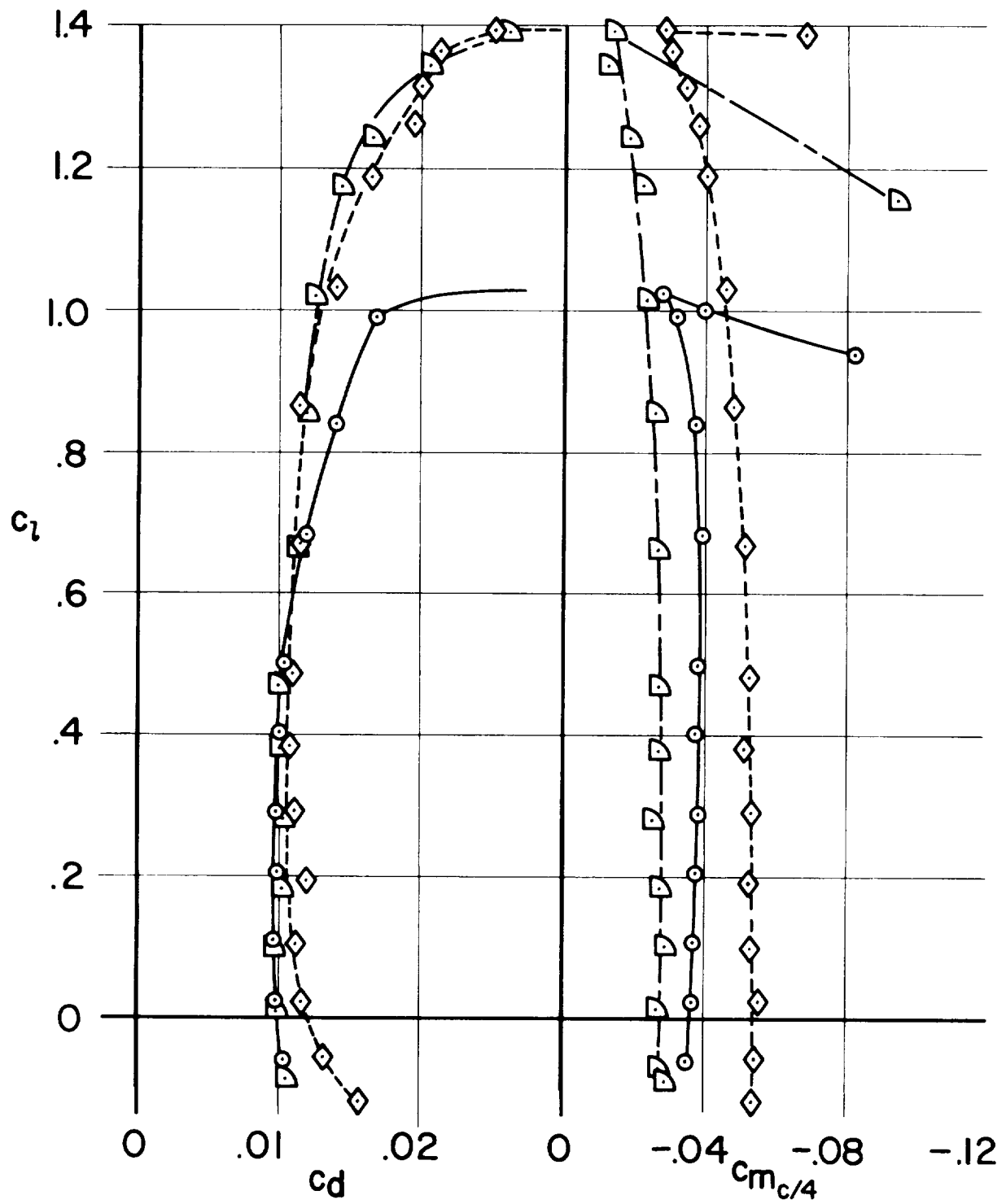
(d) $M = 0.3, Re = 1.0 \times 10^6$ - Concluded.

Figure 4.— Continued.



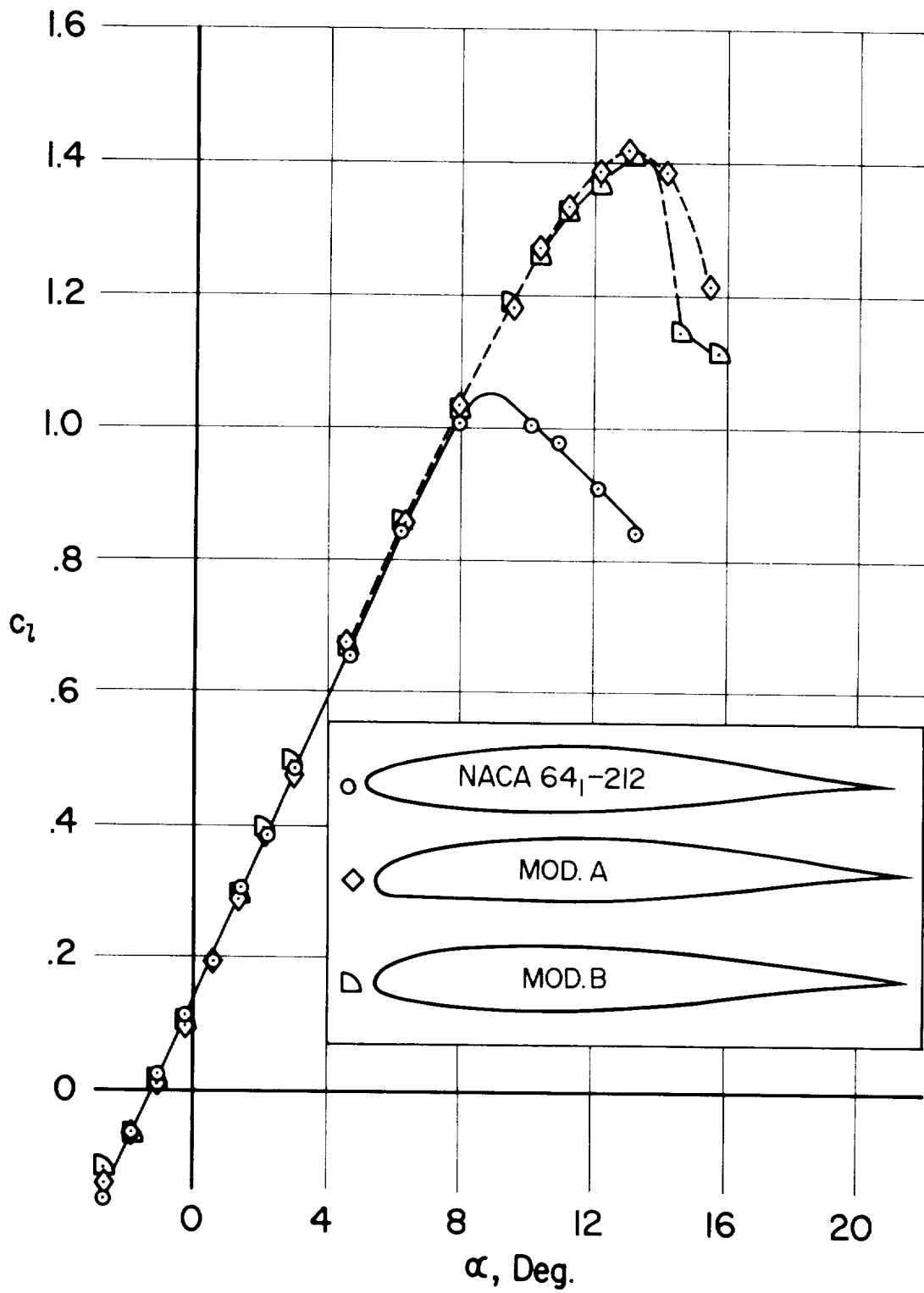
(e) $M = 0.3, Re = 1.5 \times 10^6$.

Figure 4.— Continued.



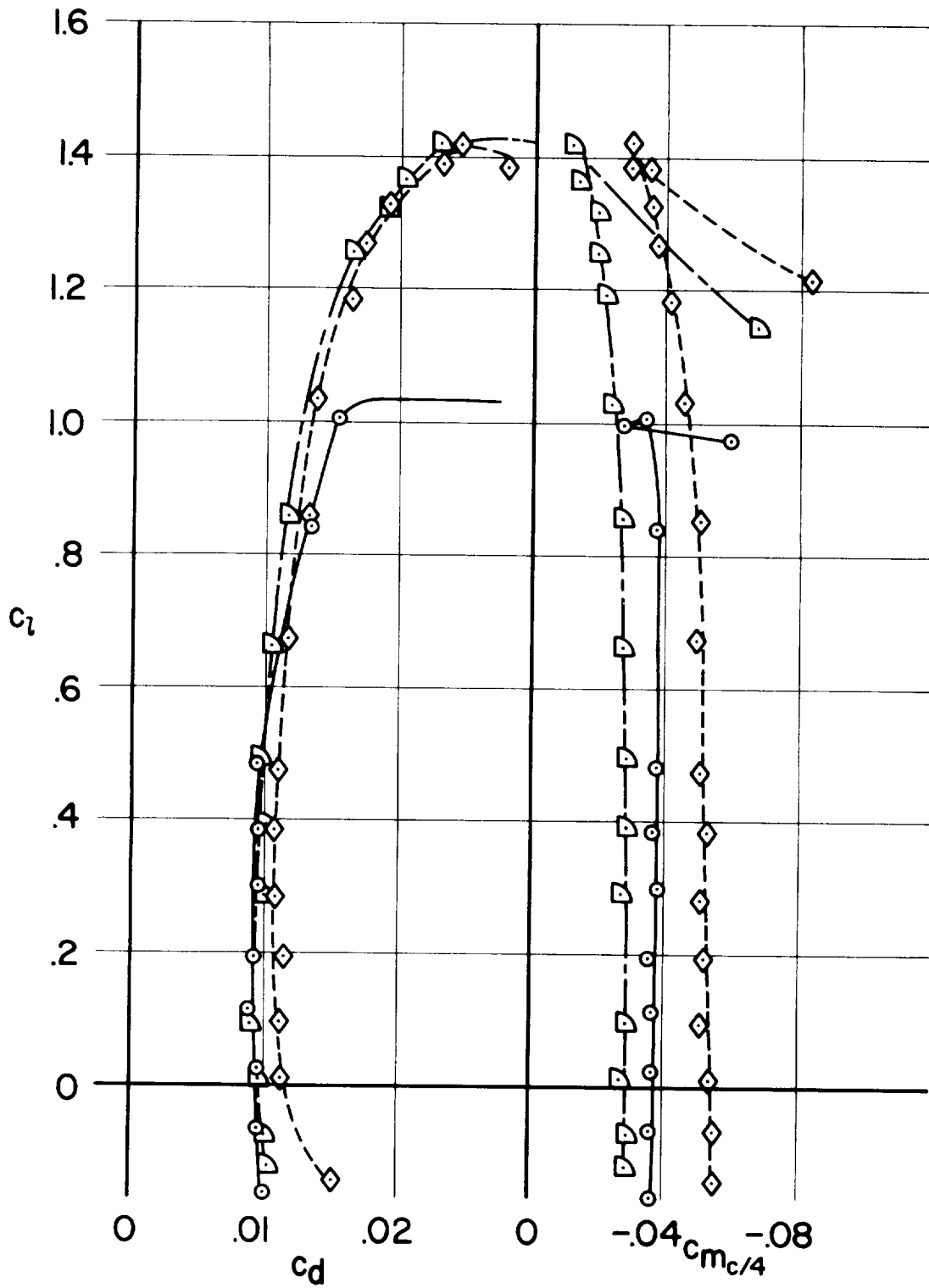
(e) $M = 0.3, Re = 1.5 \times 10^6$ - Concluded.

Figure 4. - Continued.



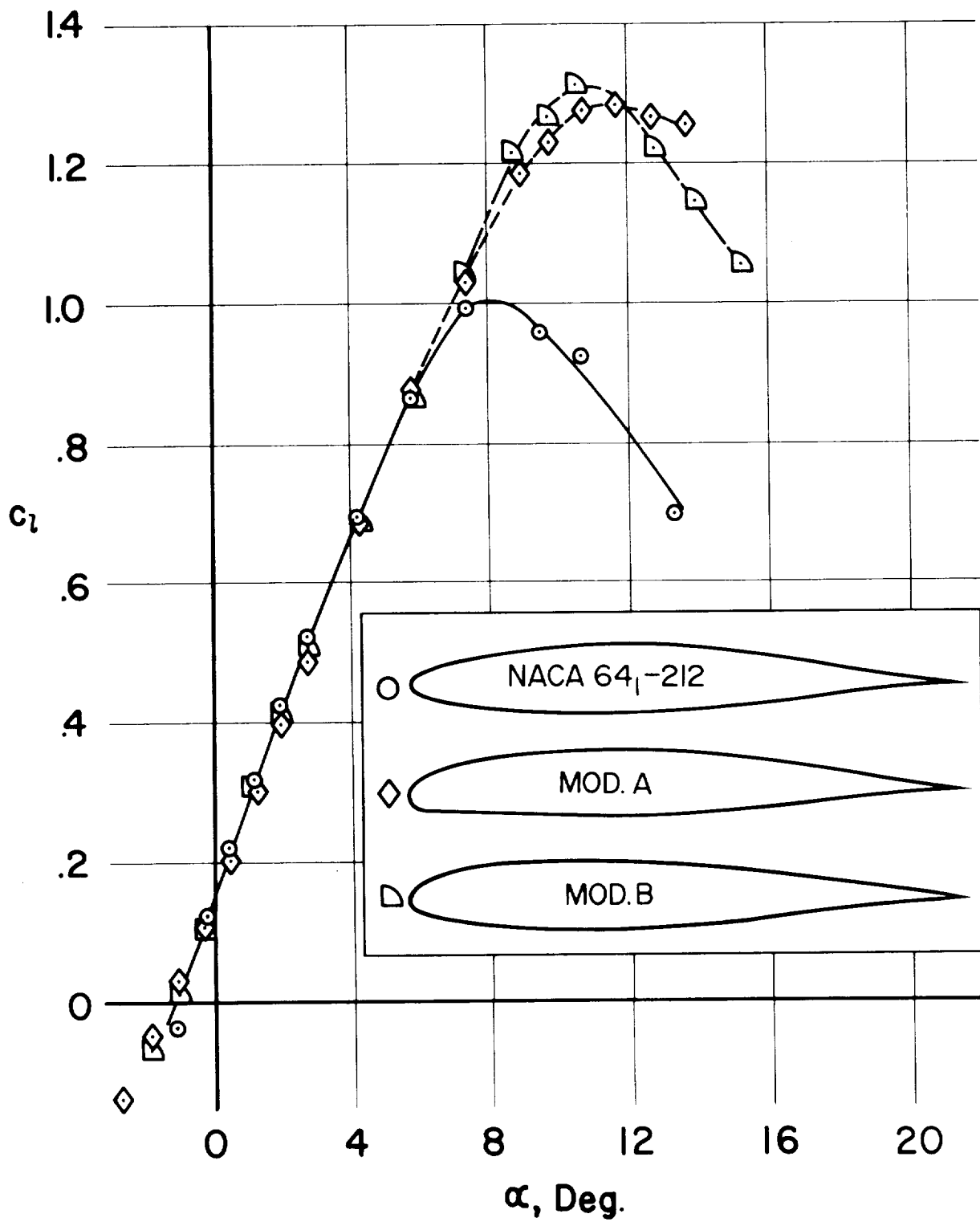
(f) $M = 0.3, Re = 1.9 \times 10^6$.

Figure 4.— Continued.



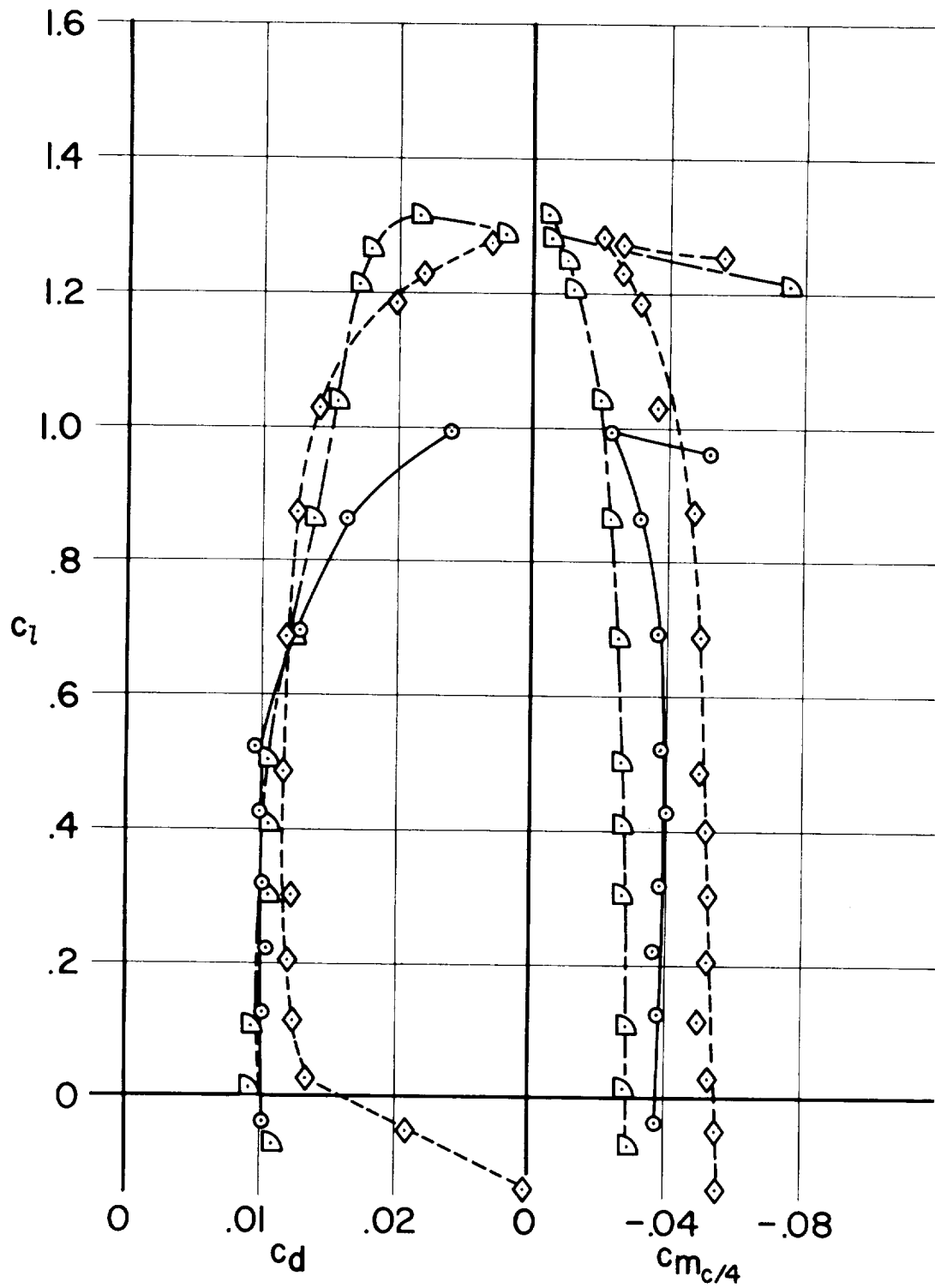
(f) $M = 0.3, Re = 1.9 \times 10^6$ - Concluded.

Figure 4.- Continued.



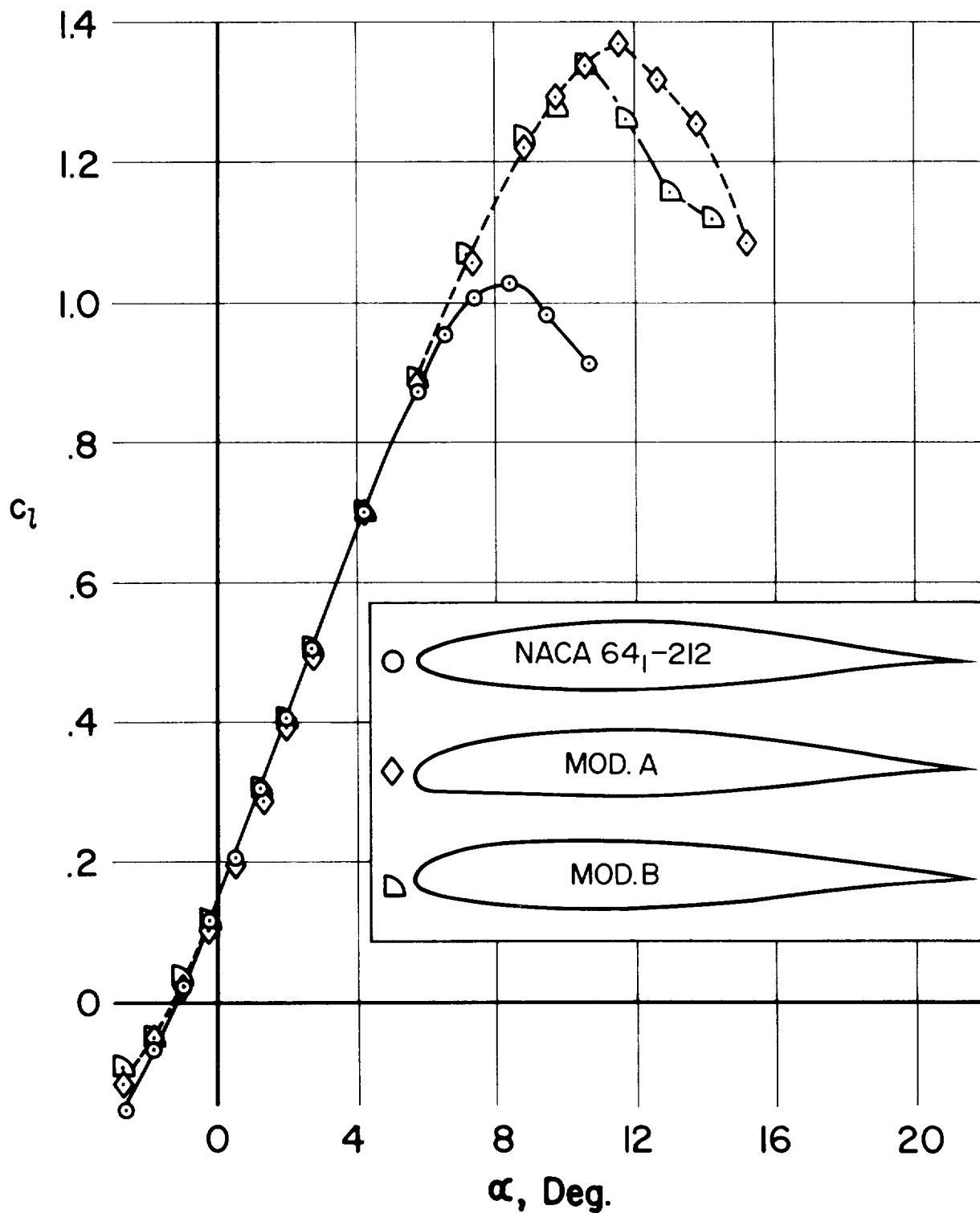
(g) $M = 0.4, Re = 1.0 \times 10^6$.

Figure 4.— Continued.



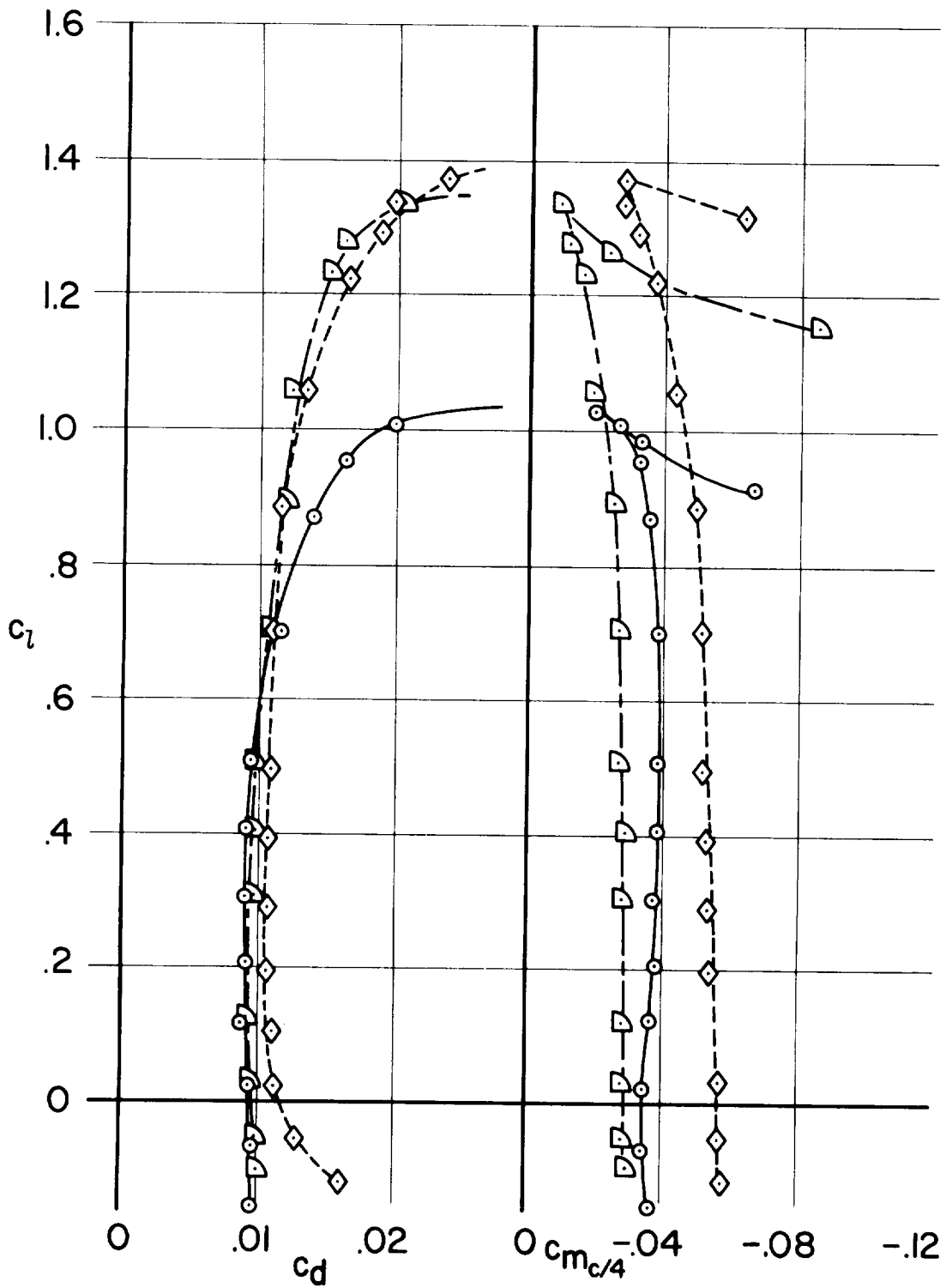
(g) $M = 0.4, Re = 1.0 \times 10^6$ - Concluded.

Figure 4.- Continued.



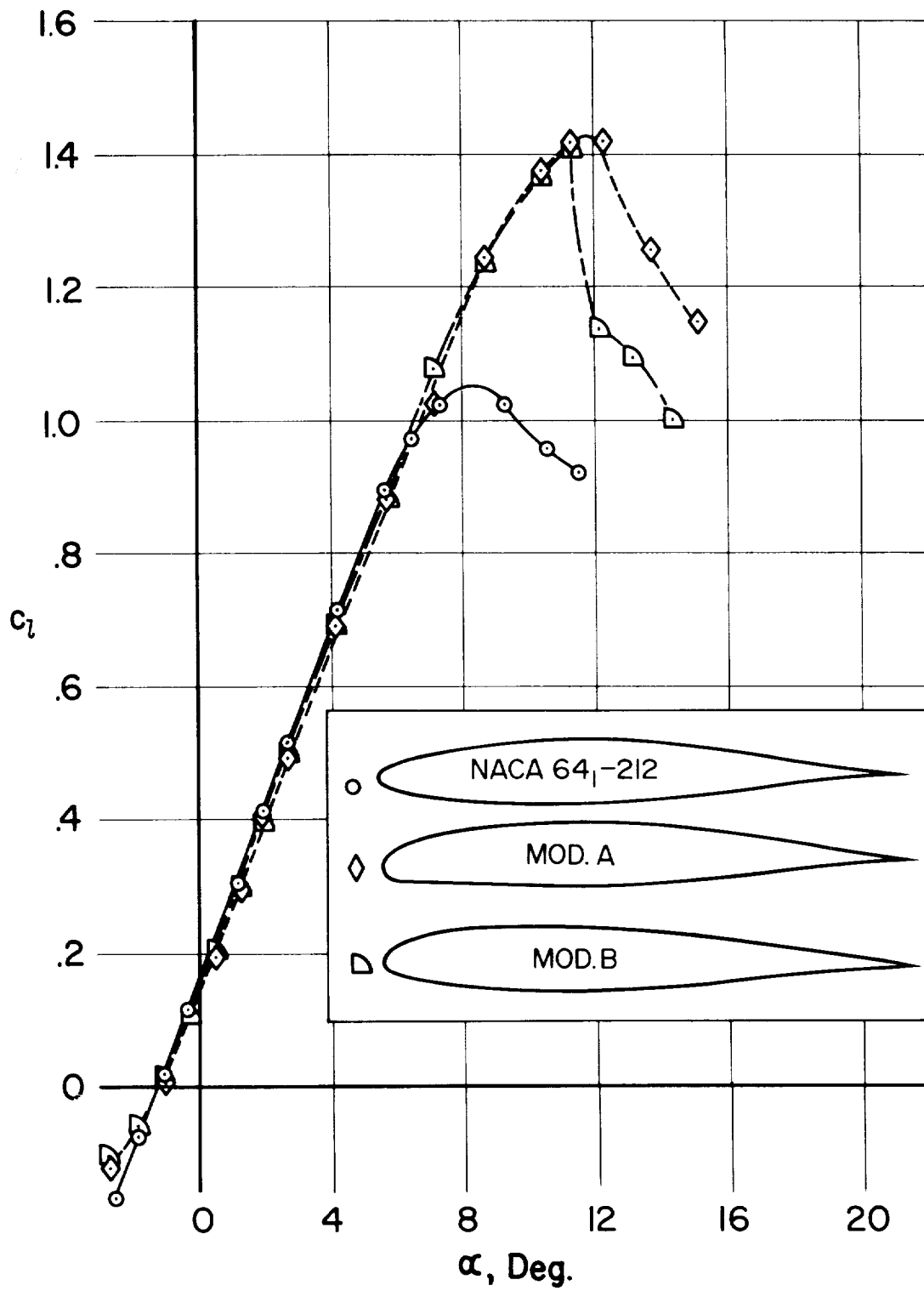
(h) $M = 0.4, Re = 1.9 \times 10^6$.

Figure 4.— Continued.



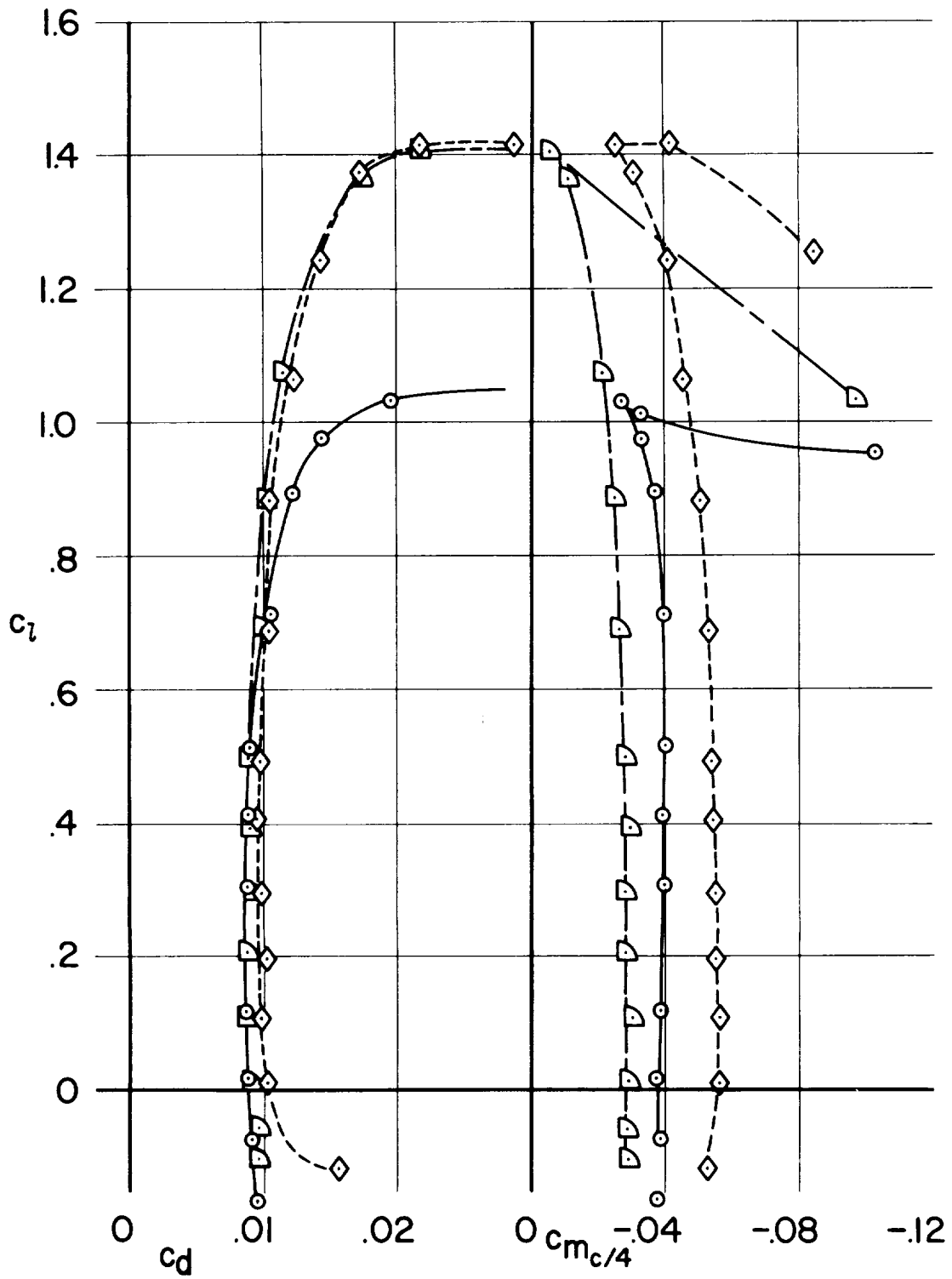
(h) $M = 0.4, Re = 1.9 \times 10^6$ - Concluded.

Figure 4.- Continued.



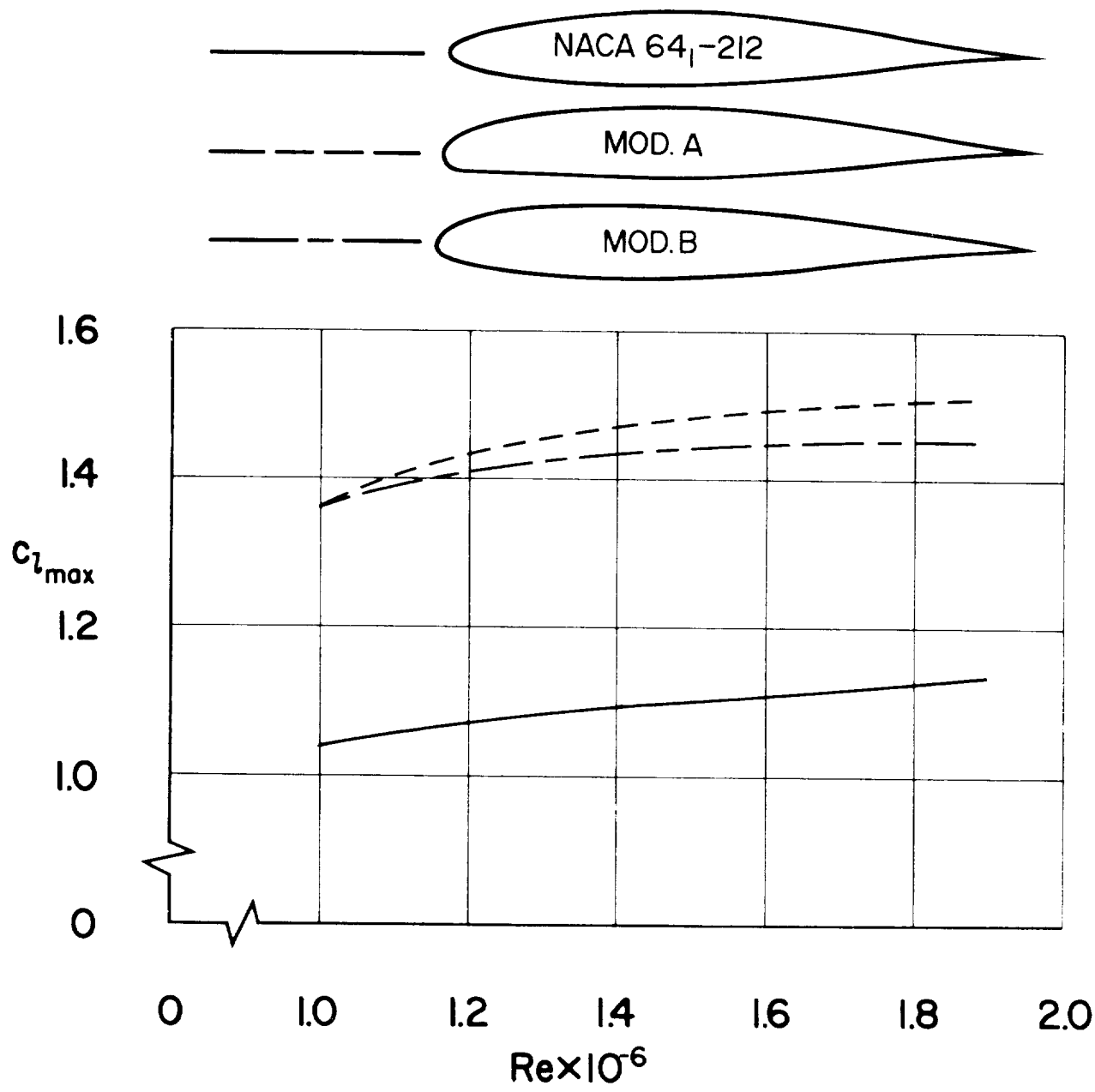
(i) $M = 0.4, Re = 3 \times 10^6$.

Figure 4.- Continued.



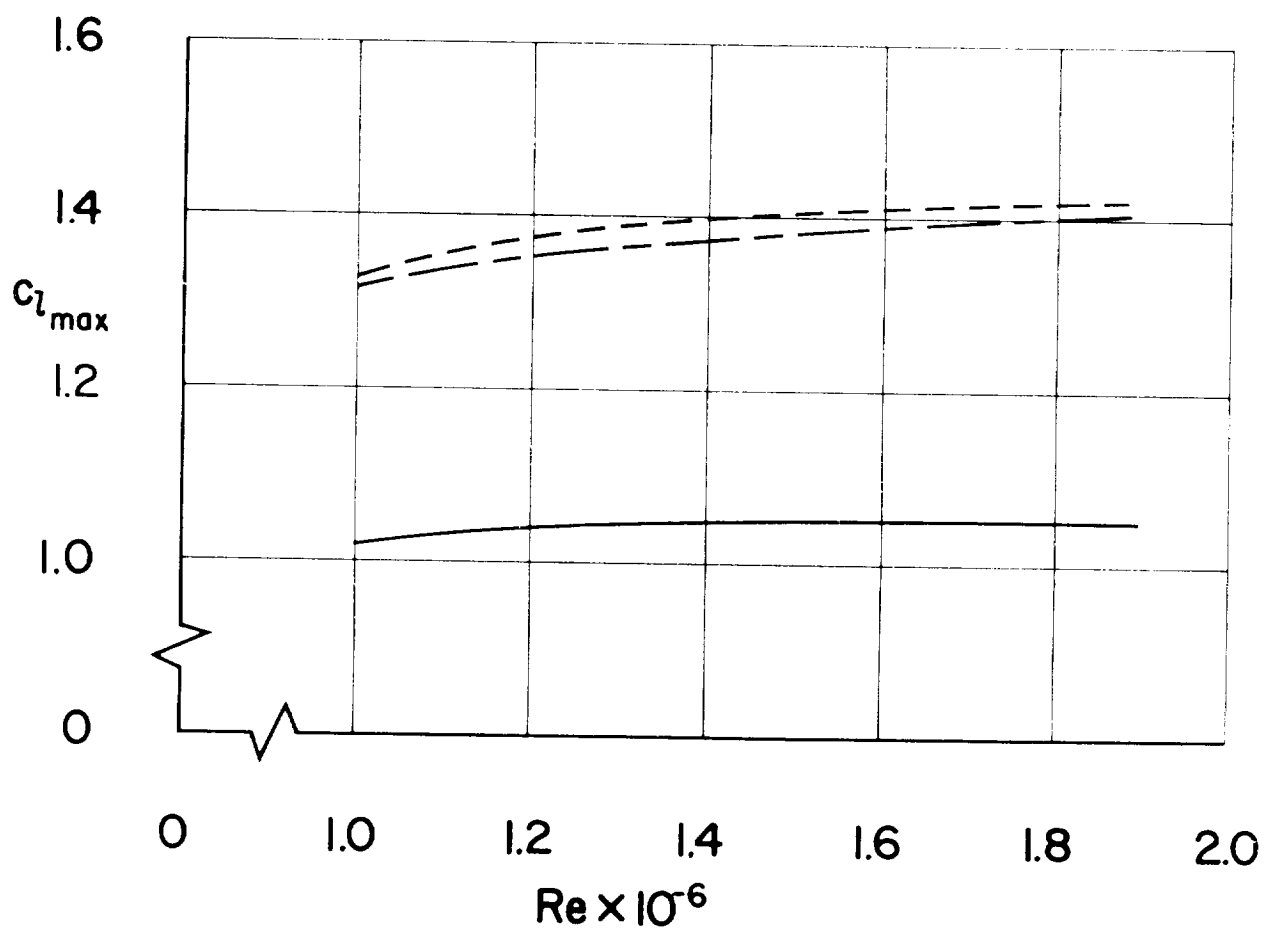
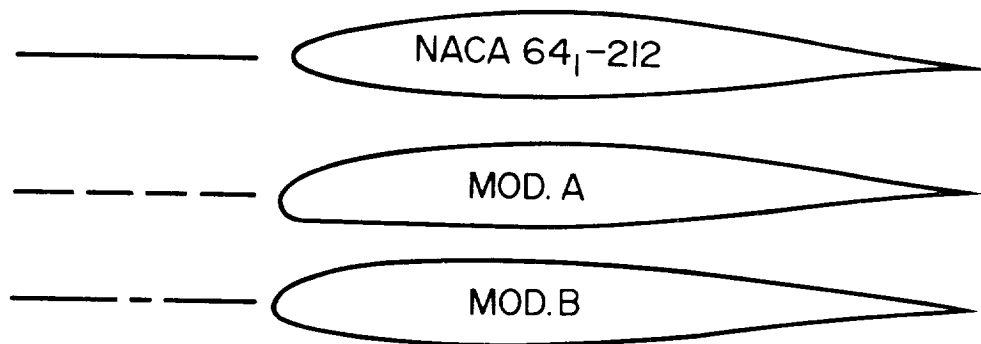
(i) $M = 0.4, Re = 3.0 \times 10^6$ - Concluded.

Figure 4.- Concluded.



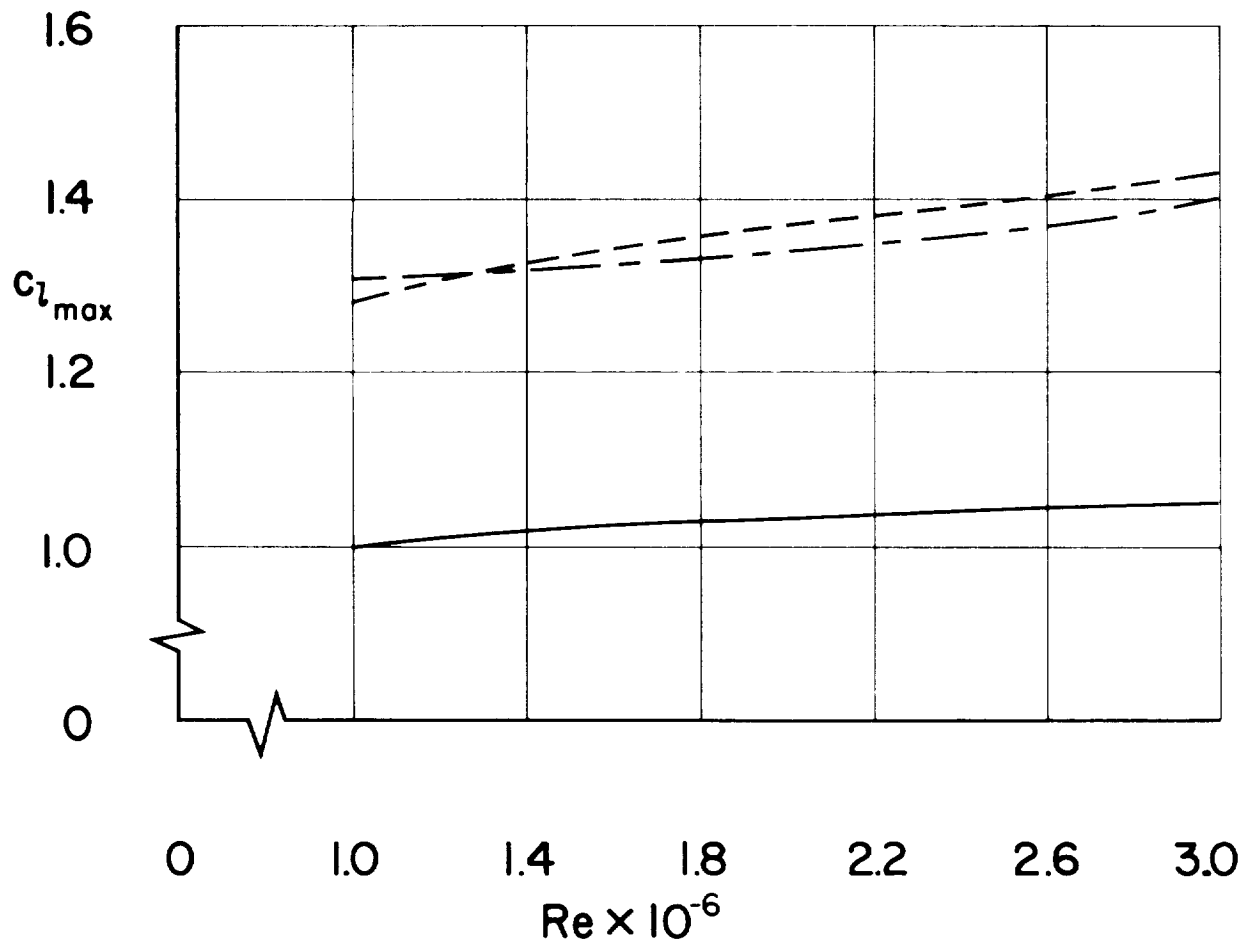
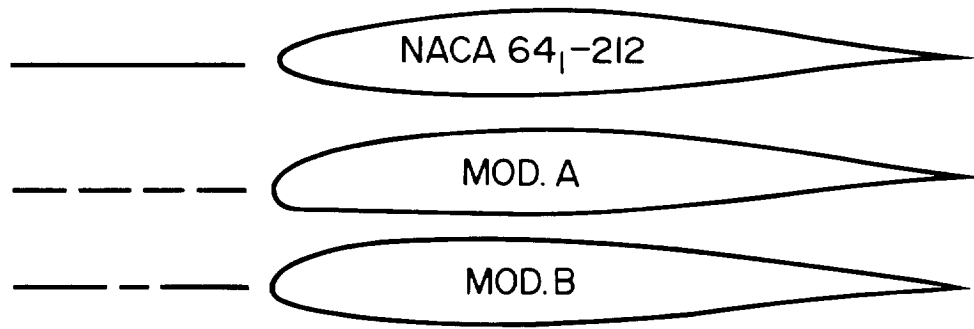
(a) $M = 0.2$.

Figure 5.— Effect of airfoil contour modification on maximum lift coefficient, roughness at $0.12c$.



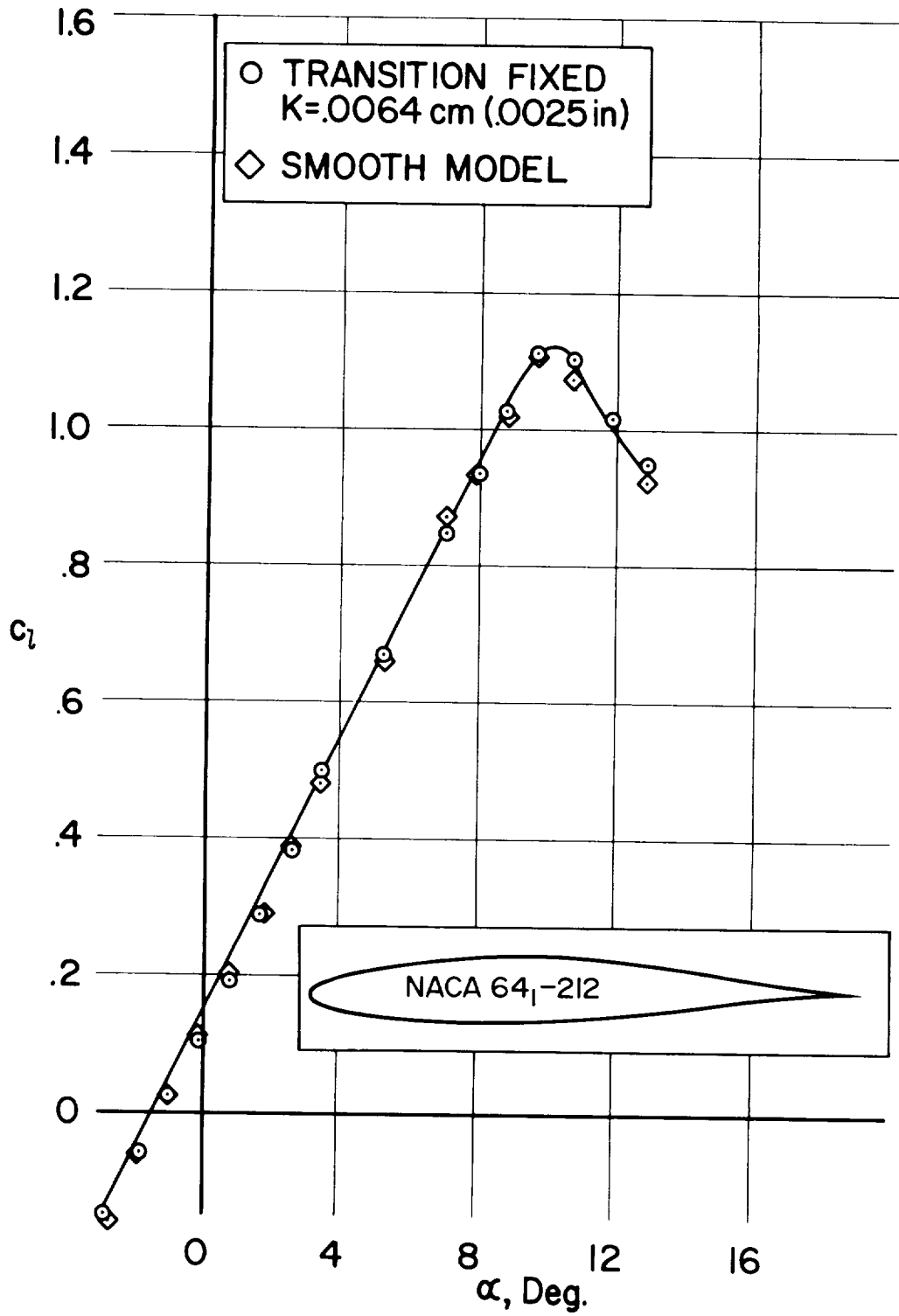
(b) $M = 0.3$.

Figure 5.— Continued.



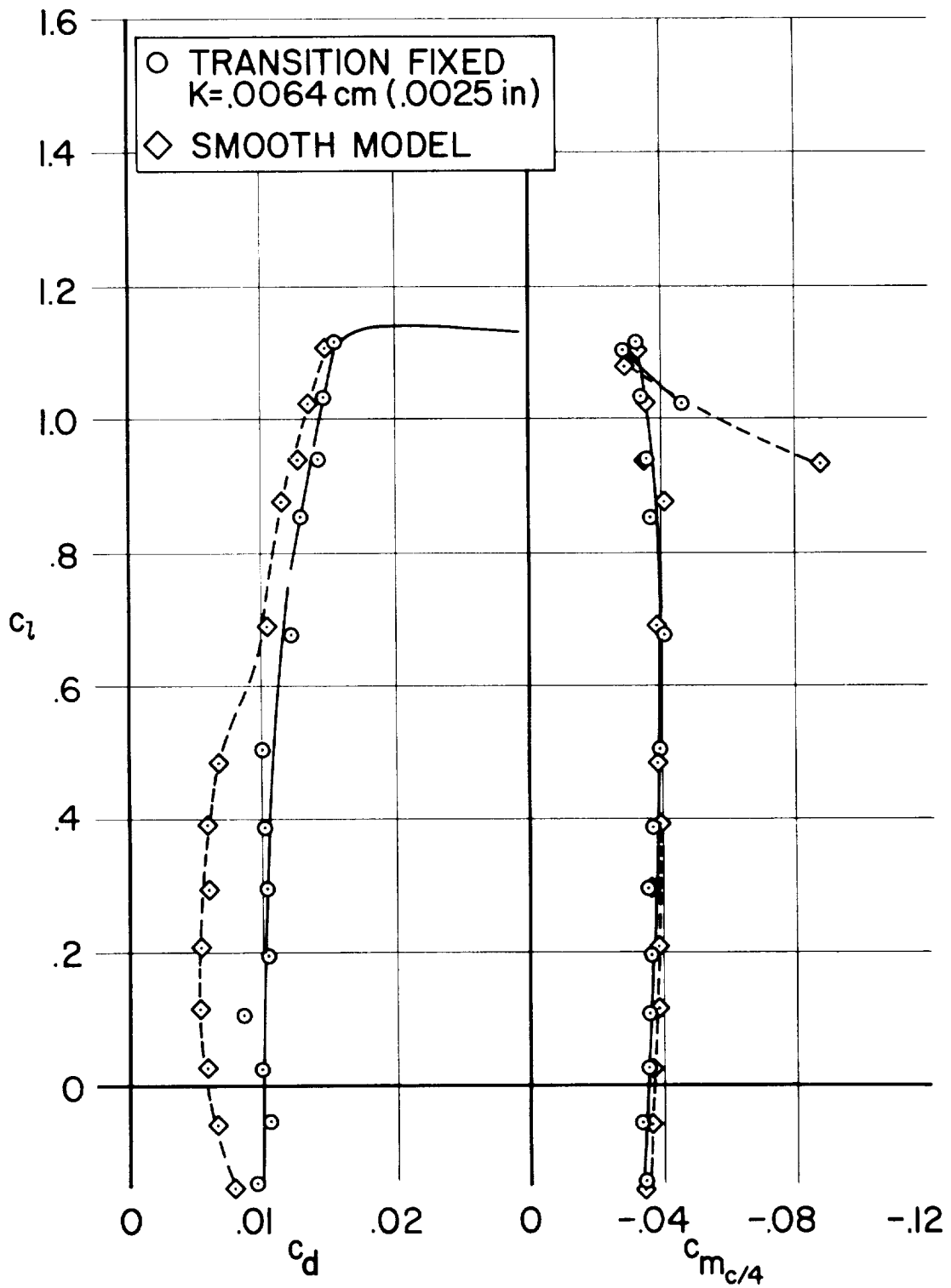
(c) $M = 0.4$.

Figure 5.— Concluded.



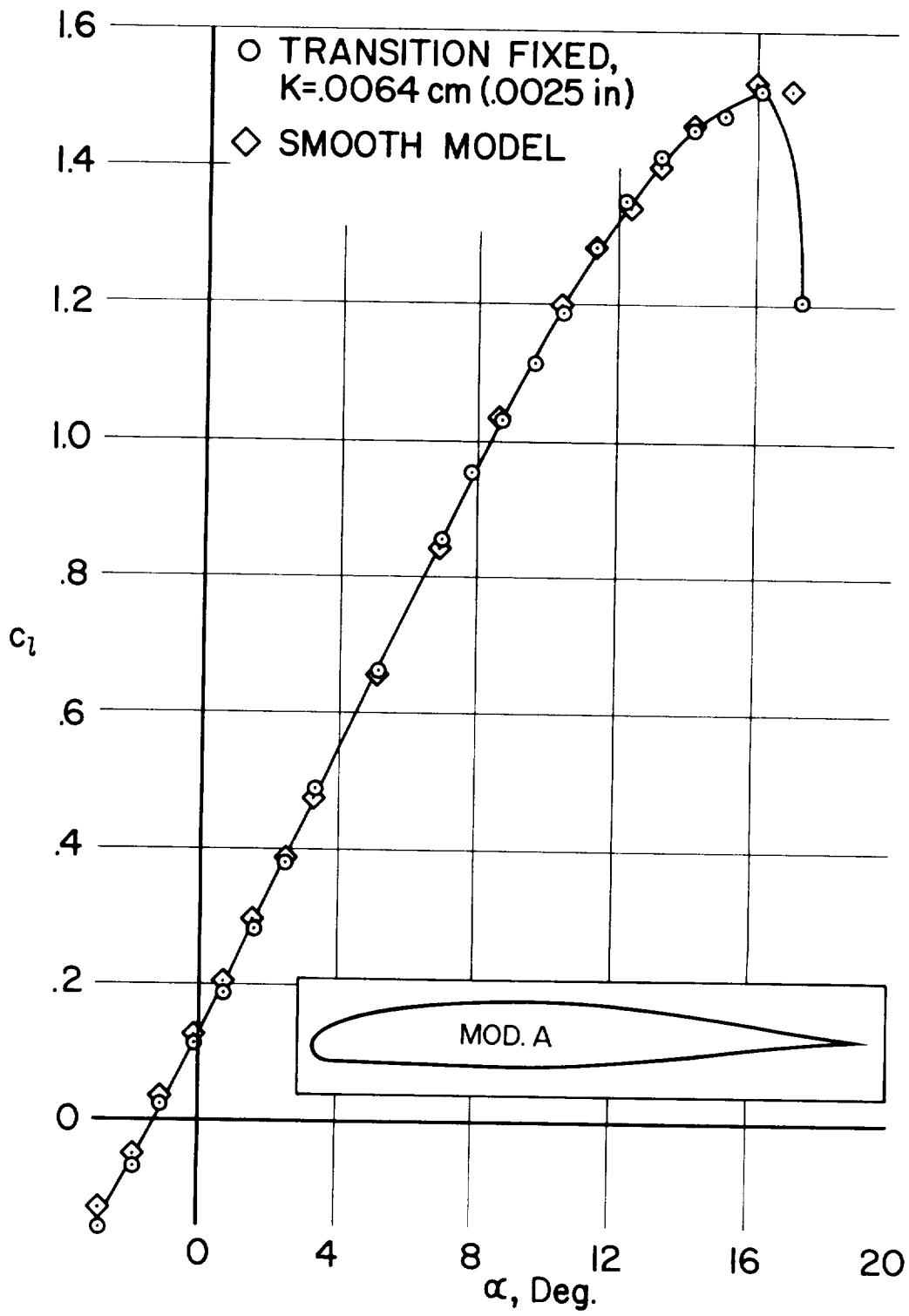
(a) NACA 64₁-212.

Figure 6.— Effect of roughness on section characteristics; $M = 0.2$, $Re = 1.9 \times 10^6$.



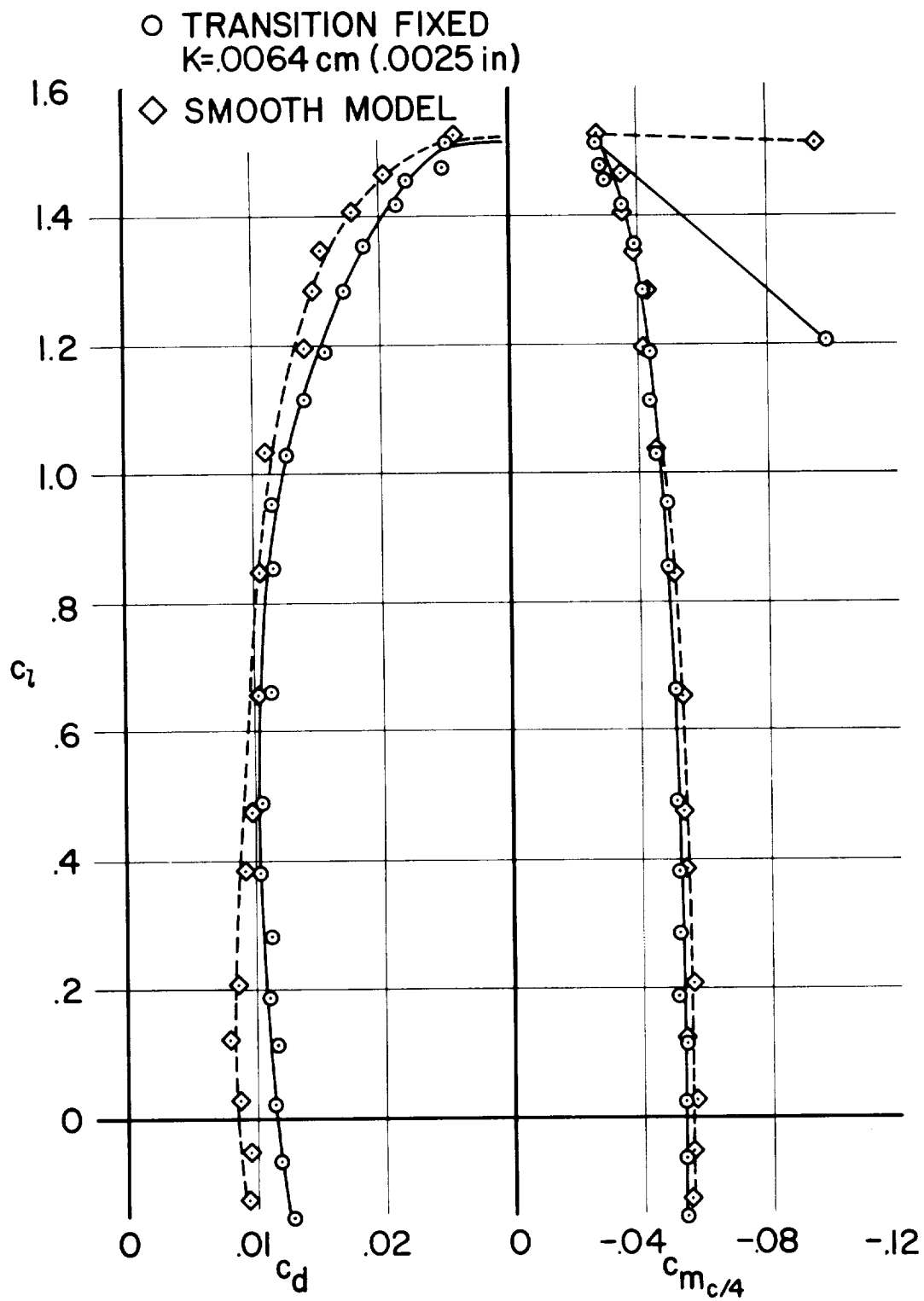
(a) NACA 64₁-212 - Concluded.

Figure 6.- Continued.



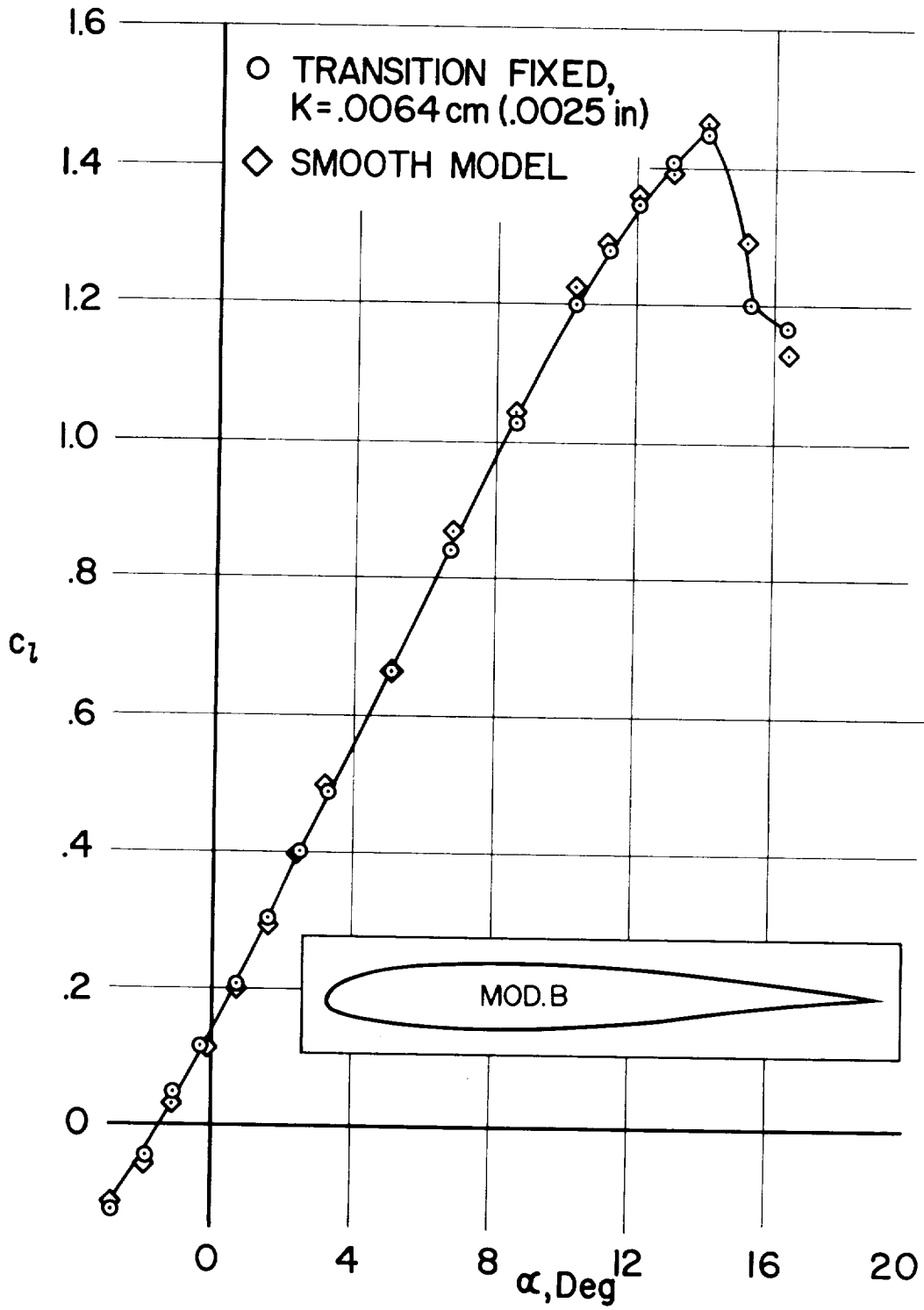
(b) Mod. A.

Figure 6.— Continued.



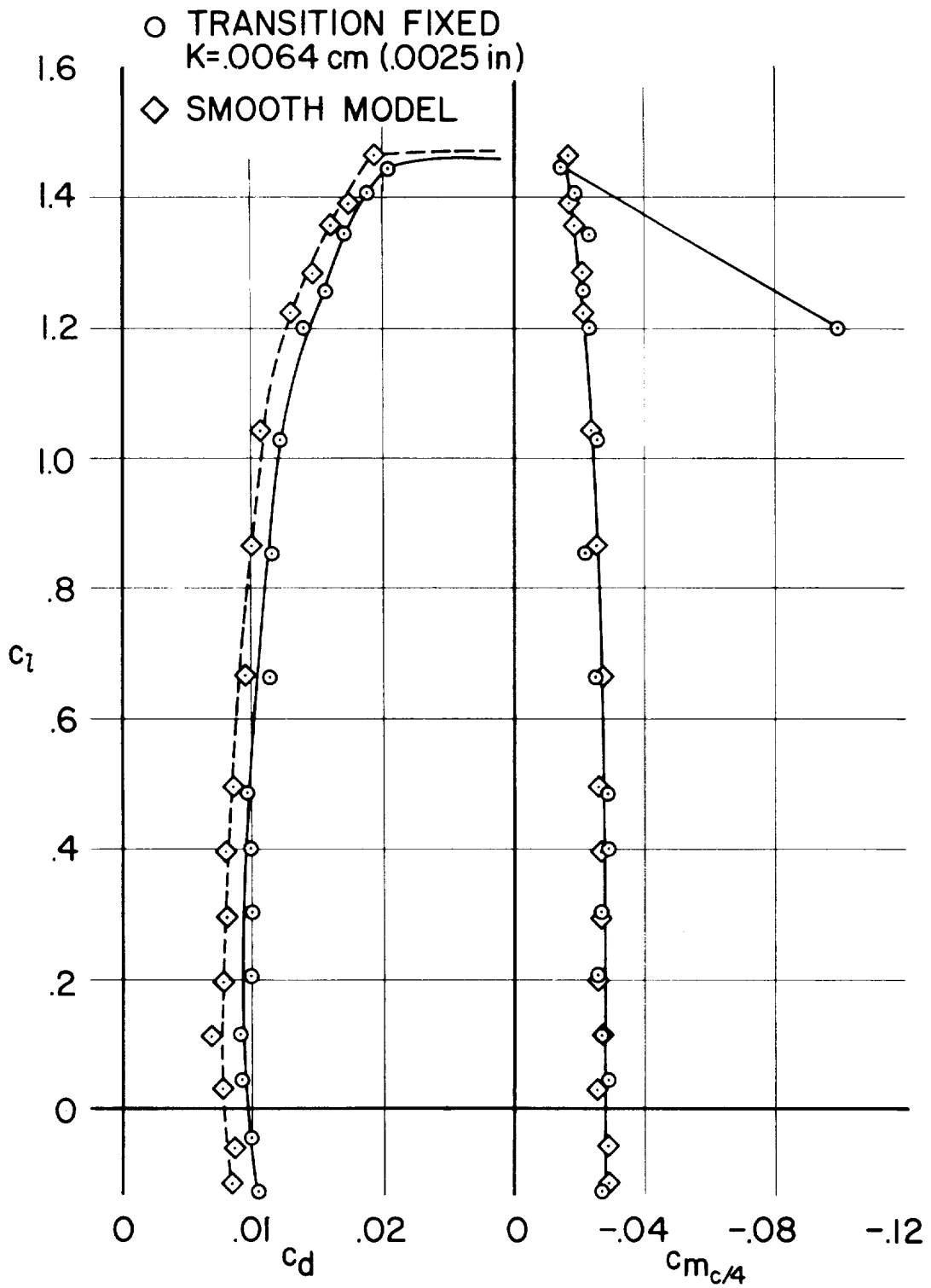
(b) Mod. A - Concluded.

Figure 6.— Continued.



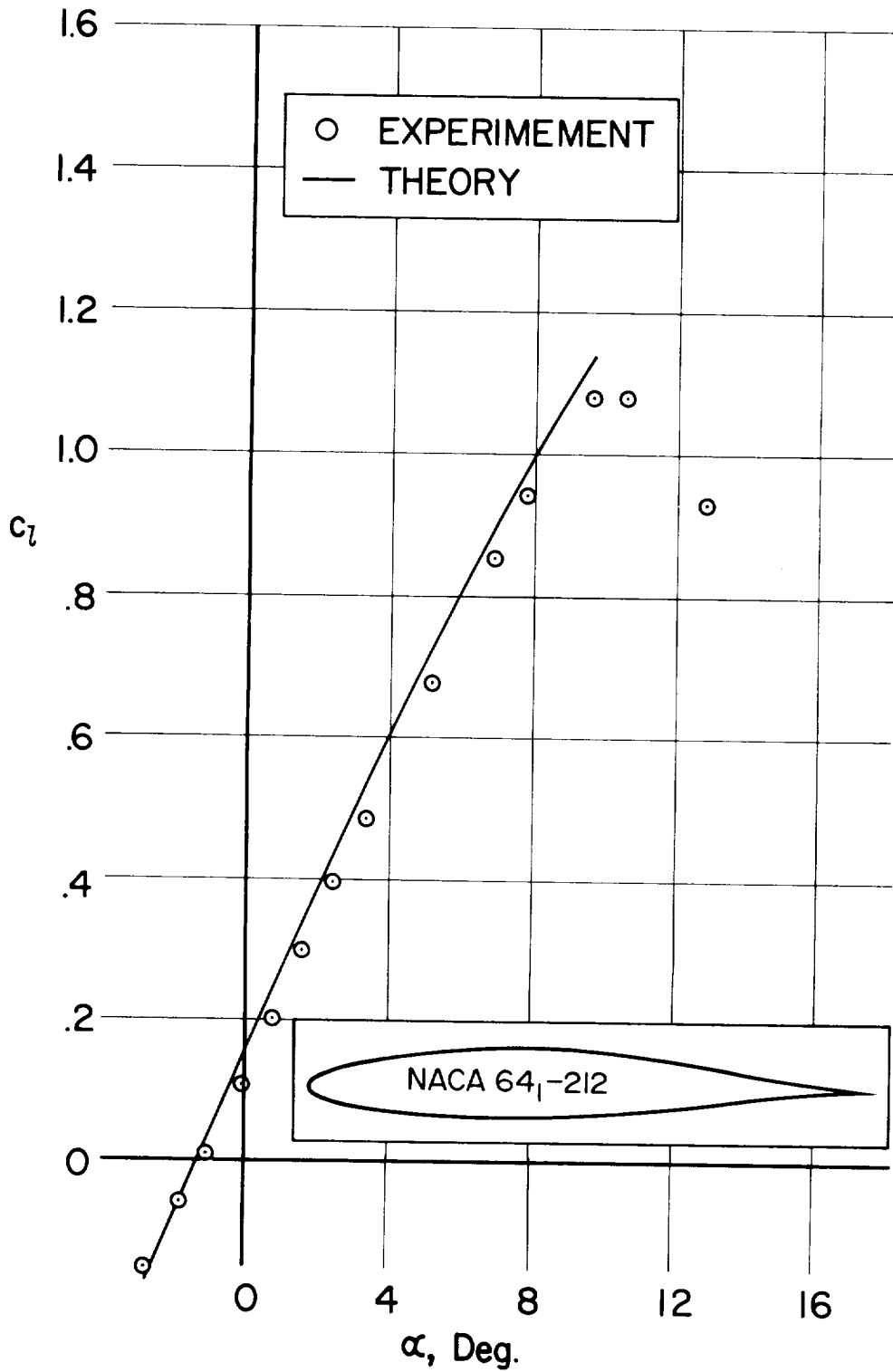
(c) Mod. B.

Figure 6.— Continued.



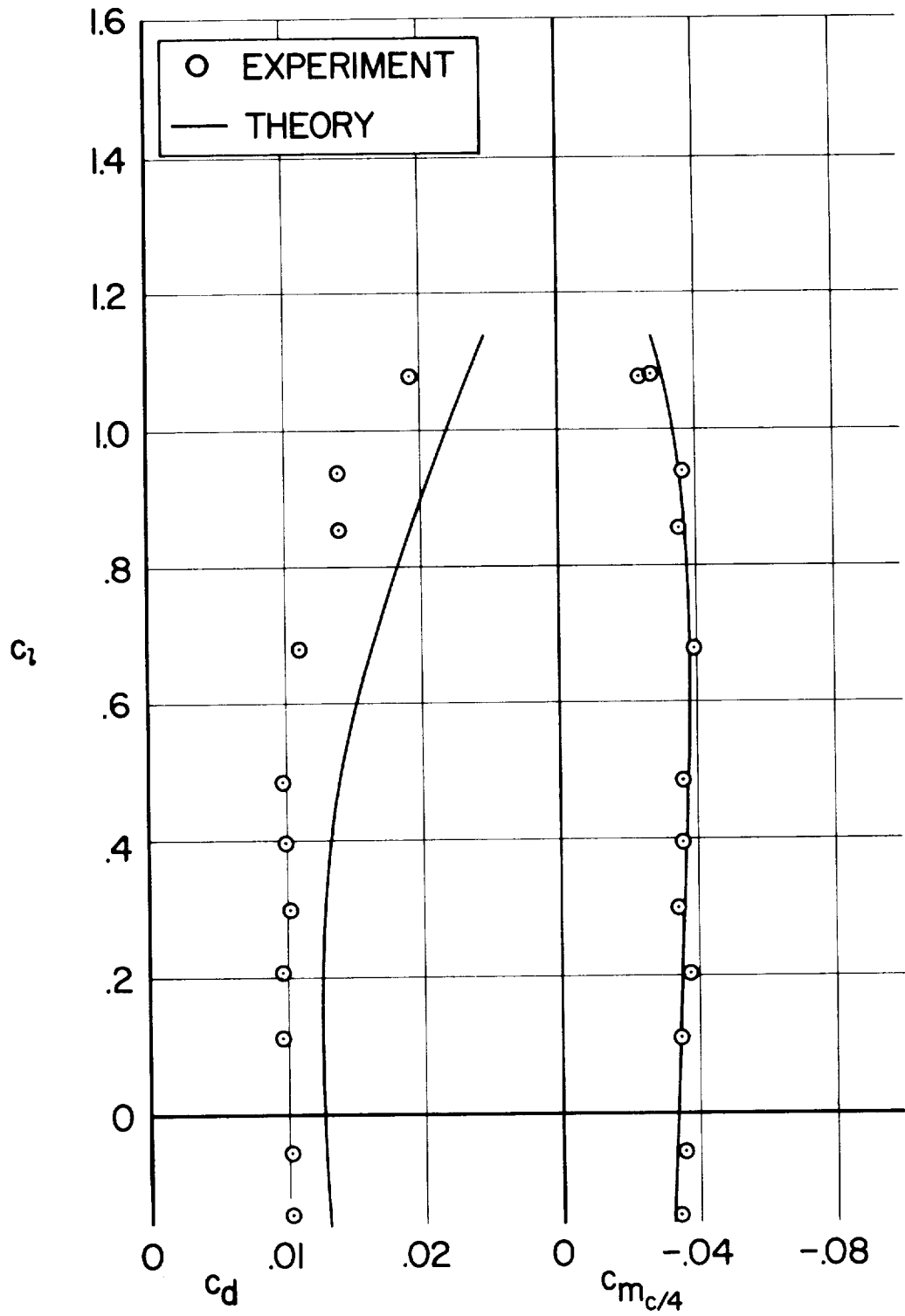
(c) Mod. B - Concluded.

Figure 6.- Concluded.



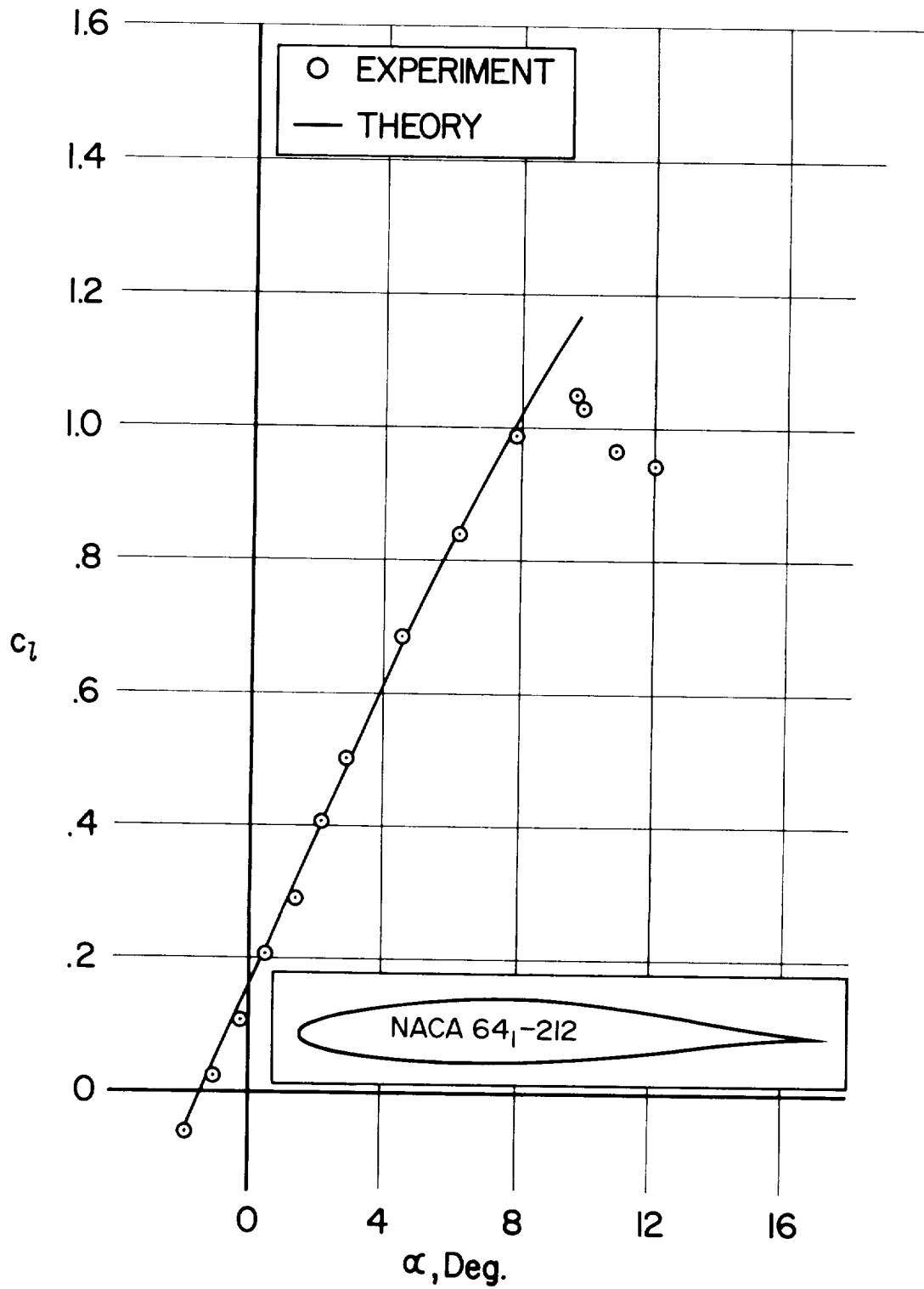
(a) $M = 0.2, Re = 1.5 \times 10^6$.

Figure 7.— Comparison of experimental and theoretical aerodynamic force coefficients. Transition fixed at $0.12c$.



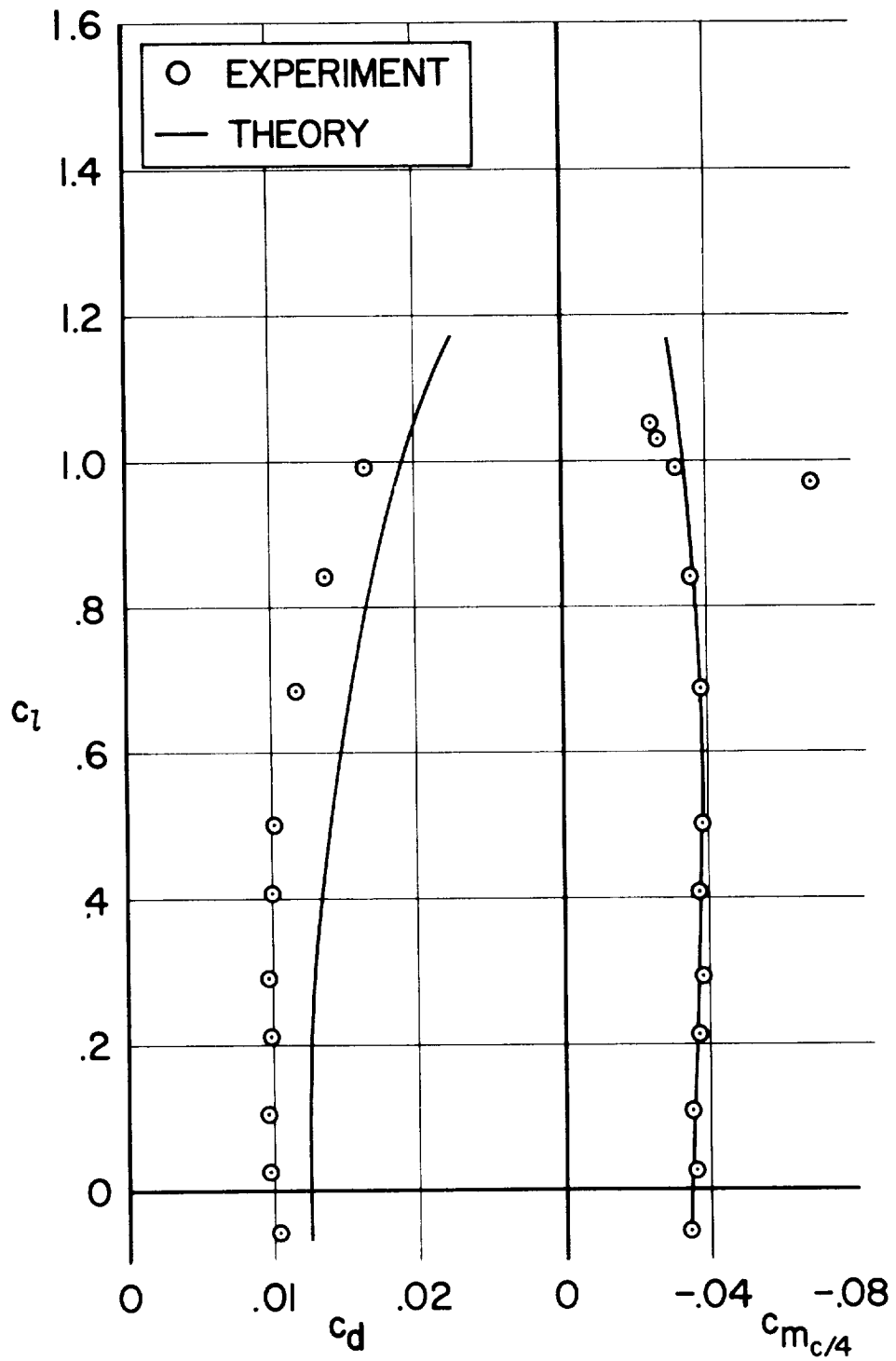
(a) $M = 0.2, Re = 1.5 \times 10^6$ - Concluded.

Figure 7.- Continued.



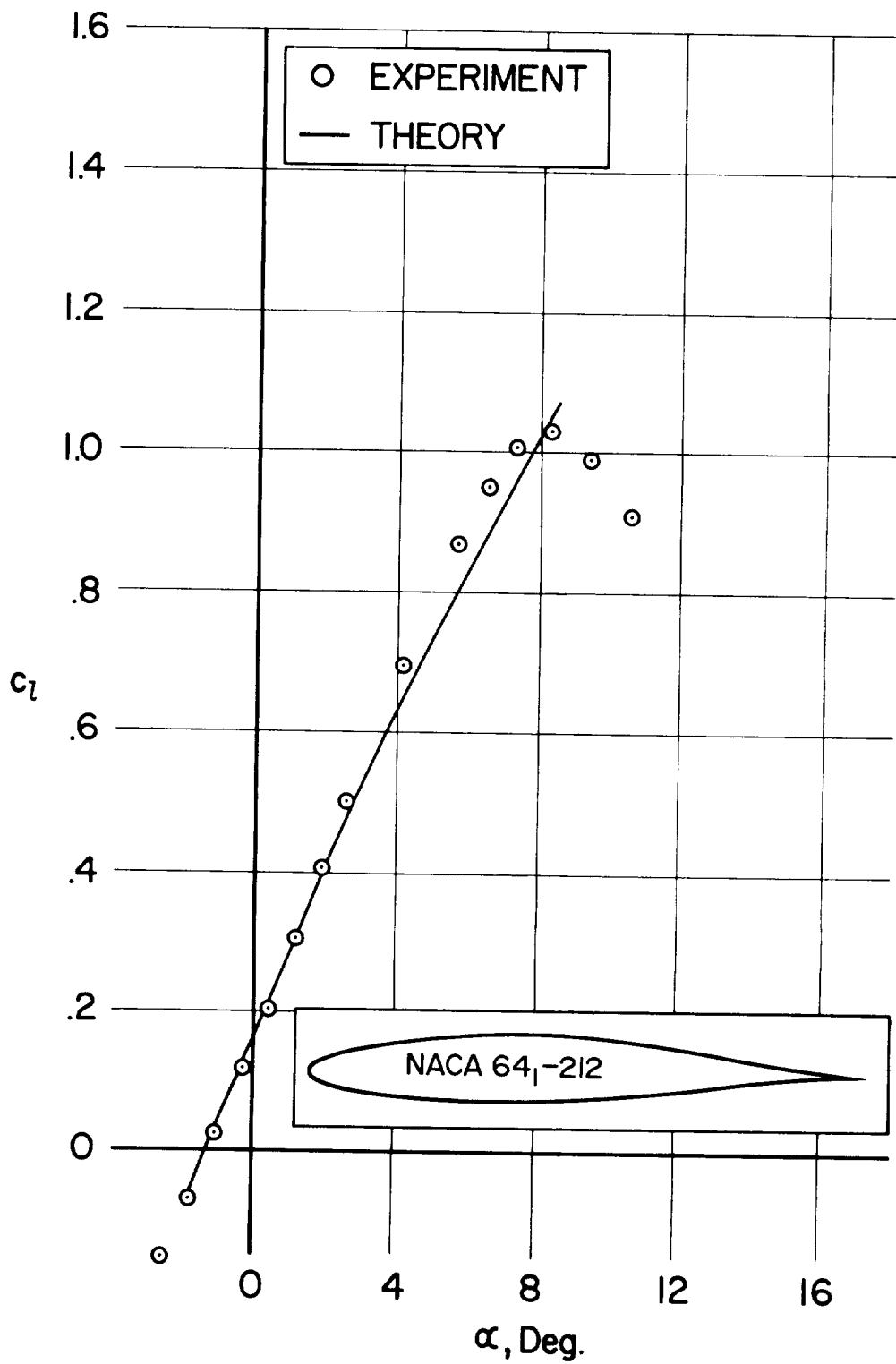
(b) $M = 0.3, Re = 1.5 \times 10^6$.

Figure 7.— Continued.



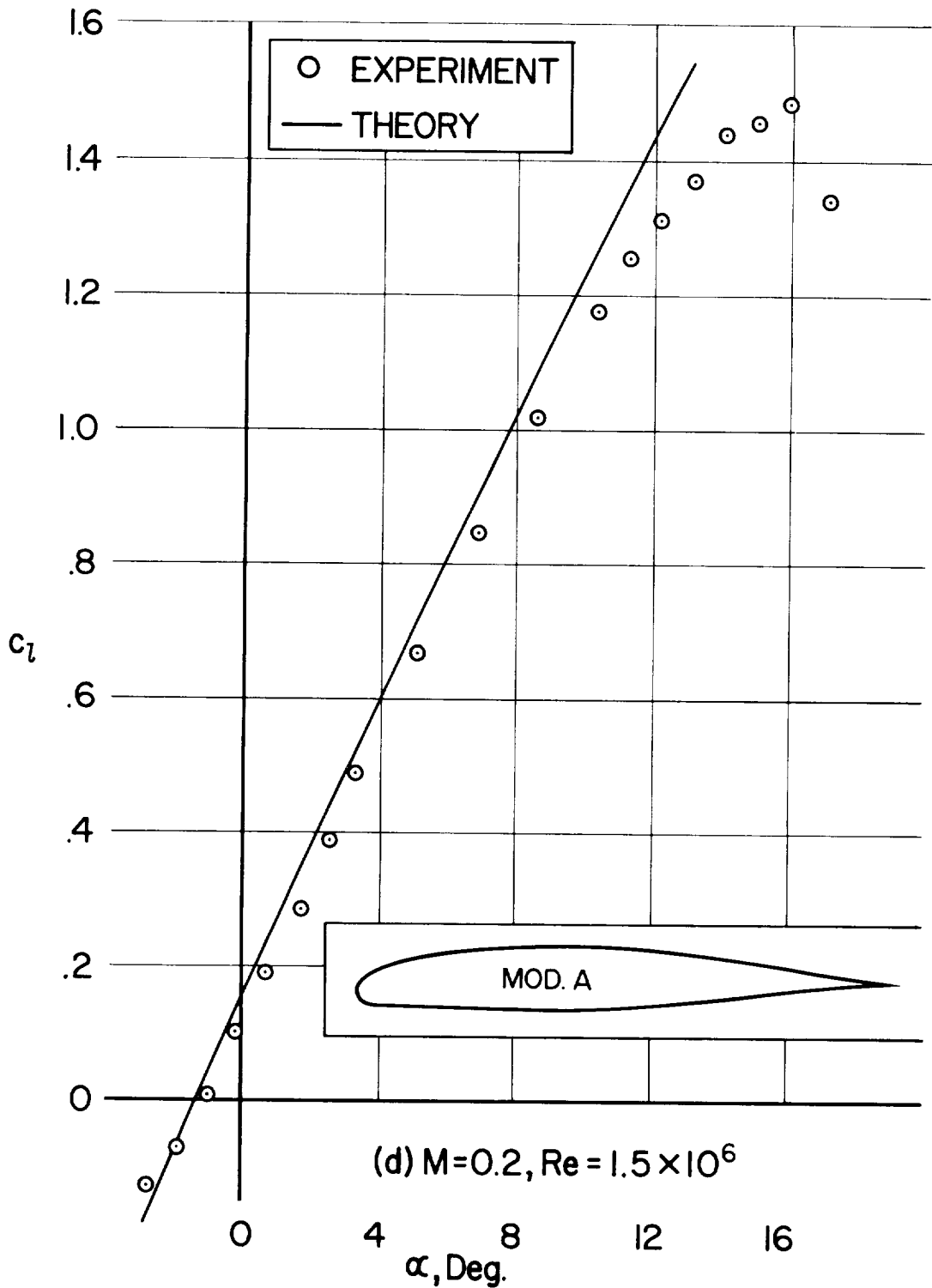
(b) $M = 0.3, Re = 1.5 \times 10^6$ - Concluded.

Figure 7.- Continued.



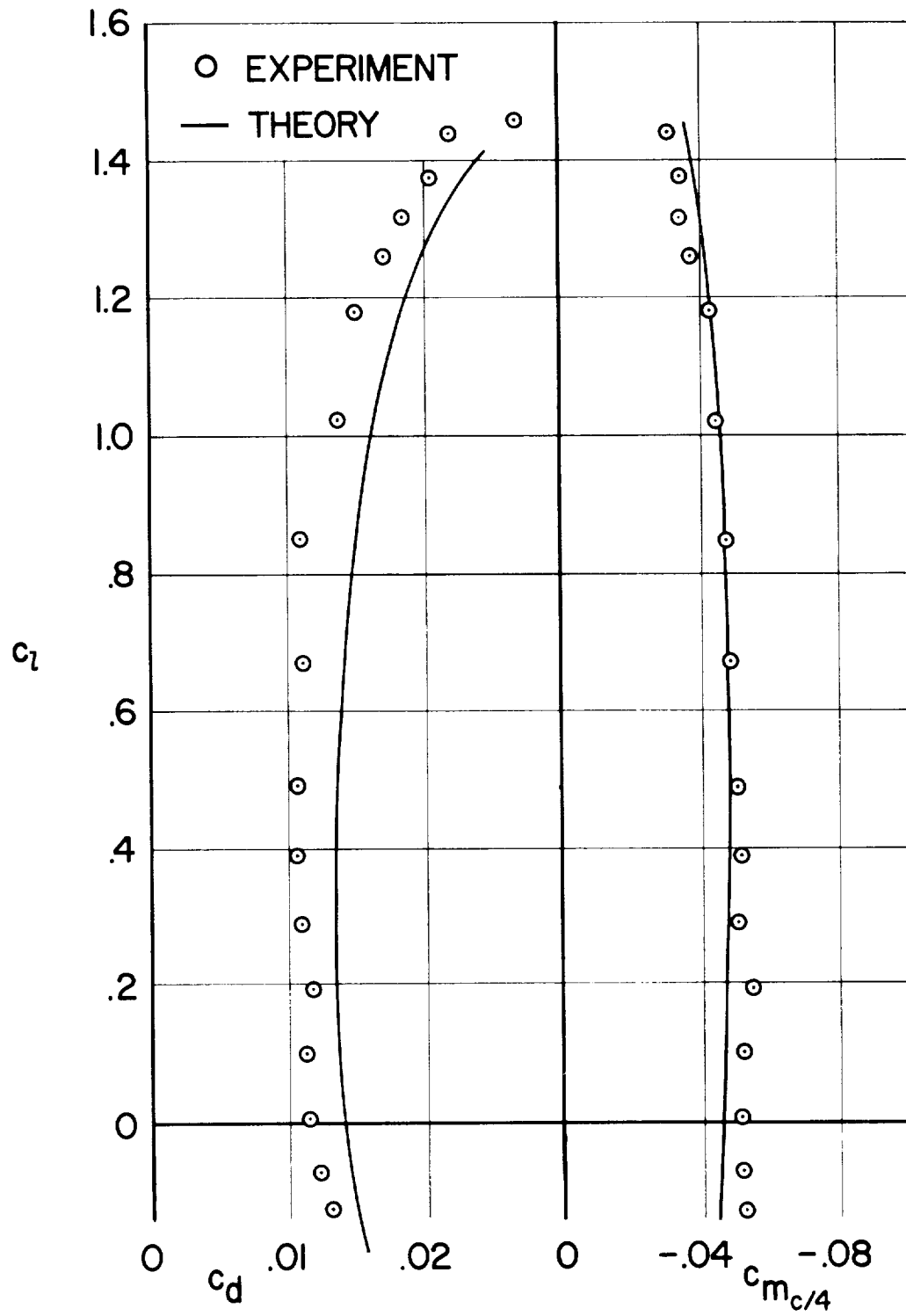
(c) $M = 0.4, Re = 1.9 \times 10^6$.

Figure 7.— Continued.



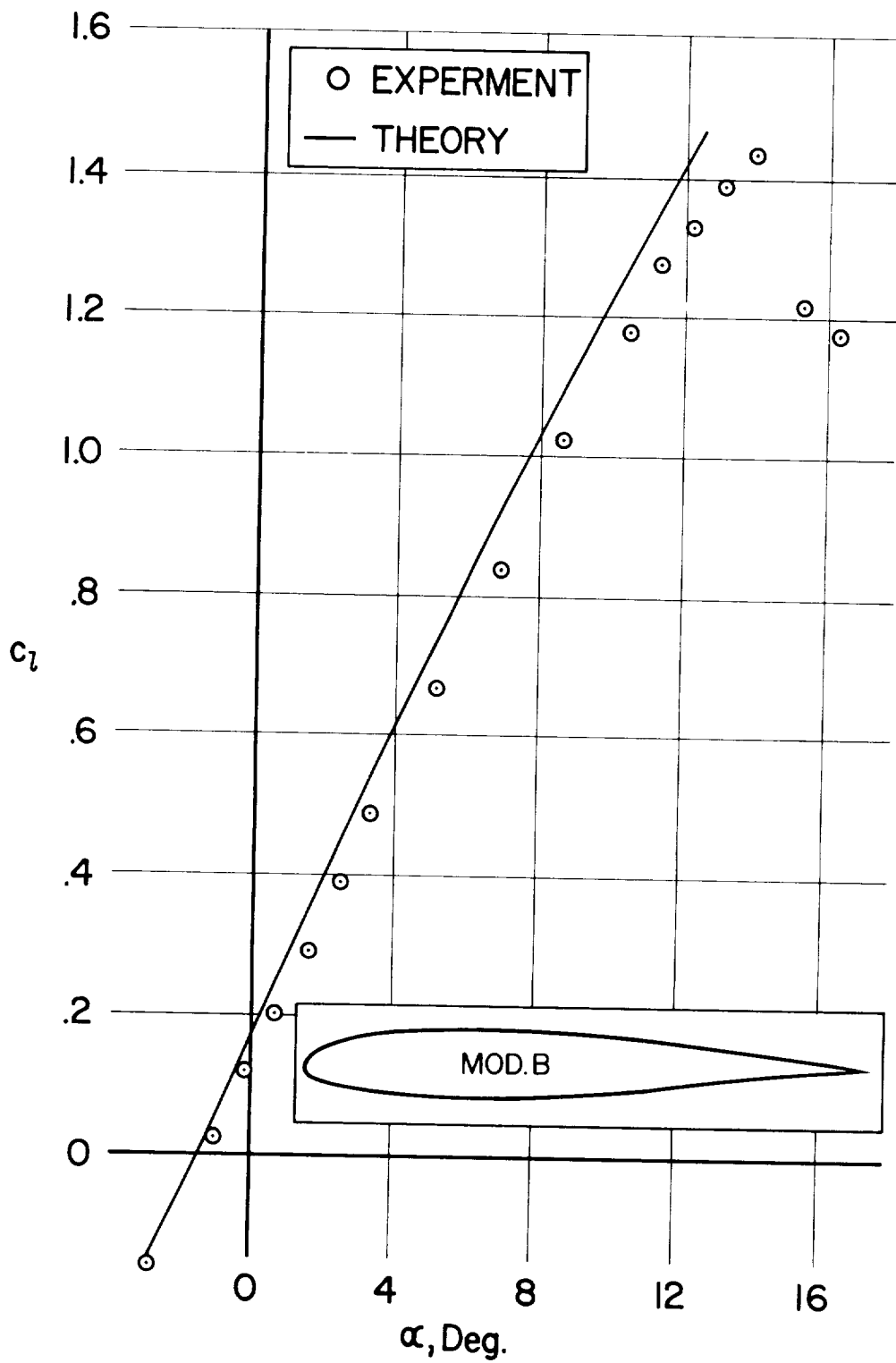
(d) $M = 0.2, Re = 1.5 \times 10^6$.

Figure 7.— Continued.



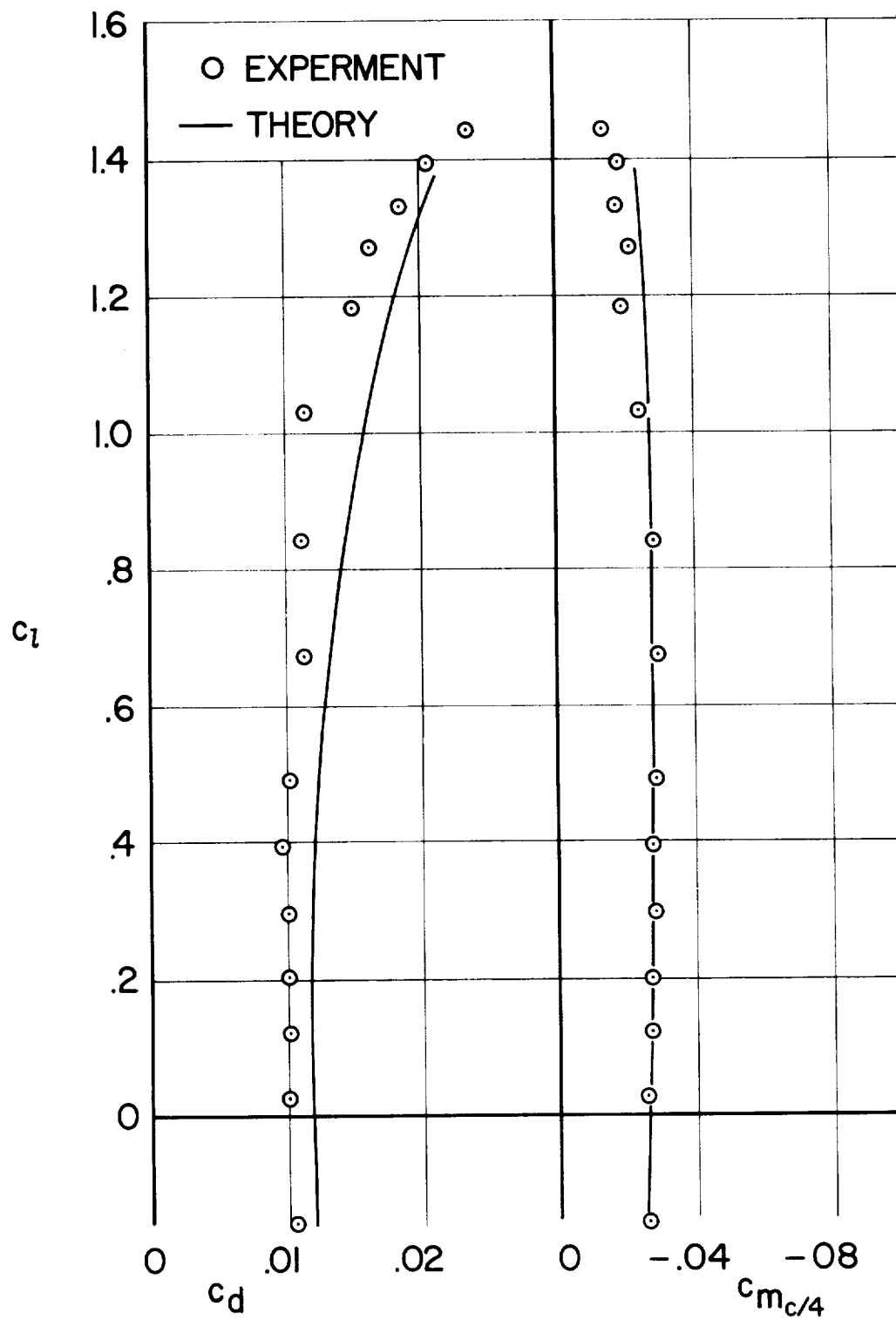
(d) $M = 0.2, Re = 1.5 \times 10^6$ - Concluded.

Figure 7.- Continued.



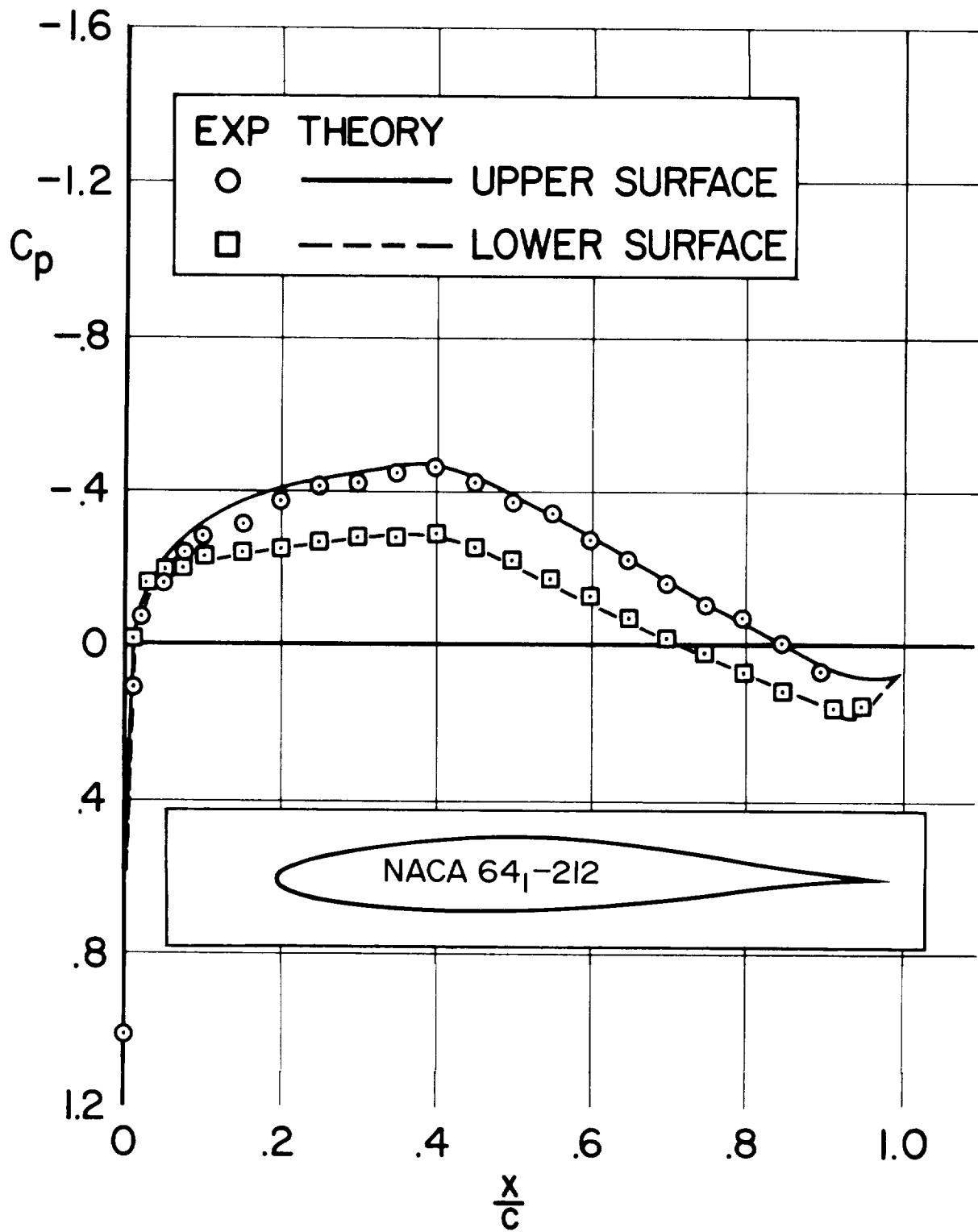
(e) $M = 0.2, Re = 1.5 \times 10^6$.

Figure 7.— Continued.



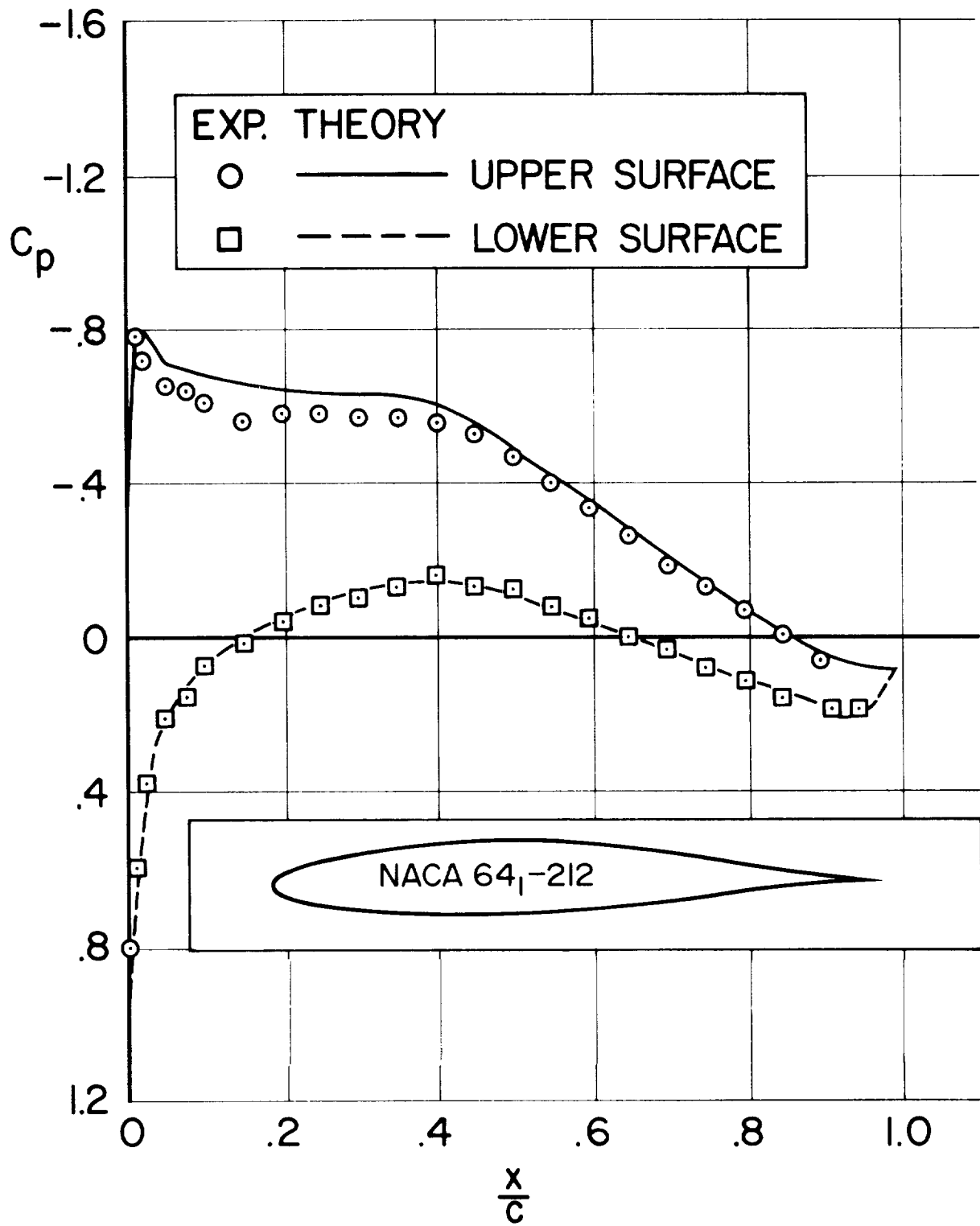
(e) $M = 0.2, Re = 1.5 \times 10^6$ - Concluded.

Figure 7.- Concluded.



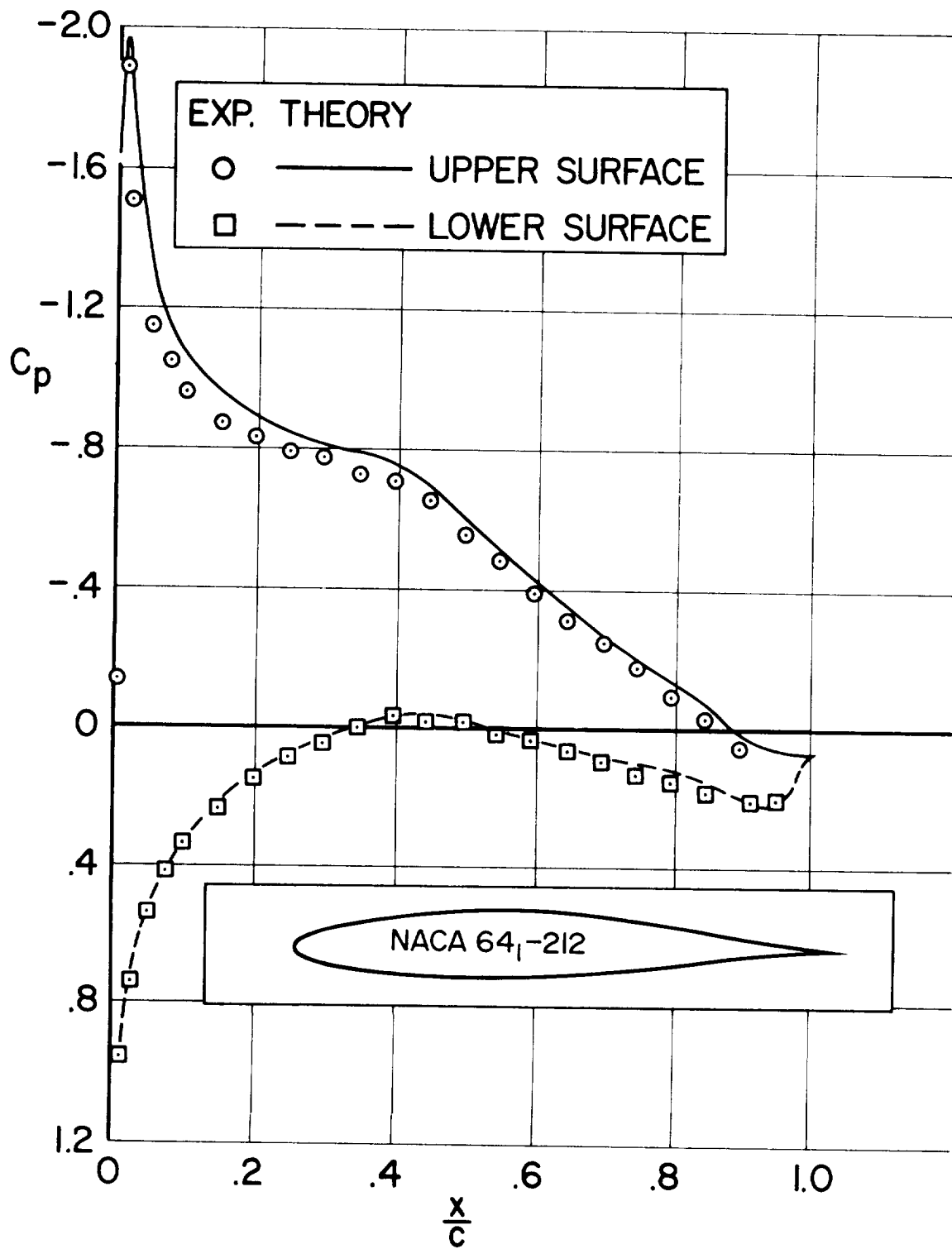
(a) $M = 0.2$, $Re = 1.5 \times 10^6$, $\alpha = -0.13^\circ$, $c_l = 0.115$.

Figure 8.— Comparison of experimental and theoretical pressure distributions.



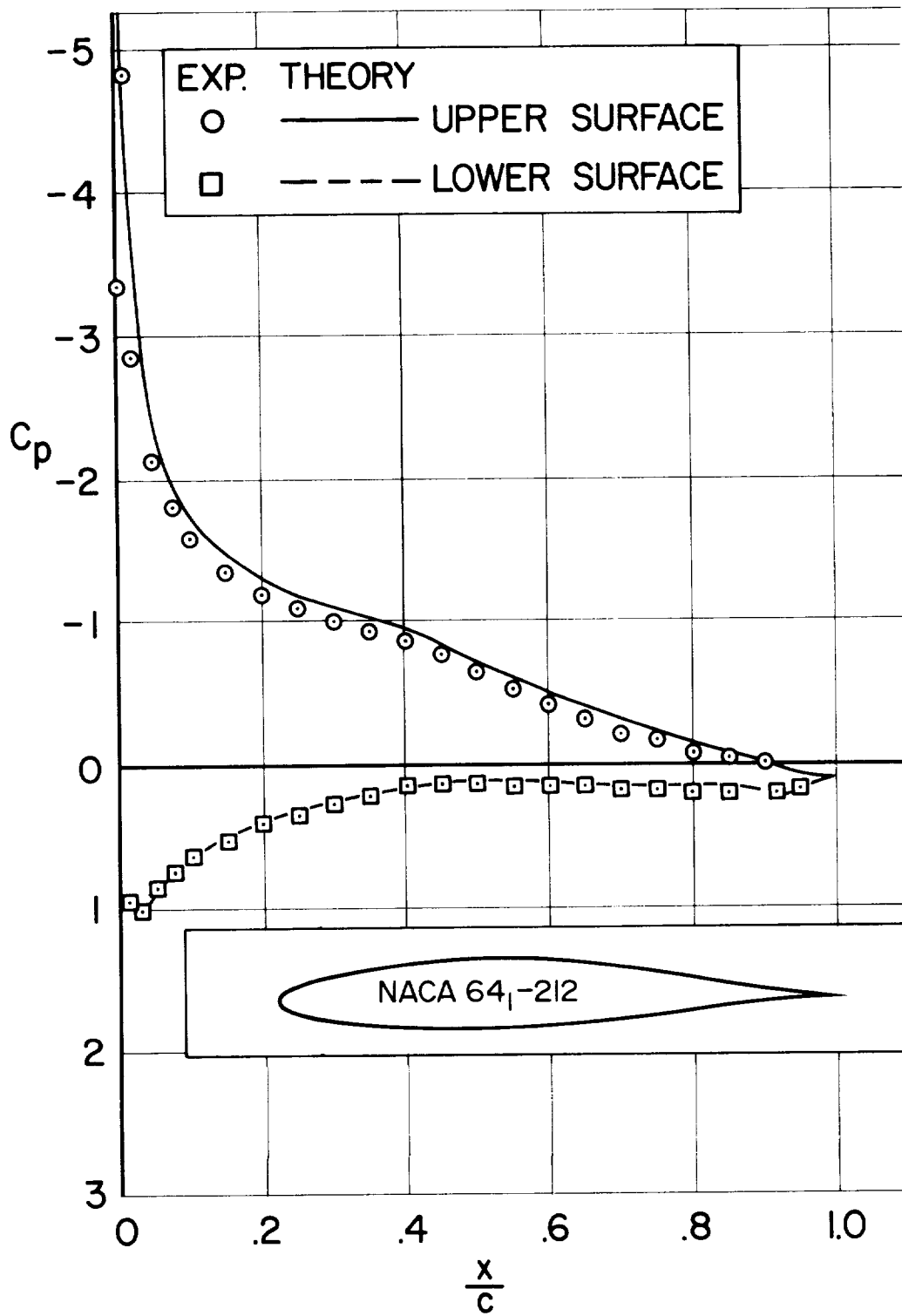
(b) $M = 0.2$, $Re = 1.5 \times 10^6$, $\alpha = 2.44^\circ$, $c_l = 0.394$.

Figure 8.— Continued.



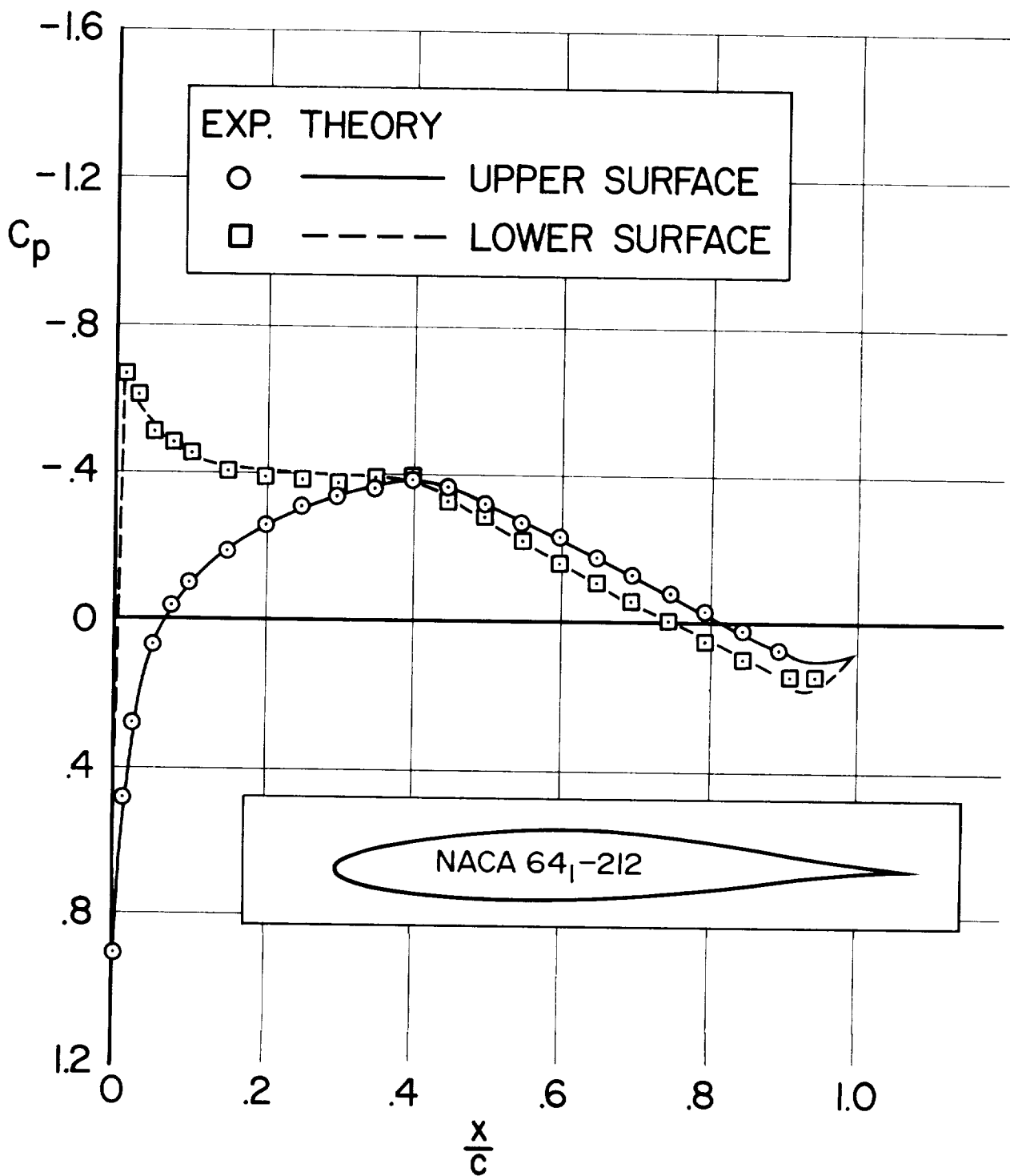
(c) $M = 0.2$, $Re = 1.5 \times 10^6$, $\alpha = 5.11^\circ$, $c_l = 0.678$.

Figure 8.— Continued.



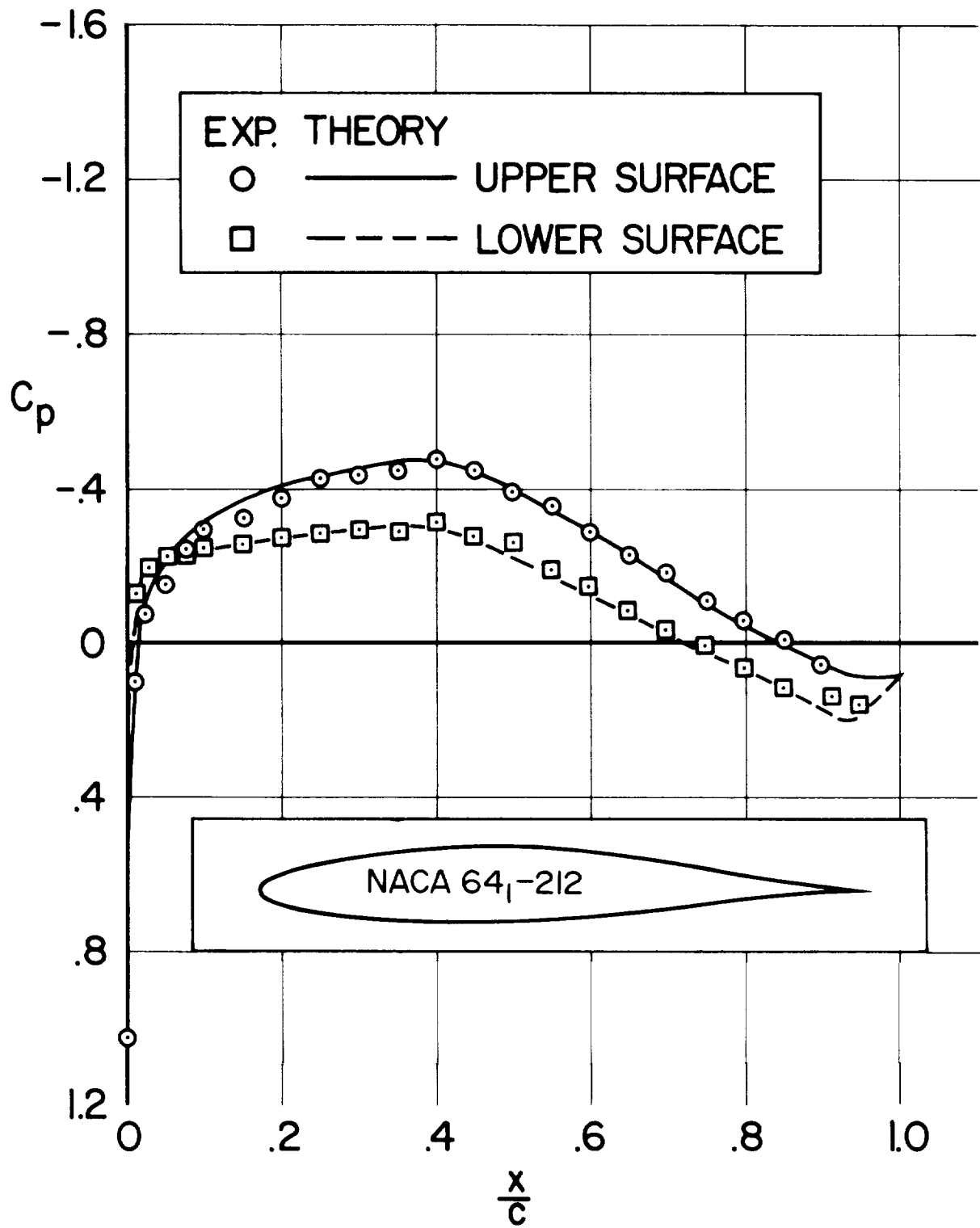
(d) $M = 0.2, Re = 1.5 \times 10^6, \alpha = 9.58^\circ, c_l = 1.081$.

Figure 8.— Continued.



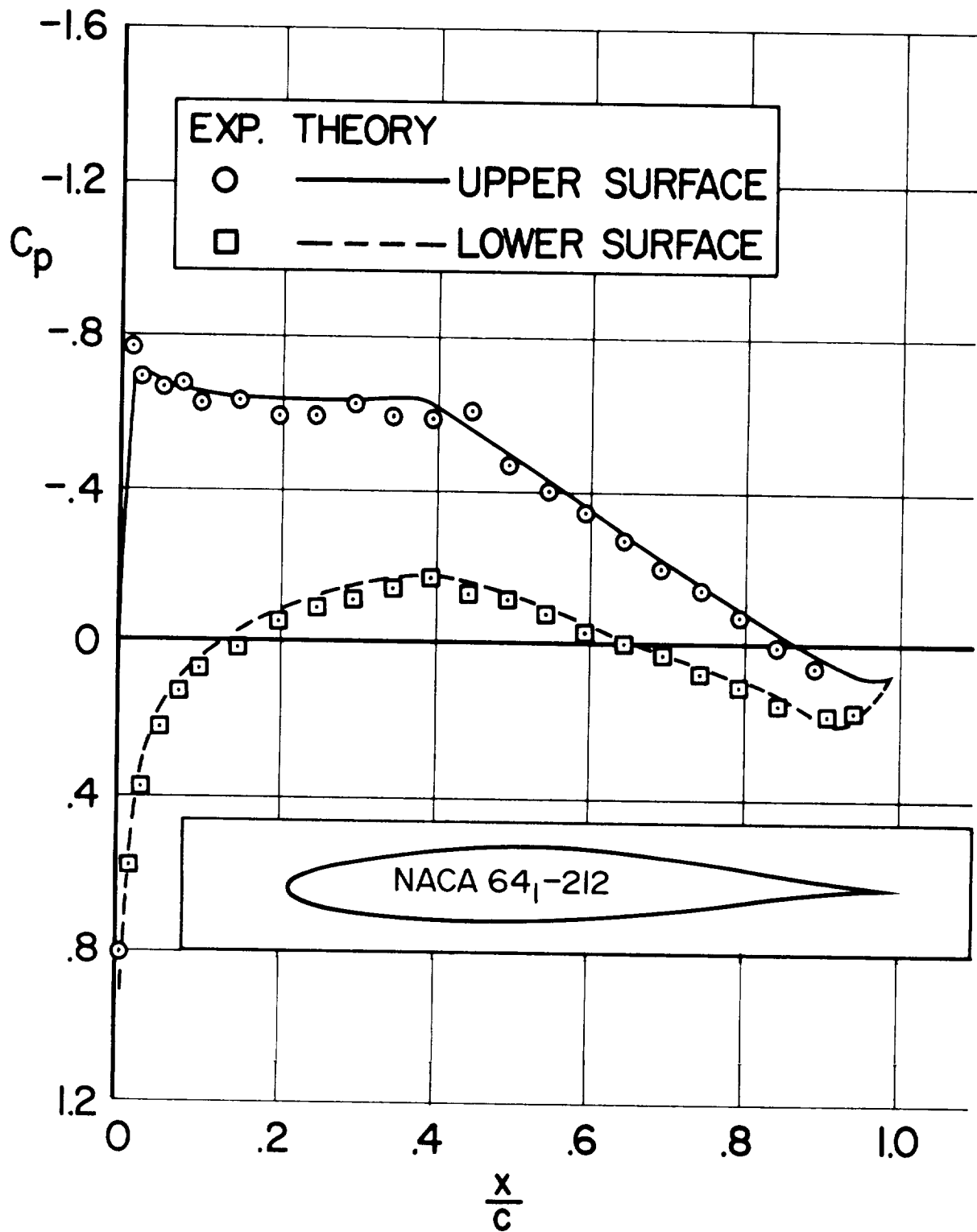
(e) $M = 0.3, Re = 1.5 \times 10^6, \alpha = -1.9^\circ, c_l = -0.059.$

Figure 8.— Continued.



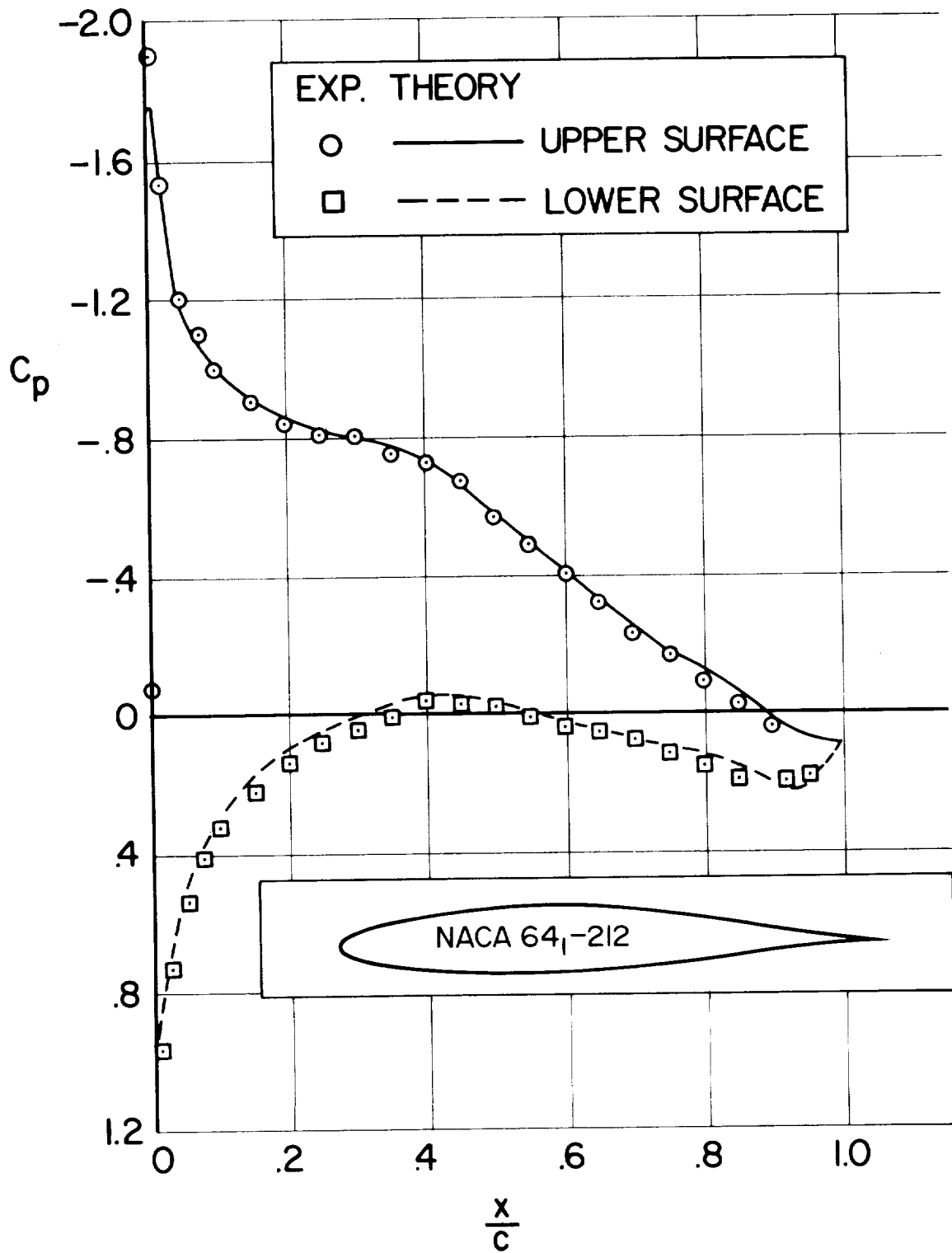
(f) $M = 0.3, Re = 1.5 \times 10^6, \alpha = -0.23^\circ, c_l = 0.107.$

Figure 8.— Continued.



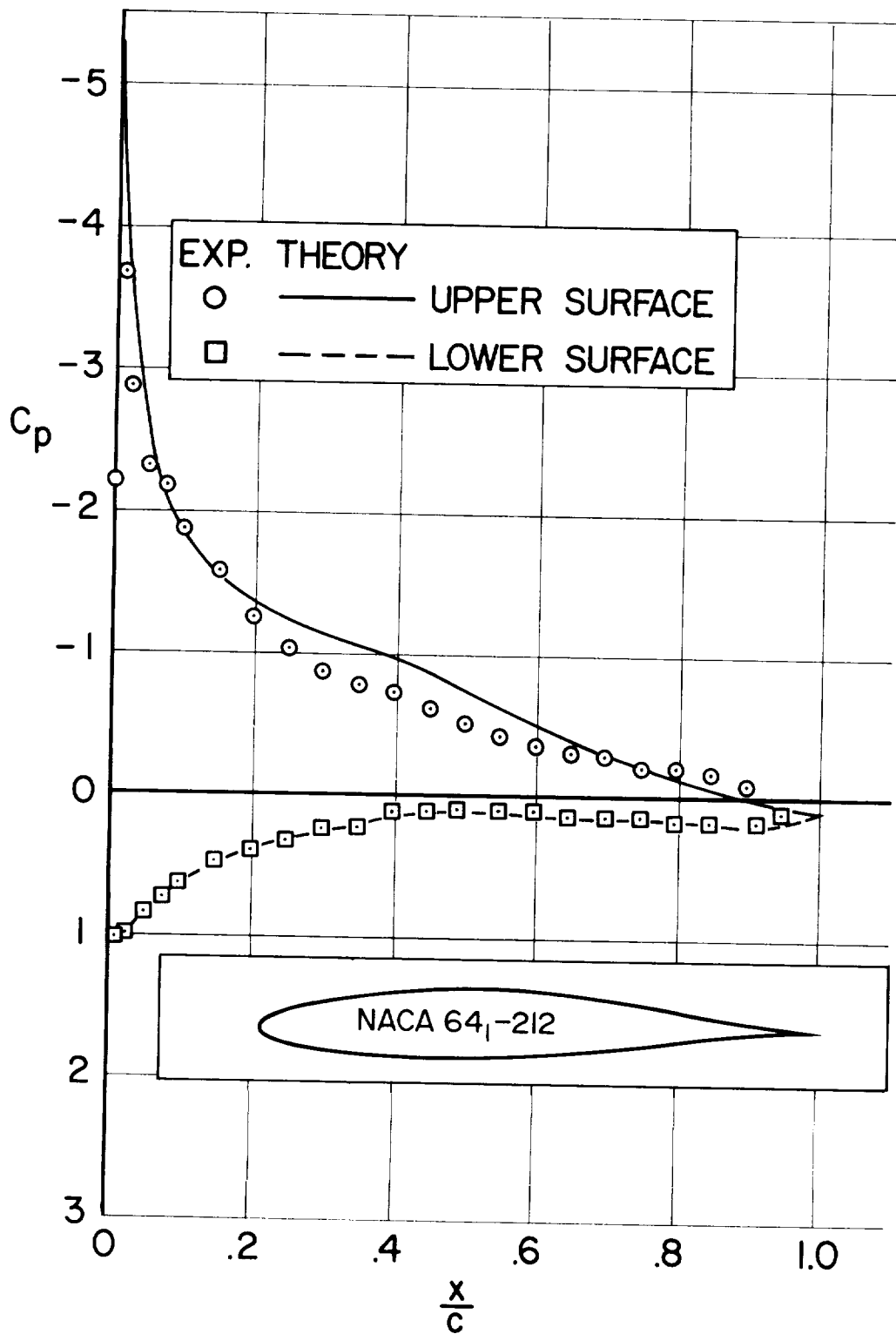
(g) $M = 0.3, Re = 1.5 \times 10^6, \alpha = 2.16^\circ, c_l = 0.407.$

Figure 8.— Continued.



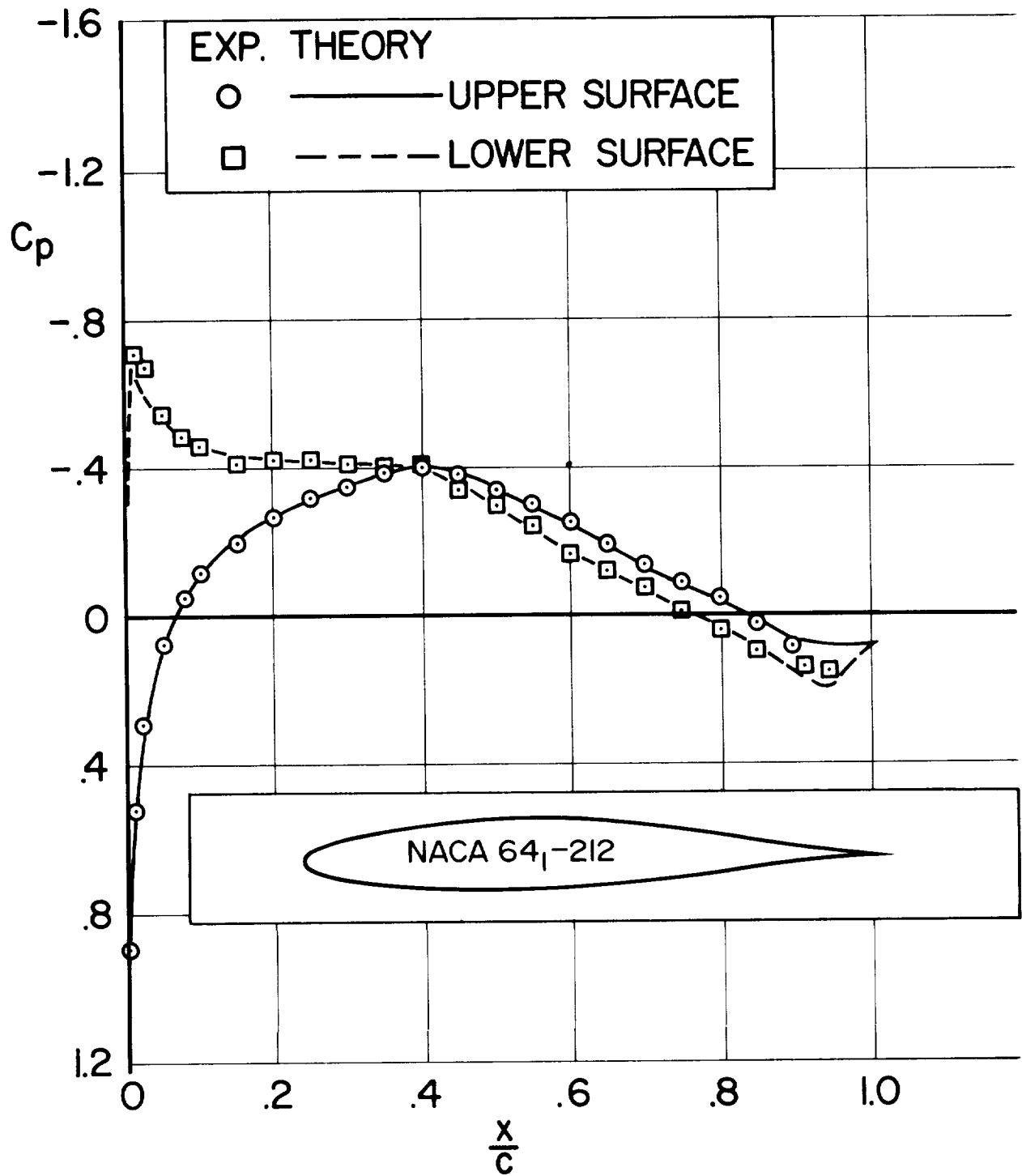
(h) $M = 0.3$, $Re = 1.5 \times 10^6$, $\alpha = 4.55^\circ$, $c_l = 0.685$.

Figure 8.— Continued.



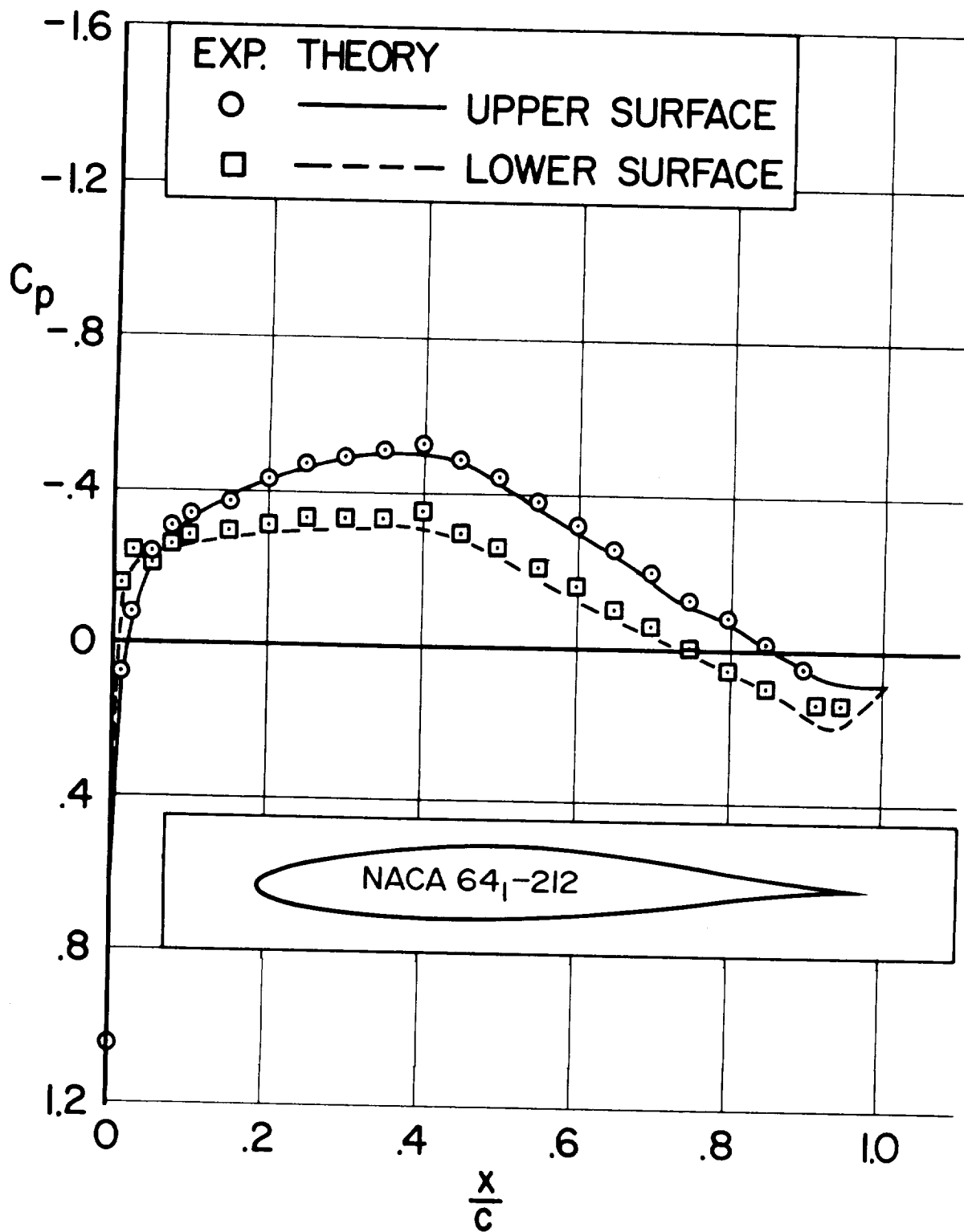
(i) $M = 0.3, Re = 1.5 \times 10^6, \alpha = 9.74, c_l = 1.048.$

Figure 8.- Continued.



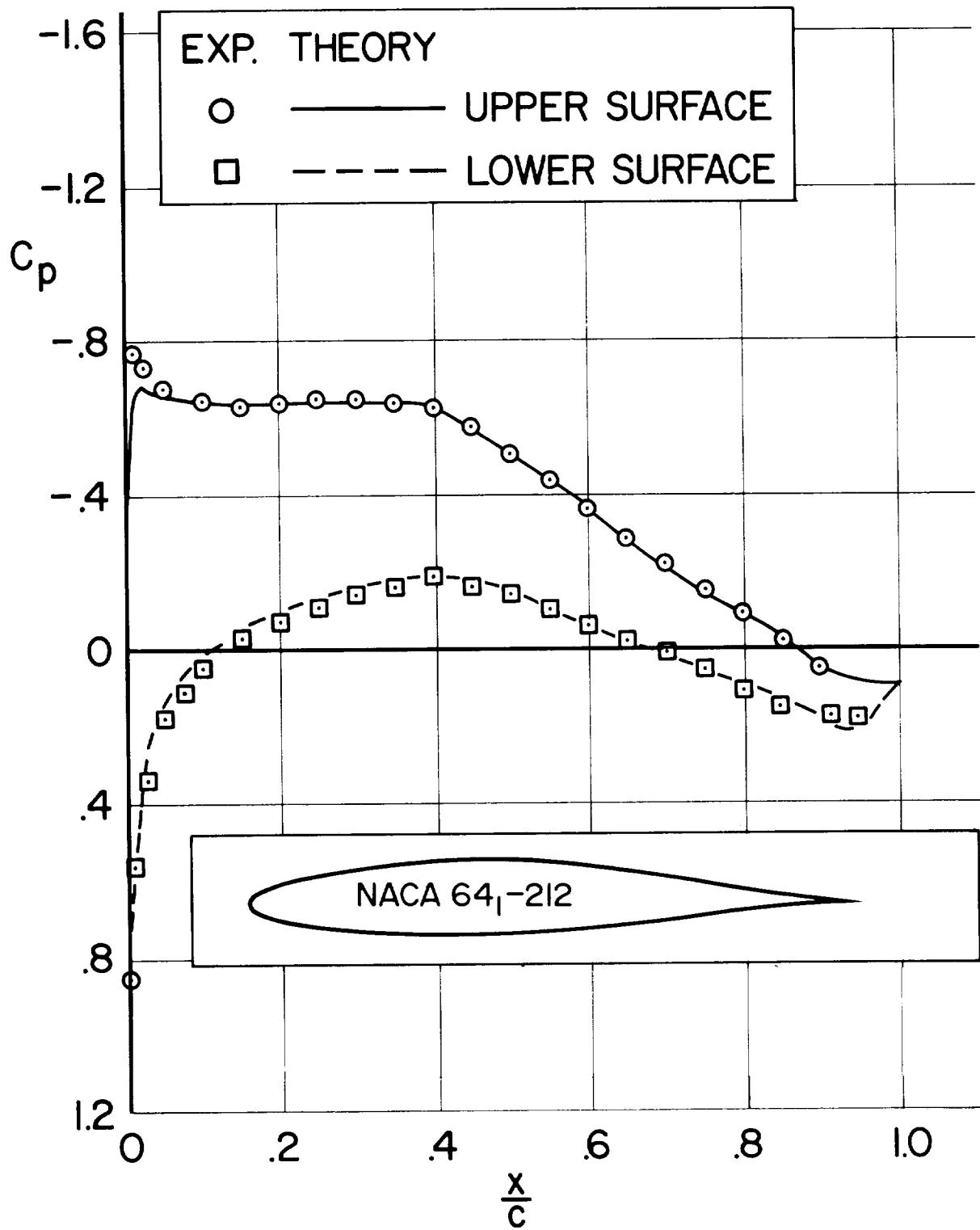
(j) $M = 0.4$, $Re = 1.9 \times 10^6$, $\alpha = -1.84^\circ$, $c_l = 0.067$.

Figure 8.— Continued.



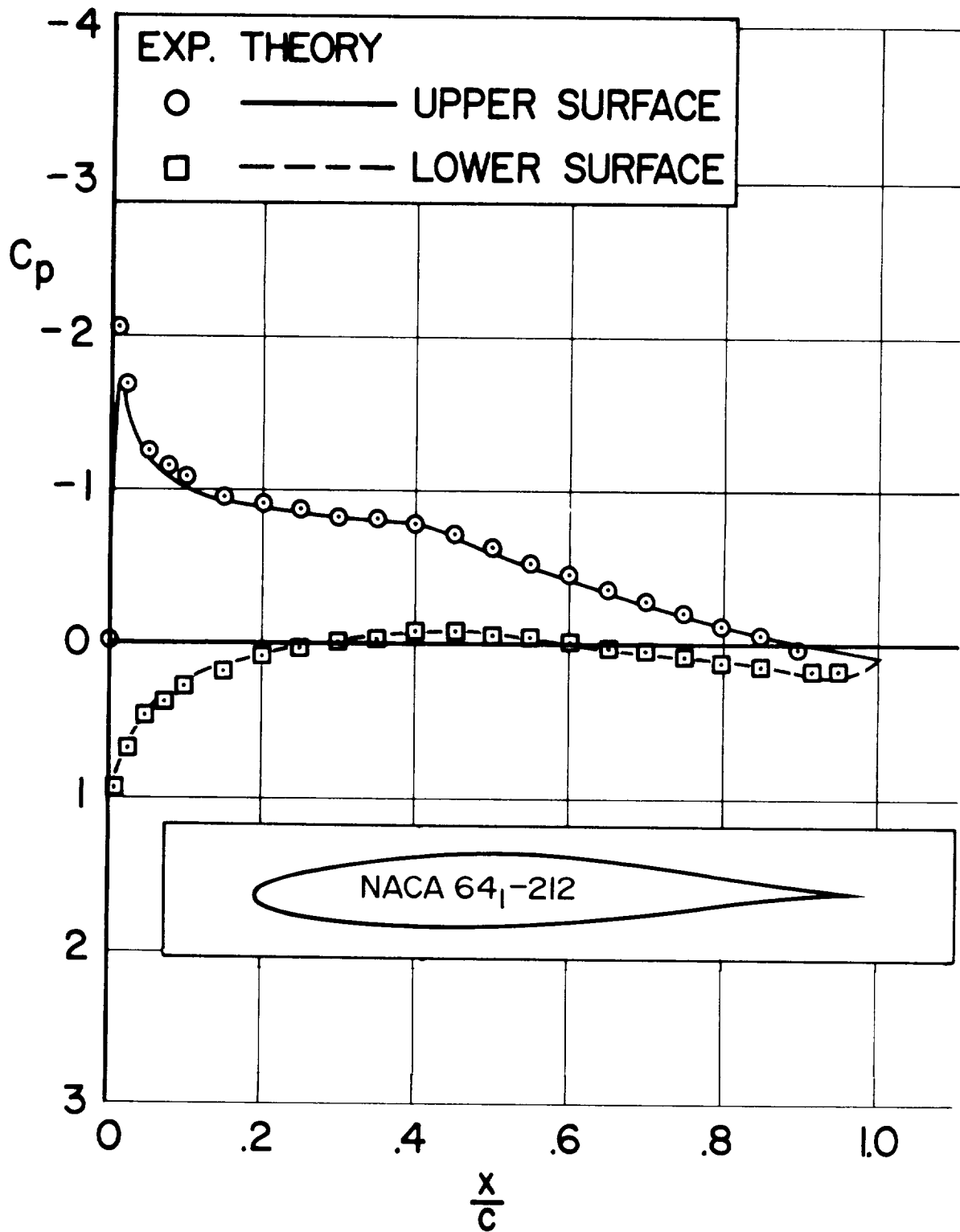
(k) $M = 0.4$, $Re = 1.9 \times 10^6$, $\alpha = -0.27^\circ$, $c_l = 0.122$.

Figure 8.— Continued.



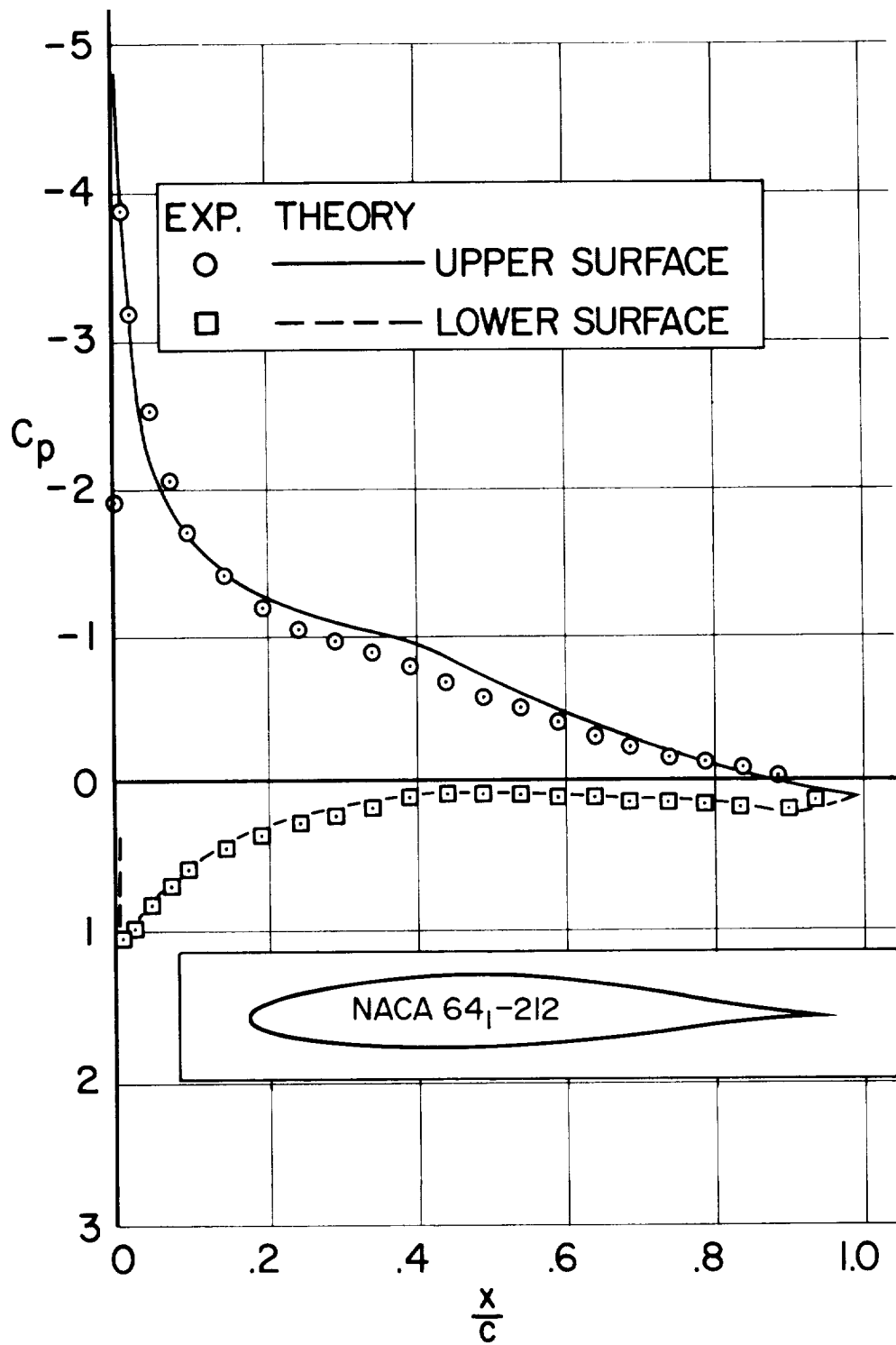
(l) $M = 0.4, Re = 1.9 \times 10^6, \alpha = 1.91^\circ, c_l = 0.409$.

Figure 8.— Continued.



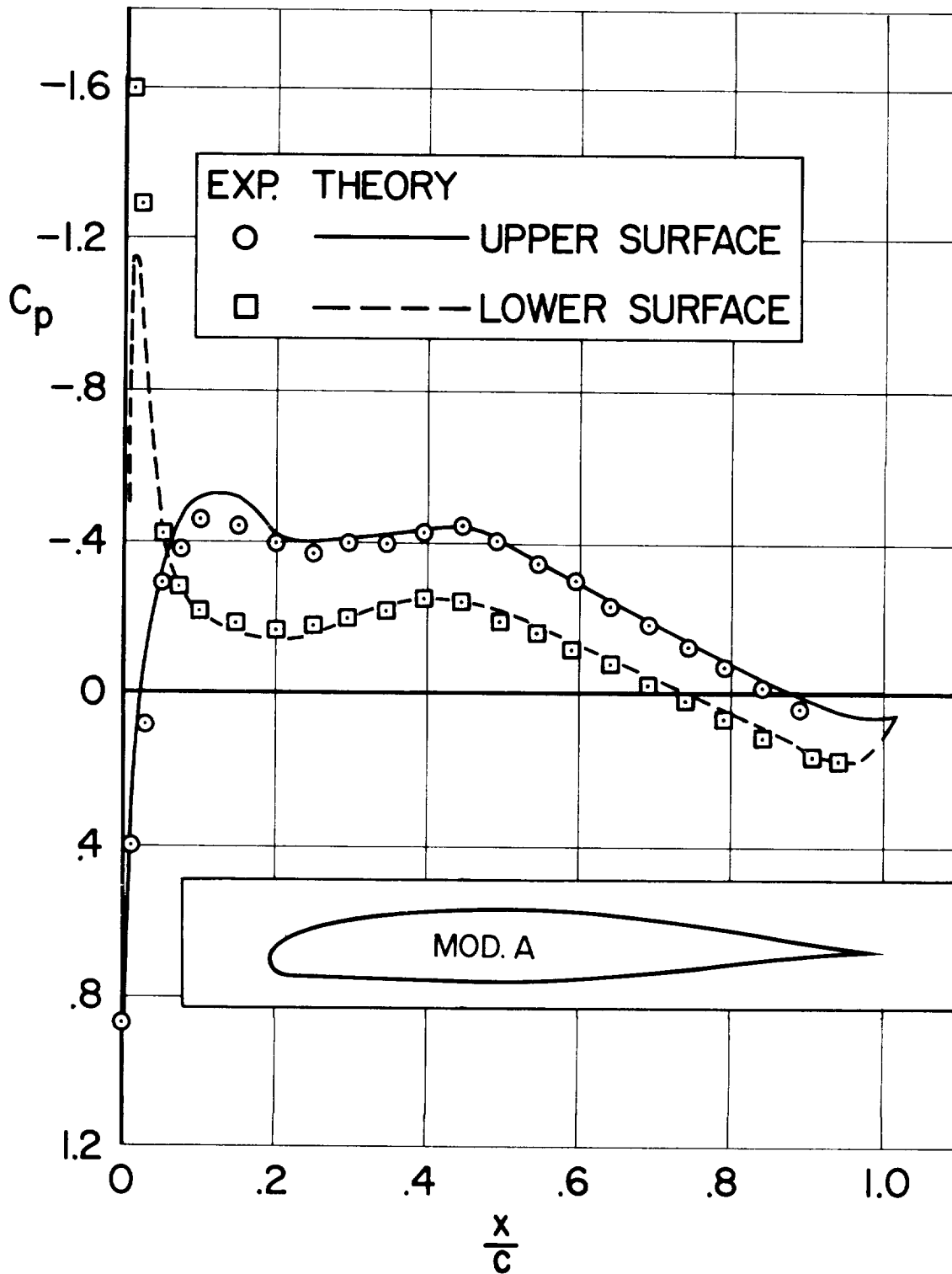
(m) $M = 0.4, Re = 1.9 \times 10^6, \alpha = 4.16^\circ, c_l = 0.699.$

Figure 8.— Continued.



(n) $M = 0.4, Re = 1.9 \times 10^6, \alpha = 8.3^\circ, c_l = 1.03.$

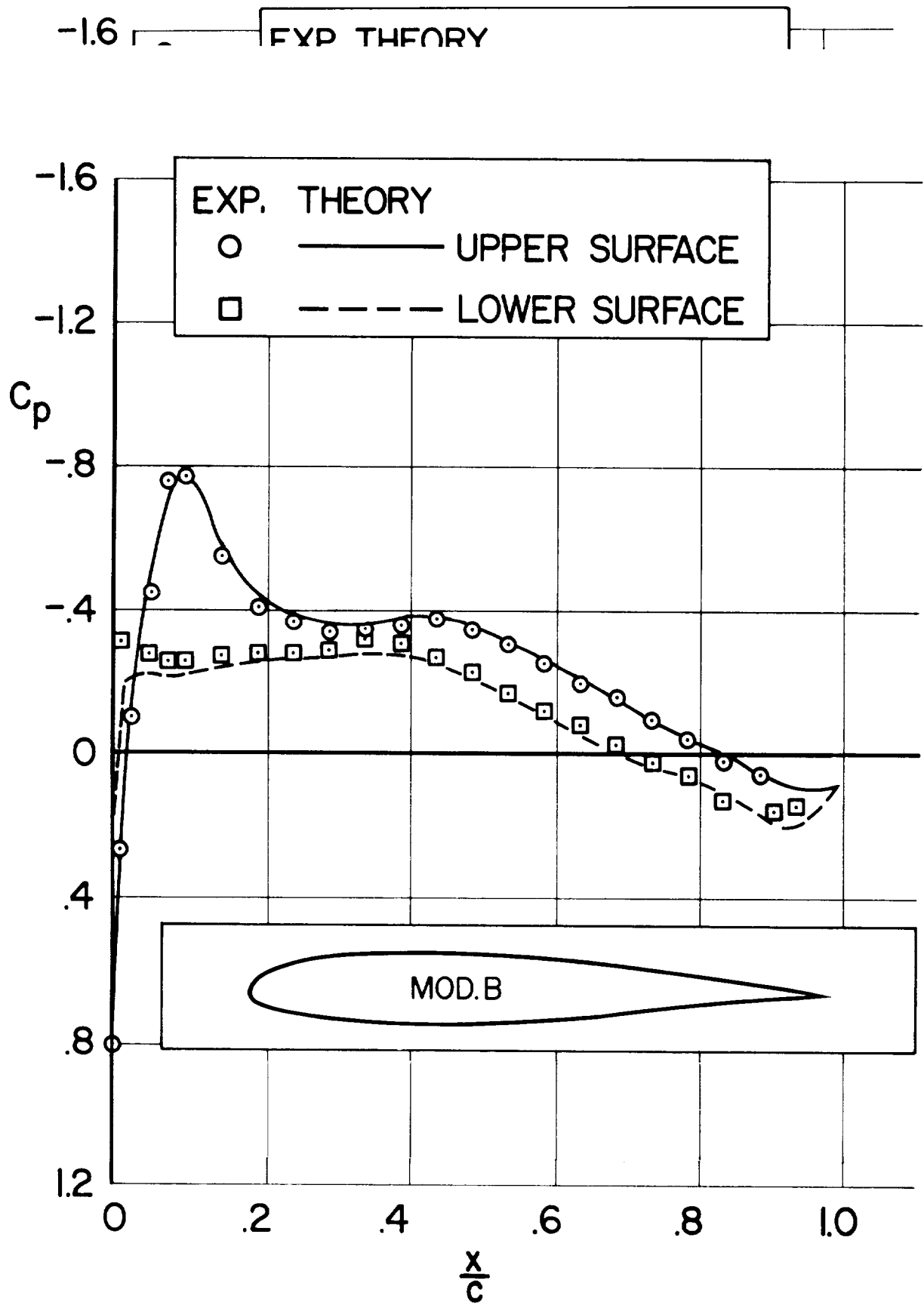
Figure 8.— Continued.



(o) $M = 0.2$, $Re = 1.5 \times 10^6$, $\alpha = -0.12^\circ$, $c_l = 0.103$.

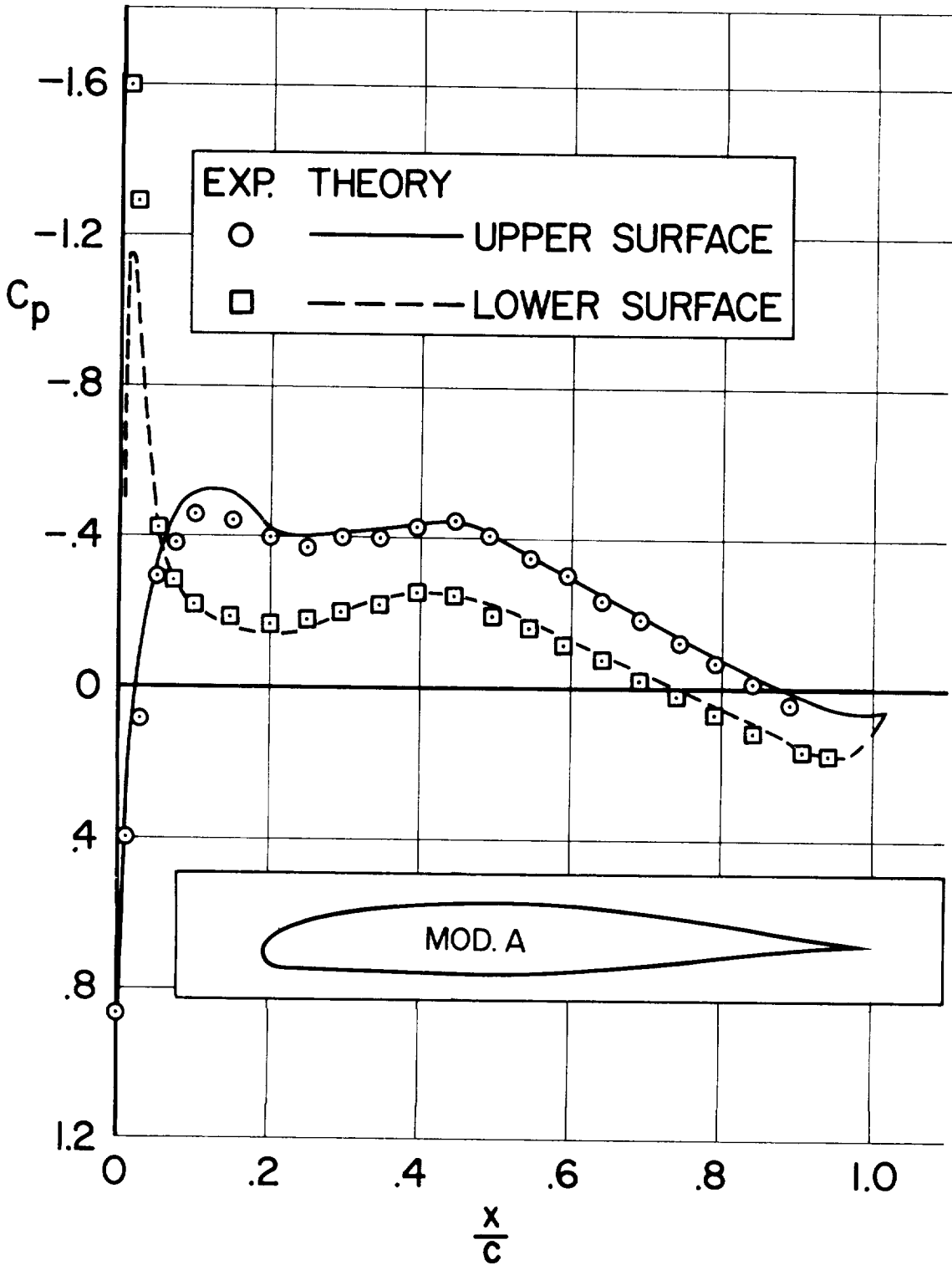
Figure 8.— Continued.

Figure 8.— Continued.



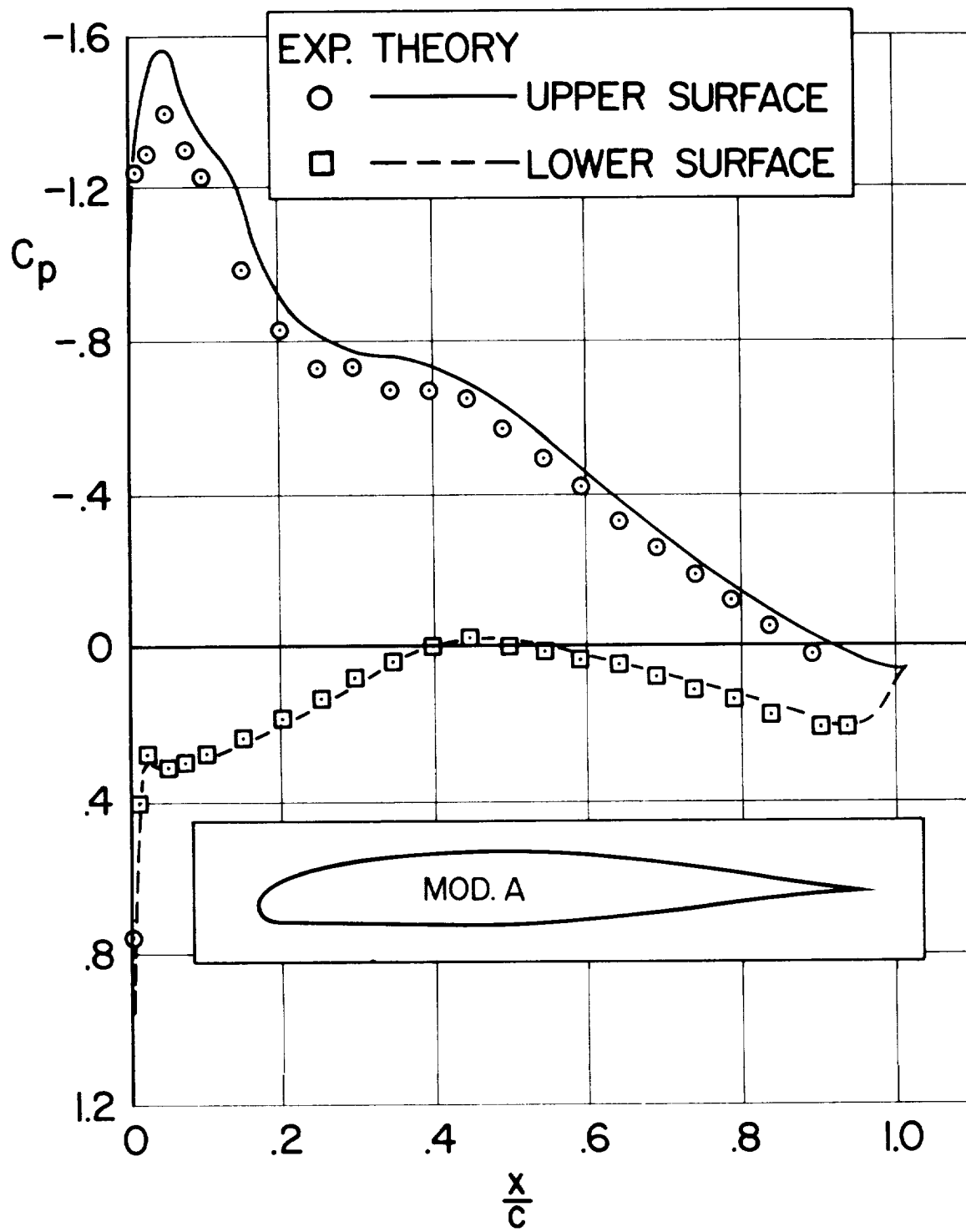
(r) $M = 0.2, Re = 1.5 \times 10^6, \alpha = -0.15^\circ, c_l = 0.119.$

Figure 8.— Continued.



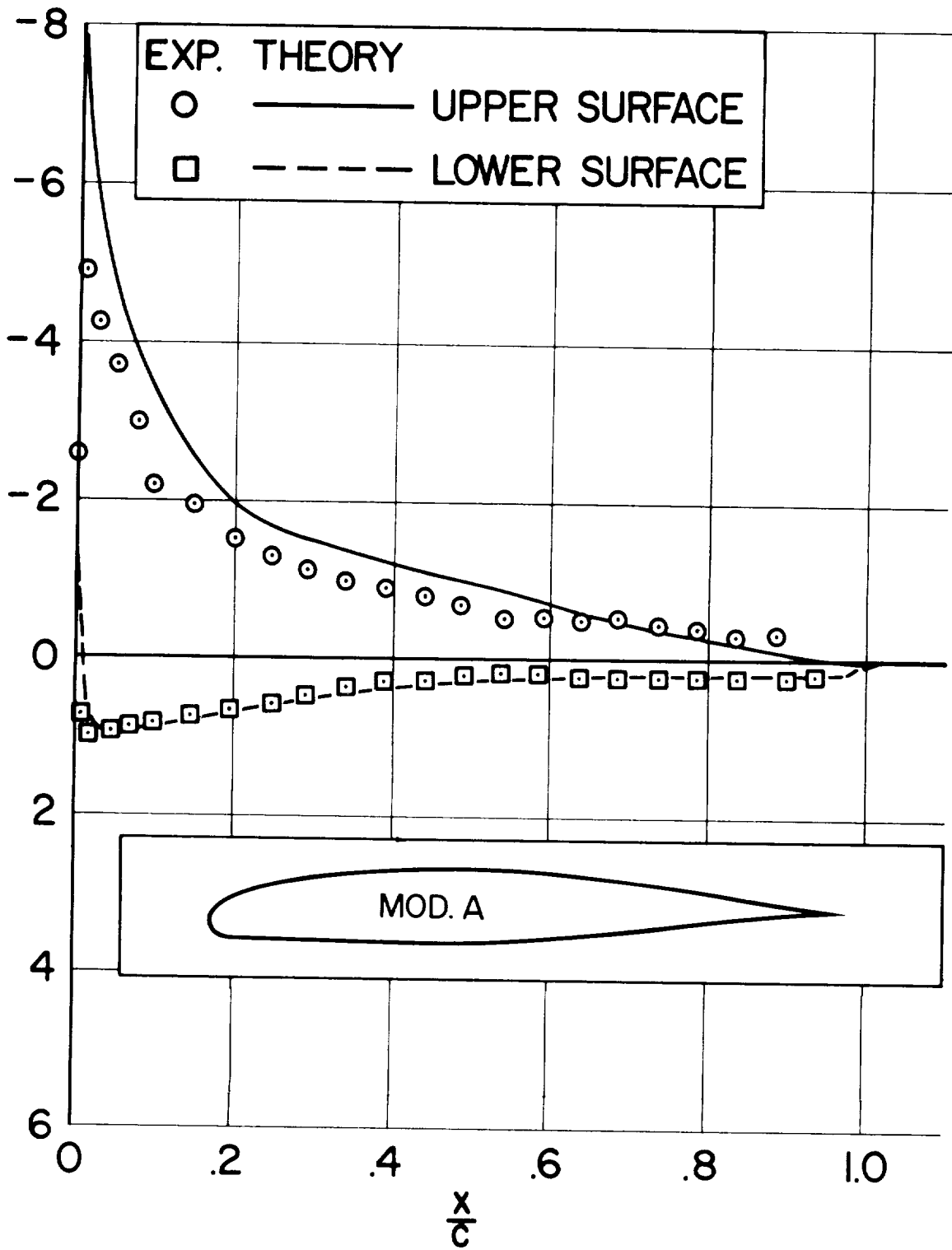
(o) $M = 0.2$, $Re = 1.5 \times 10^6$, $\alpha = -0.12^\circ$, $c_l = 0.103$.

Figure 8.— Continued.



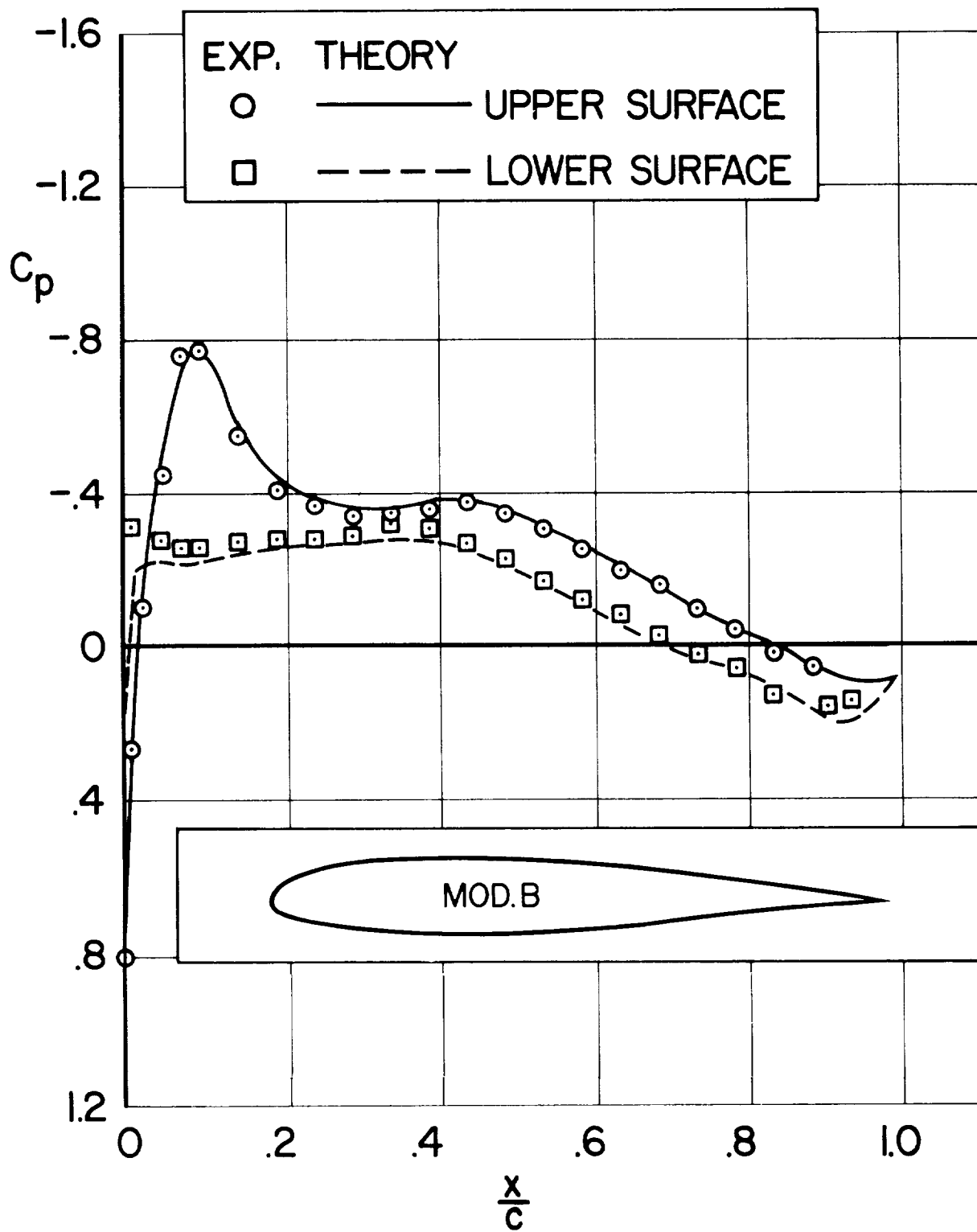
(p) $M = 0.2, Re = 1.5 \times 10^6, \alpha = 5.1^\circ, c_l = 0.670$.

Figure 8.— Continued.



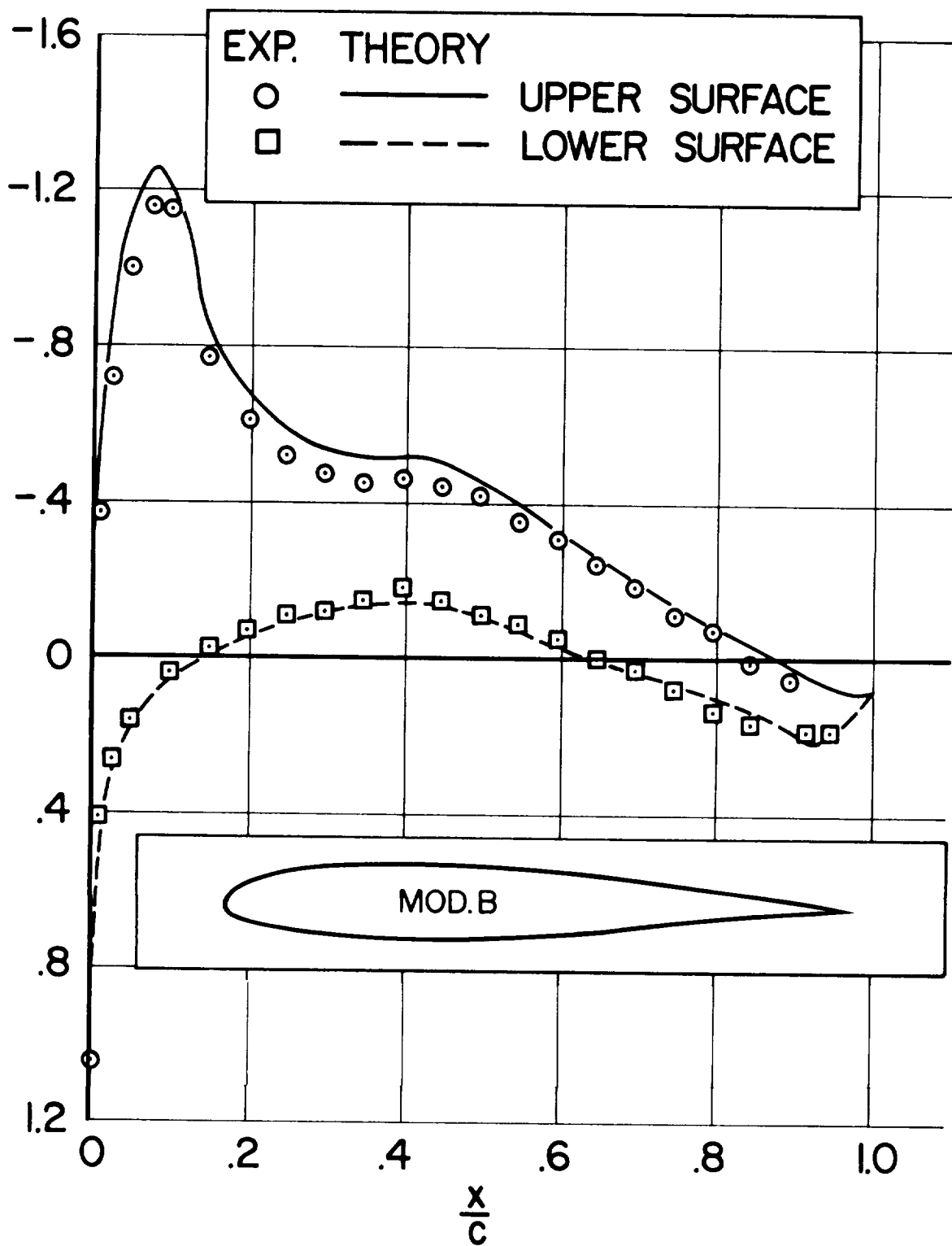
(q) $M = 0.2, Re = 1.5 \times 10^6, \alpha = 15.99^\circ, c_l = 1.488.$

Figure 8.— Continued.



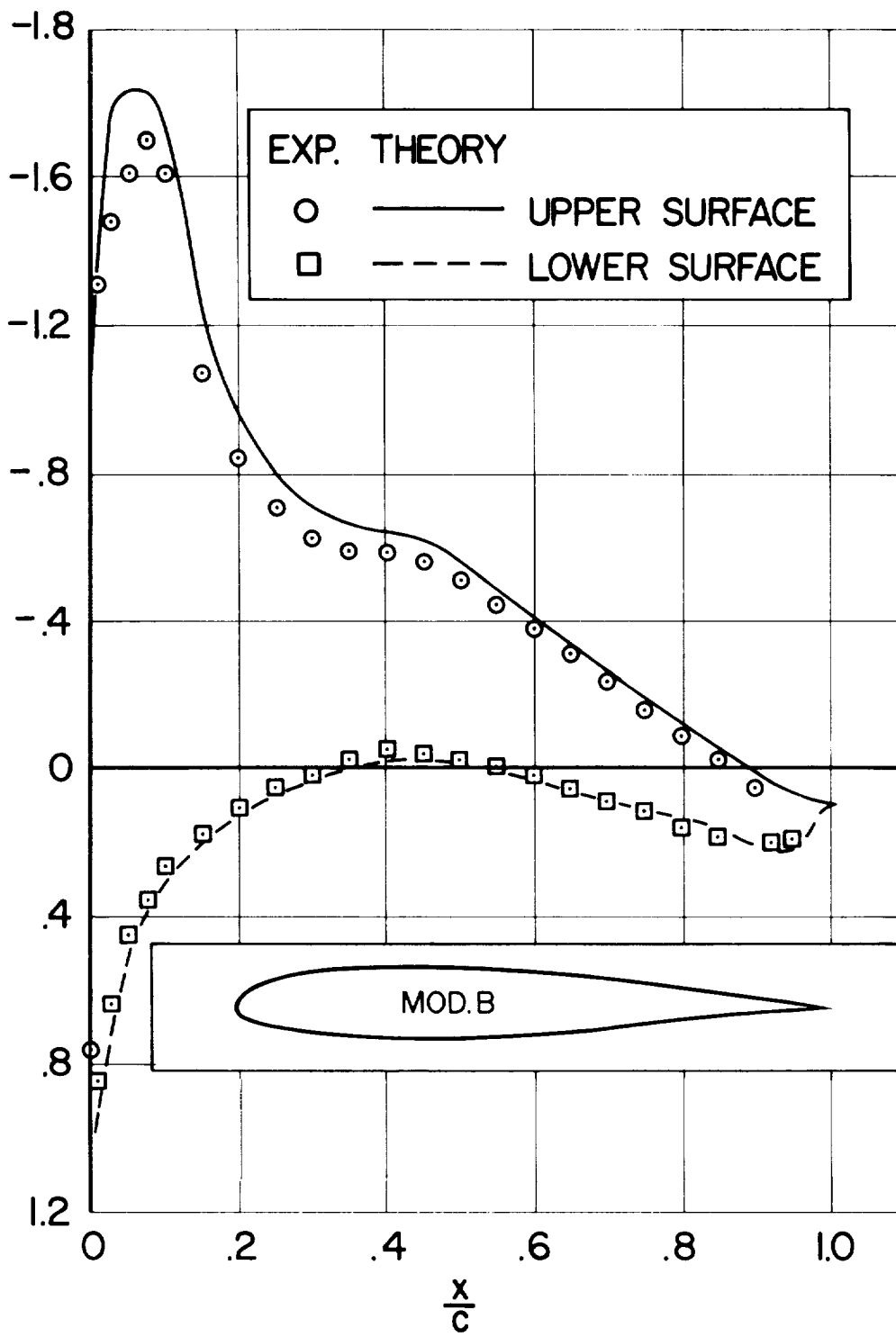
(r) $M = 0.2, Re = 1.5 \times 10^6, \alpha = -0.15^\circ, c_l = 0.119.$

Figure 8.— Continued.



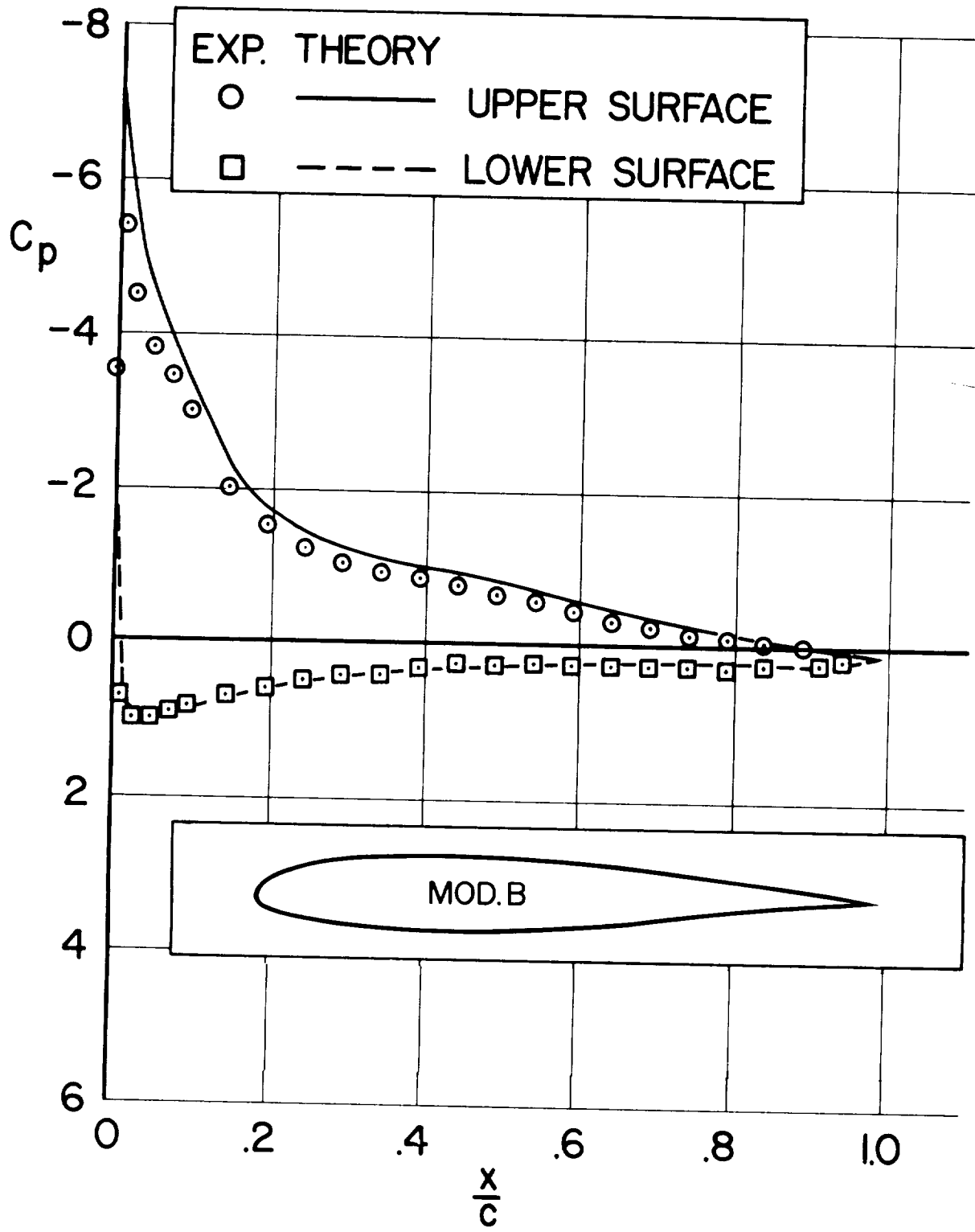
(s) $M = 0.2$, $Re = 1.5 \times 10^6$, $\alpha = 2.47^\circ$, $c_l = 0.393$.

Figure 8.— Continued.



(t) $M = 0.2, Re = 1.5 \times 10^6, \alpha = 5.09, c_l = 0.671.$

Figure 8.— Continued.



(u) $M = 0.2, Re = 1.5 \times 10^6, \alpha = 14.05^\circ, c_l = 1.437.$

Figure 8.— Concluded.

